



NASA CR 54815
AGC 8800-72

MECHANICAL DESIGN OF A CURTIS
TURBINE FOR THE OXIDIZER TURBOPUMP
OF THE M-1 ENGINE

GPO PRICE \$ _____

CFSTI PRICE(S) \$ _____

Hard copy (HC) 5.00

Microfiche (MF) 1.00

FACILITY FORM 602

N66 31625

(ACCESSION NUMBER)

169

(PAGES)

CR-54815

(NASA CR OR TMX OR AD NUMBER)

(THRU)

1

(CODE)

(CATEGORY)

By

E. Roesch

ff 653 July 65

Prepared for
National Aeronautics and Space Administration

Contract NAS 3-2555



AEROJET-GENERAL CORPORATION

SACRAMENTO, CALIFORNIA

NASA CR 54815
AGC 8800-72

TECHNOLOGY REPORT
MECHANICAL DESIGN OF A CURTIS TURBINE
FOR THE OXIDIZER TURBOPUMP
OF THE M-1 ENGINE

Prepared For

NATIONAL AERONAUTICS AND SPACE ADMINISTRATION

15 June 1966

CONTRACT NAS3-2555

PREPARED BY:
AEROJET-GENERAL CORPORATION
LIQUID ROCKET OPERATIONS
SACRAMENTO, CALIFORNIA

TECHNICAL MANAGEMENT:
NASA LEWIS RESEARCH CENTER
CLEVELAND, OHIO

AUTHOR: E. Roesch
APPROVED: W. E. Watters
Manager
M-1 Turbopump Project

TECHNICAL MANAGER: W. W. Wilcox
APPROVED: W. W. Wilcox
M-1 Project Manager

31625

ABSTRACT

The mechanical design of the 36,000 horsepower, 4,000 rpm Curtis turbine for the M-1 Engine Oxidizer Turbopump is described. Unusual design features include an inlet manifold which is integral with the backplate of the adjacent centrifugal pump, and the light-weight hollow blade stator and rotor designs principally made possible by electron-beam welding fabrication techniques. Inconel 718 alloy is used almost exclusively. The technology used in fabricating the unitized turbine inlet manifold and pump backplate assembly is also discussed.

TABLE OF CONTENTS

	<u>Page</u>
I. <u>SUMMARY</u>	1
II. <u>INTRODUCTION</u>	1
III. <u>TECHNICAL DISCUSSION</u>	4
A. DESIGN REQUIREMENTS AND SPECIFICATIONS	4
1. <u>Aerodynamic</u>	4
2. <u>Mechanical</u>	9
3. <u>System Functions and Interfaces</u>	11
4. <u>Structural and Weight</u>	11
5. <u>Material Properties</u>	11
6. <u>Producibility</u>	13
B. DESIGN DESCRIPTION	17
1. <u>Rotor Assembly</u>	17
2. <u>Inlet Nozzle</u>	26
3. <u>Reversing Row Assembly</u>	27
4. <u>Inlet Manifold and Support Structure</u>	31
5. <u>Exhaust Manifold</u>	37
IV. <u>CONCLUSIONS</u>	39
Bibliography	41

APPENDIXES

- A. Structural Design Criteria
- B. Temperature Analysis, Mod II Oxidizer Turbine Inlet Manifold - Backplate Assembly
- C. Stress Analysis of the M-1 Mod II Oxidizer Turbine Inlet Manifold and Backplate Assembly
- D. Technology Used in Fabricating the Turbine Inlet Manifold, Pump Backplate, and Turbine Support Structure Assembly

LIST OF FIGURES

<u>Figure</u>		<u>Page</u>
1	M-1 Engine Mockup	2
2	M-1 Oxidizer Turbopump Assembly	3
3	Blade Layout	6
4	Axial Plan in Hot Condition	7
5	Velocity Triangles at the Mean Diameter	8
6	Turbine and Turbopump Interface	12
7	Inconel 718, Tensile Properties	14
8	Inconel 718, Tensile Properties	15
9	Inconel 718, Elastic Properties	16
10	Rotor, Turbine - AGC Drawing No. 286527	18
11	Rotor Blade Configuration	19
12	Typical Electron Beam Weld Configuration	20
13	Disc, Turbine - 1st, AGC Drawing No. 286528	22
14	Disc, Turbine - 2nd, AGC Drawing No. 286533	23
15	Hub, Turbine Rotor, AGC Drawing No. 1119263	25
16	Nozzle, Turbine, AGC Drawing No. 286513	28
17	Stator Assembly	29
18	Stator, Turbine, AGC Drawing No. 286557	30
19	Vane, Stator, AGC Drawing No. 286556	32
20	Stator and Casing Joint	34
21	Machined Inlet Manifold Weldment	36
22	Manifold, Exhaust-Weldment - AGC Drawing No. 286520	38

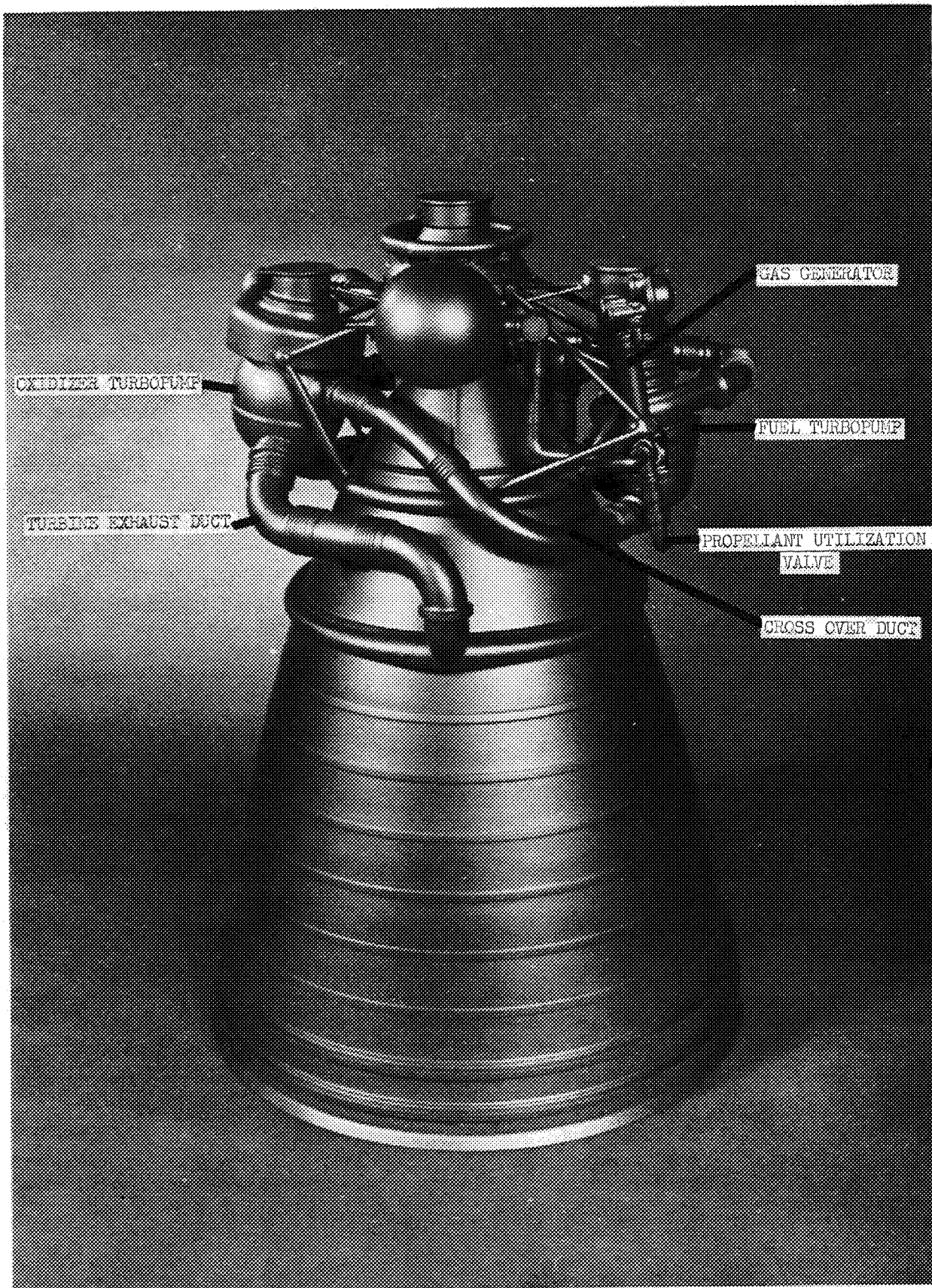


Figure 1

M-1 Engine Mockup

I. SUMMARY

This report describes the mechanical design of a flight-weight 36,000 horsepower 4,000 rpm, two-row Curtis turbine for the M-1 engine oxidizer turbopump. The primary design criterion was minimum weight for all turbine components, both stationary and rotating. This criterion was satisfied by incorporating design features utilizing electron--beam weld techniques. A significant weight reduction feature is provided by the design of the inlet manifold assembly which is unusual in that it is structurally integrated with the backplate of the adjacent centrifugal pump. The weight of the rotor assembly was minimized by applying thin conical discs. The stationary turbine nozzles and the moving blades are of hollow, sheet metal construction and are attached to their respective assemblies by means of electron-beam welding. Inconel 718, a nickel-chromium alloy, is used exclusively for all major components. One set of components was successfully fabricated and the technology used in fabricating the structurally integrated turbine inlet manifold and pump backplate assembly is delineated. Unfortunately, for reasons of directed early program terminations, there was no opportunity for development and testing.

II. INTRODUCTION

The subject turbine was designed by the Aerojet-General Corporation under contract to the National Aeronautics and Space Administration for the oxidizer turbopump of the M-1 Engine. To provide brief background information, the function of this machine, its application, and the preceding development are presented.

Two separate turbopump assemblies are used in the M-1 rocket engine; one for pumping liquid hydrogen and one for pumping liquid oxygen to the respective injector manifolds of the thrust chamber. Each turbopump has its own direct-drive turbine. The turbine drive gas is supplied by a gas generator. This gas initially drives the liquid hydrogen pump turbine, then it is further expanded to feed the liquid oxygen turbopump turbine (see Figure No. 1).

Initial development and testing of the liquid oxygen turbopump began by using a "workhorse" type of turbopump configuration (Model I) powered by a one-stage impulse turbine. This previously-designed turbine was well-suited for turbopump testing, but was not sized in accordance with the engine system balance parameters. Consequently, for this phase of the program, the turbine drive gas conditions were not restricted to those specified for the engine system, but were adjusted to meet the speed and power requirements for pump testing.

The next planned program phase was to power the same pump with a flight-weight turbine design that would be sized aerodynamically to the exact turbine drive gas conditions specified for the M-1 Engine system. For this, a two-row Curtis stage turbine was selected and this report describes the mechanical and structural design of this turbine configuration for use in the M-1 Engine Configuration Liquid Oxygen Turbopump (see Figure No. 2).

SACRAMENTO PLANT

GENERAL

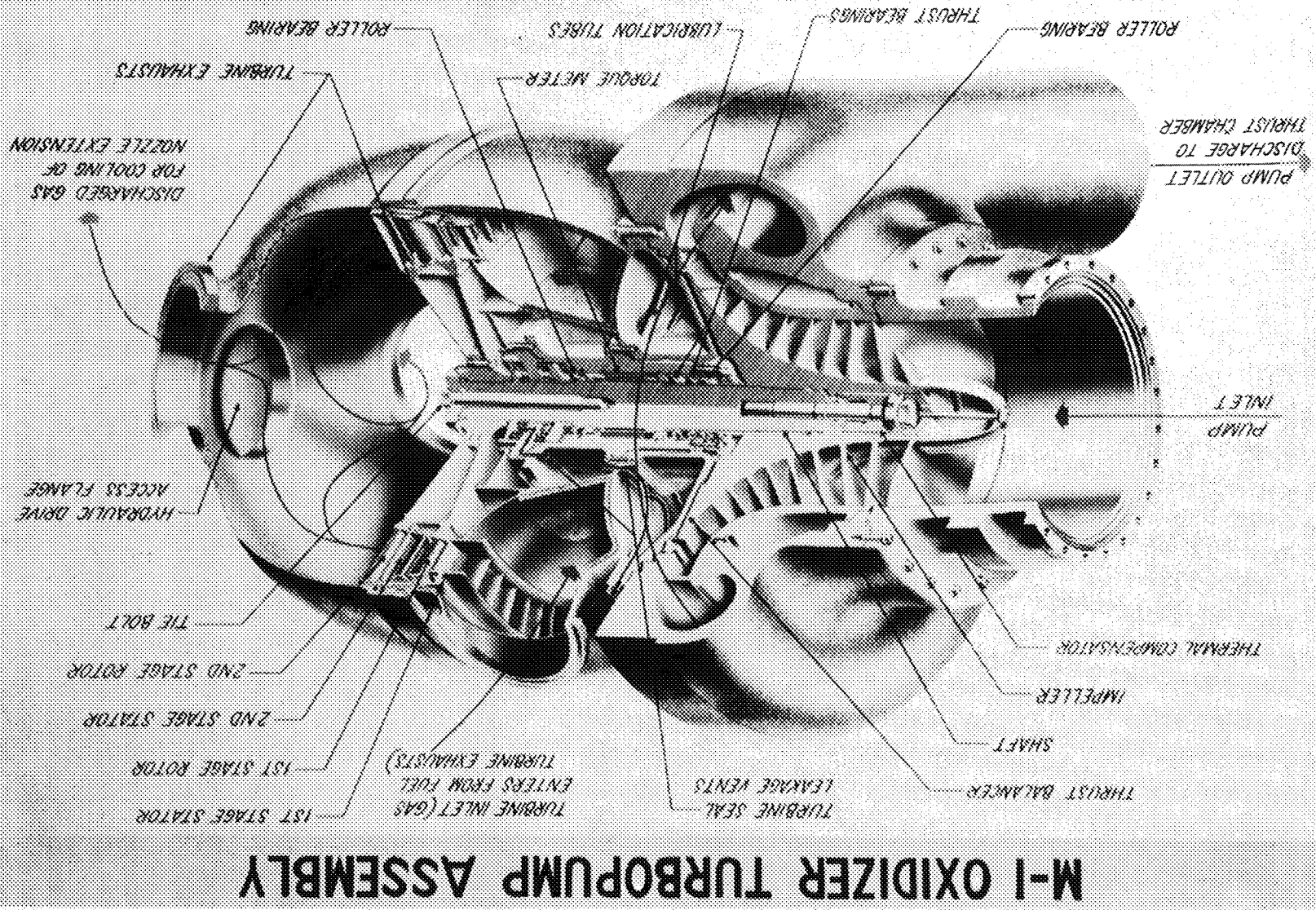


Figure 2

Operating Conditions and Specifications (cont.)

- Gas Inlet Total Temperature
(at Nozzle Inlet) 1190°R
- Gas Outlet Static Pressure 120 psia
- Gas Outlet Total Temperature 1099.5°R
- Gas Flow Rate 115 lb/sec

The turbine drive gas is the combustion product of oxygen and hydrogen at a mixture ratio, $\frac{\dot{m}_O}{\dot{m}_F} = 0.8$, having a molecular weight, $M = 3.66$.

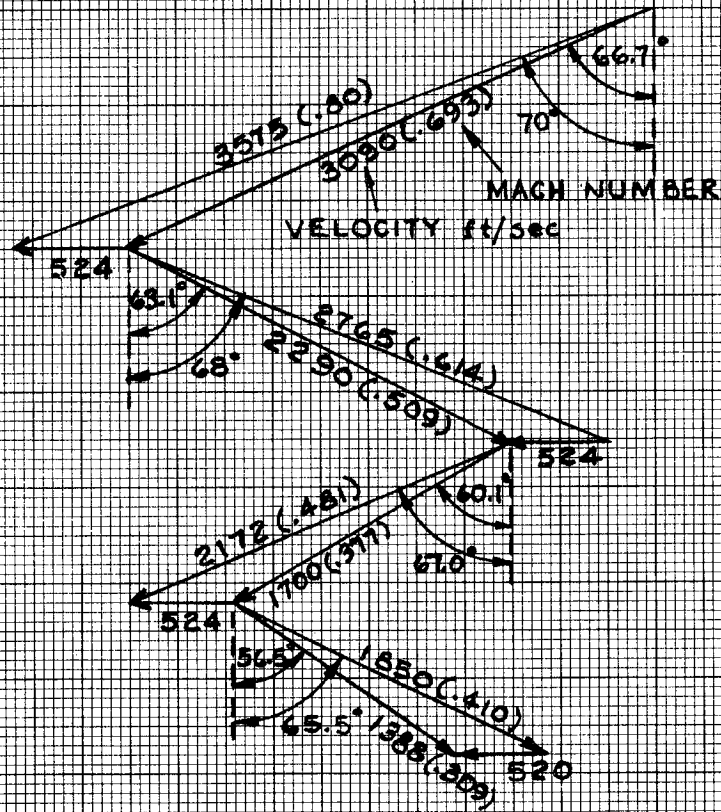
The aerodynamic calculations for turbine blading resulted in the following:

	<u>Inlet Nozzle</u>	<u>Rotor 1st Row</u>	<u>Reversing Vanes</u>	<u>Rotor 2nd Row</u>
Number of Blades	43	98	97	94
Blade Throat Area, in. ²	111.5	141.5	184.5	227.5

The blade layout is delineated in Figure No. 3 and an axial cross-section for the blading of the stators and rotors is shown in Figure No. 4, establishing the geometry necessary to meet the calculated aerodynamic requirements. The velocity triangles at the Mean Diameter are presented in the vector diagram, Figure No. 5.

An important feature of the selected blade profile is a blunt leading edge, as compared to the thin leading edge of classical impulse blading. A blade with a blunt leading edge can be manufactured from sheet metal by simple forming. The blunt blade profile is efficient over a large variance in incidence angle, a feature which is also of benefit in achieving good off-design performance. Another reason for the selection of this profile was the consideration of a fast start transient and operation in the combustion products of hydrogen and oxygen. Under these conditions, extreme heat transfer rates to the blades have caused cracking of sharp leading edges. The blade profile is identical for both rotors and for the reversing row, which simplifies tooling and manufacture of the hardware.

M-1 OXIDIZER TURBINE



Velocity Triangles at the Mean Diameter

Figure 5

VIII. Dual Seal Joints and Special Methods (cont.)

The temperatures shown are gas temperatures; therefore, the actual metal temperature of the respective parts exposed to the gas are subject to the heat transfer conditions existing and design values must be determined accordingly.

Other general mechanical design specifications include:

a. Leakage, Purges, Drains

(1) No leakage allowed at external joints for Flight Model Units.

(2) The design must provide for monitoring of any leakage past primary static seals into the intervening cavity of dual seal joints. Steps must be initiated to eliminate any leakage detected during development. Leakage must be collected and disposed of into a non-hazardous area during tests.

(3) Decontamination and drying purges must be provided to remove all air and moisture from the turbopump prior to the admission of propellant for the chill-down cycle.

b. Separable Flange Seals

M-1 leakage criteria requires an inner and outer seal with a vented cavity between the two seals at each external joint. This sealing arrangement is required at all separable joints and assemblies in the hydrogen, oxygen, and hot gas circuits where static seals are necessary. (During design the only recommended seal design was the Conoseal* or seal welds with grind-off provisions for disassembly).

c. Instrumentation Bosses

(1) All instrumentation bosses shall be brazed, welded, cast, or forged in place and shall conform to leakage requirements discussed in Section III, A,2,a,(1) of this report.

(2) Instrumentation bosses shall have a threaded connection per Specification AND 10050 for use with K seal MC 252, Teflon-coated.

d. Torquing

(1) Access ports with removable covers must be provided in the turbine exhaust manifold to allow measurement of breakaway torque of the rotating assembly.

*Registered Trademark of the Aeroquip Corporation

2. Mechanical

Established mechanical design parameters are:

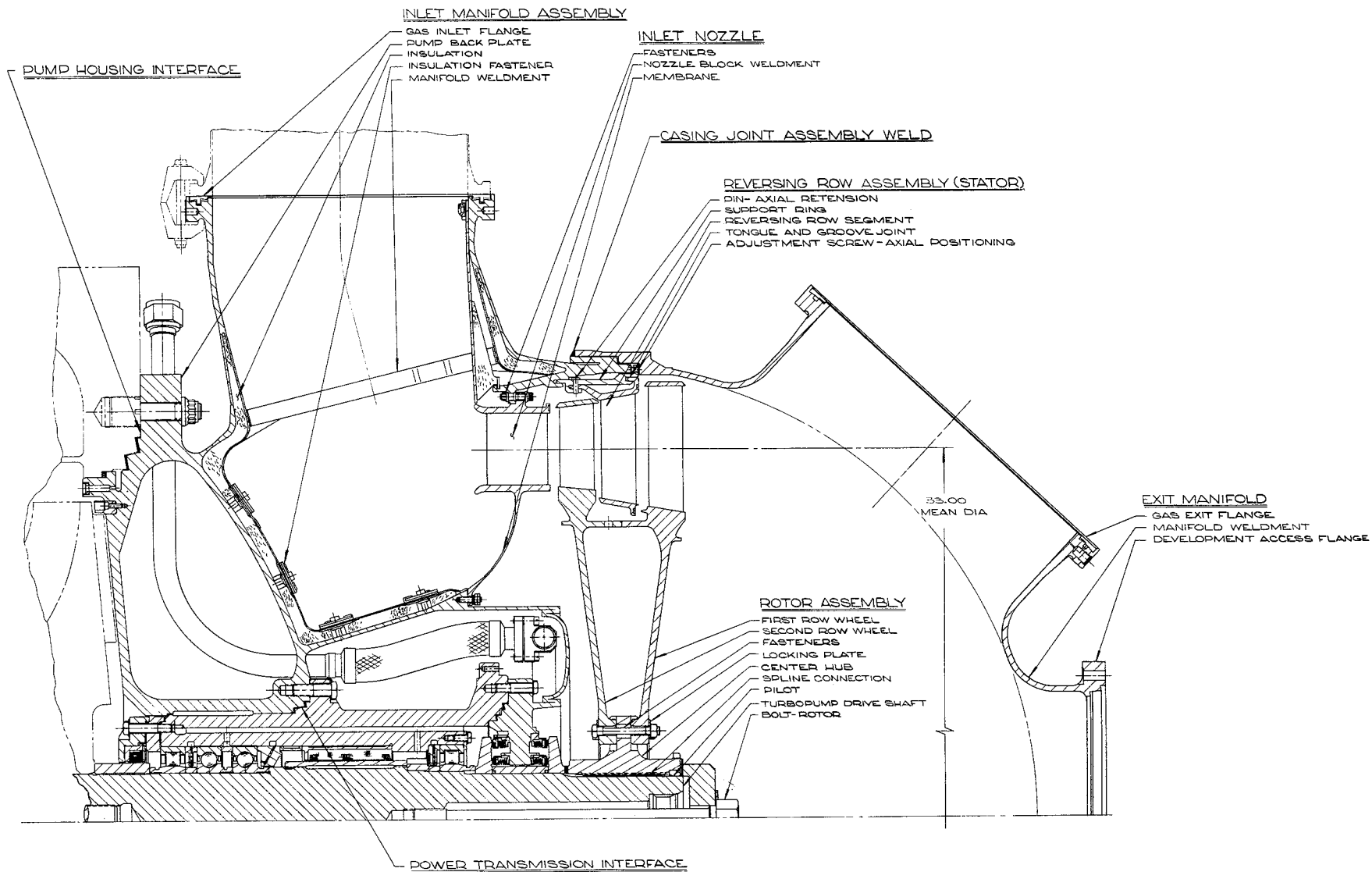
Maximum Shaft Speed	4,000 rpm
First Critical Speed, Minimum	4,600 rpm
Horsepower	35,828
Torque	47,000 ft-lb
Shaft Rotation (Viewed from Turbine Toward Pump)	Counter Clockwise
Inlet Manifold Static Pressure	310 psia
Discharge Housing Static Pressure	205 psia
Gas Inlet Temperature (Manifold)	1050°F
Pump Interface Temperature	-320°F

These values are somewhat larger than those calculated in the aerodynamic analysis because the mechanical capability for some off-design operation is to be built into the machine.

The pressures and temperatures between each blade row are:

	<u>Nozzle Outlet</u>	<u>Rotor, First Row Outlet</u>	<u>Reversing Vanes Outlet</u>	<u>Rotor, Second Row Outlet</u>
<u>Blade, Hub</u>				
Pressure, Static, psia	115.5	119.2	115.0	115.0
Temperature, Total, °R	1190	1133.8	1133.8	1102.5
<u>Blade, Mean</u>				
Pressure, Static, psia	126.8	126.8	124.8	120.0
Temperature, Total, °R	1190	1133.0	1133.0	1100.9
<u>Blade, Tip</u>				
Pressure, Static, psia	136.0	132.2	132.2	124.4
Temperature, Total, °R	1190	1132.4	1132.4	1100.3

Figure 6



Turbine and Turbopump Interface

(2) Consideration of the effect of thermal expansion or contraction at operating temperature must be factored into fastener torque values.

3. System Function and Interfaces

The interfaces of the turbine components with the turbopump assembly (see Figure No. 6) are provided by the power transmission shaft for the rotor elements and by the power transmission housing and the pump discharge housing for the stationary parts.

The rotor interface to the power transmission shaft consists of a splined connection transmitting the rotor torque, and a tie-bolt assuring axial retention of the rotor. The power transmission shaft forms a direct-drive connection between the turbine rotor and the pump impeller.

The stationary interface is provided by the pump backplate, which is an integral weldment with the turbine inlet manifold and is flange-connected to the power transmission housing and the pump discharge housing. In turn, the inlet manifold provides the connecting points of attachment for the turbine inlet nozzles, the reversing vanes, and the turbine exhaust housing.

Two flange connected 11-1/2-in. diameter inlet lines form the connection between the turbine inlet manifold and the engine. The Dual-Inlet configuration provides favorable engine packaging. In like manner, dual exhaust lines lead from the turbine exhaust manifold to the exhaust chamber skirt cooling manifold.

4. Structural and Weight

Structural adequacy must be provided in a minimum weight configuration, a requirement based upon a target weight allowance of 3000 lb for the complete oxidizer turbopump assembly. In view of this, weight reduction discipline must be practiced in the design of every turbopump part, which is especially important for the large turbine components. The structural design criteria are presented in Appendix A.

5. Material Properties

The material requirements for lightweight turbine components operating in the environment of this turbopump are:

- a. High strength at operating temperature to permit thin cross-sections and corresponding minimum weight.
- b. Good elongation characteristics at operating temperatures up to 1050°F to withstand thermal shock conditions without surface cracking.
- c. Good properties at cryogenic temperature (-320°F)

DESIGN PROPERTIES MATERIALS ENGINEERING DEPARTMENT, LRO	Inconel 718 Tensile Properties
MATERIAL: Inconel 718	Issue No. 1 Date: 1-22-65

Ultimate Tensile Stress, 0.2% Yield Stress, and Elongation vs Temperature
 Also Stress for Rupture in 1 and 10 Hours

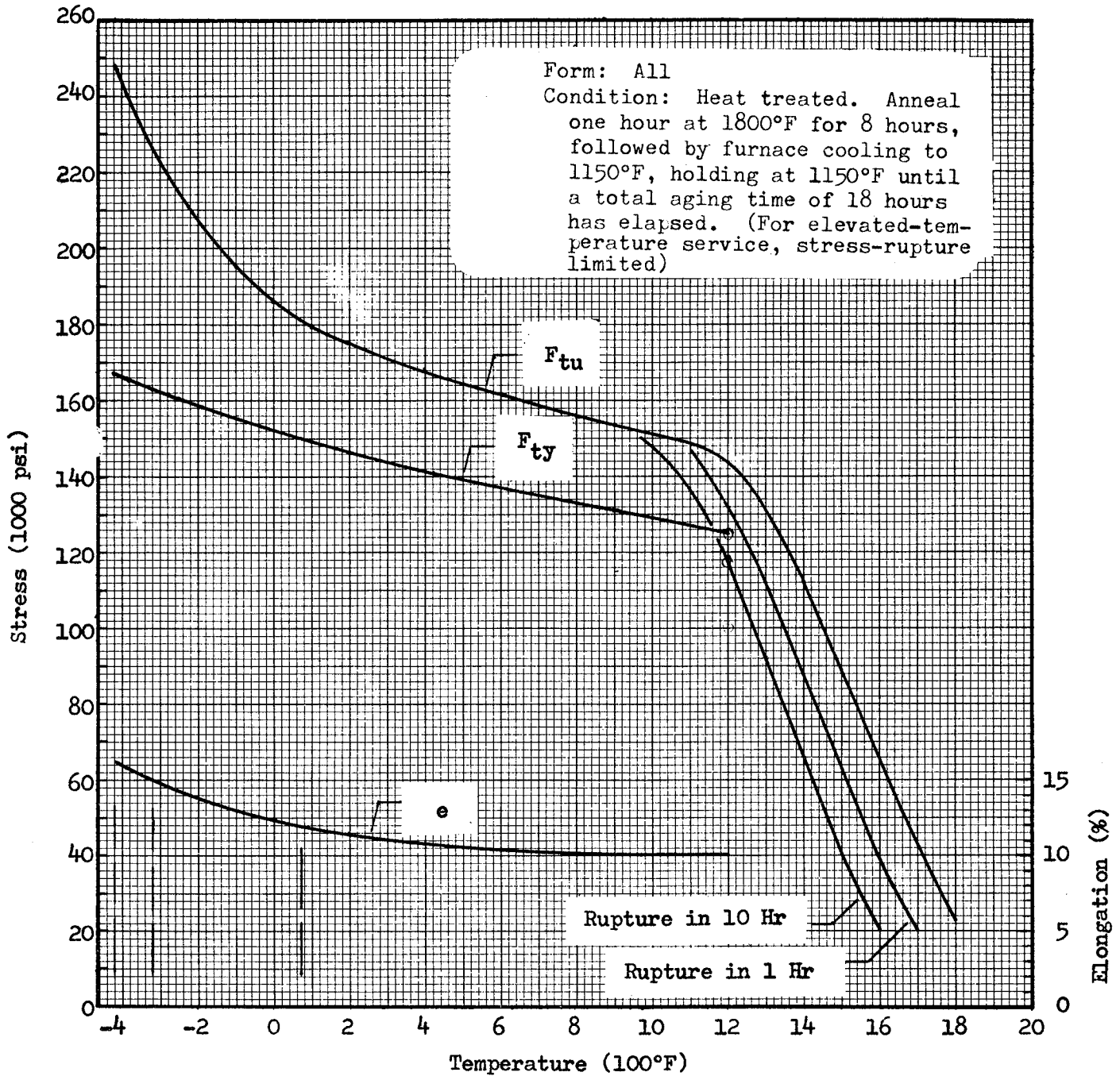


Figure 7

d. Good corrosion resistance.

e. Good machinability, metal forming qualities, and weldability, which are needed for lightweight design and manufacturing techniques.

The Nickel-Chromium Alloy, Inconel 718, conforms closely to the stated requirements and was selected for use on all major turbine components. Depending upon the heat treat specification, Inconel 718 is classified in two groups:

Group 1: The 1800°F solution treatment and 1325/1150°F aging cycle for stress rupture controlled parts where notch-ductility is important. It is recommended for high temperature applications.

Group 2: The 1950°F solution treatment and 1350/1200°F aging cycle provides improved toughness at low temperatures and is recommended for cryogenic service. It is also superior over Group 1 in its ability of ensuring age-hardening response in large forgings having coarse-grained structure.

The principal material strength properties of Inconel 718 are shown in Figures No. 7 and No. 8 for Groups 1 and 2 respectively. The elastic properties are presented in Figure No. 9.

Details of the comprehensive material selection study and metallurgical data of the Inconel 718 chromium-nickel alloy are documented. (2)

6. Producibility

The mechanical and structural requirement of minimum weight influences the component design philosophy toward manufacturing processes for thin-wall parts made from high strength materials. This establishes configurations that are fabricated by joining thin plates, formed sheet metal parts, stamping and forgings, and making the best use of advanced fabrication technology, as well as classic black-art shop techniques. Metal joining by gas tungsten arc welding, and especially by the more recently introduced electron-beam welding process, is a chief factor in making possible minimum weight design configurations for the respective turbine parts.

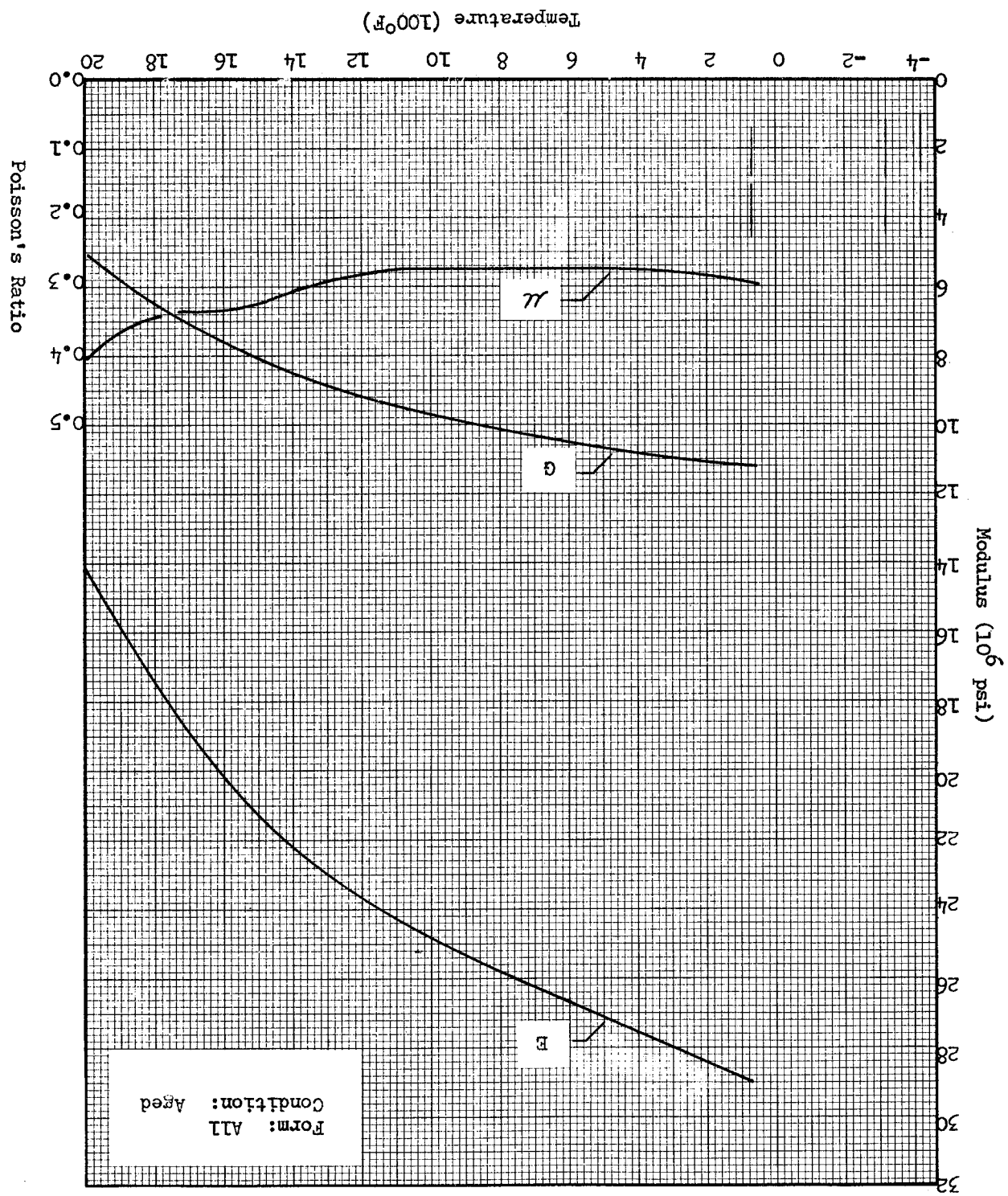
The fabrication history and fabrication techniques used in the production of the inlet nozzle, the turbine rotor, and the reversing vane, using Inconel 718 material and electron-beam welding processes, are presented in a separate report(3).

(2) Inouye, F. T., Hunt, V., Jansen, G. R., and Frick, V., Summary of Experience Using Inconel 718 on the M-1 Engine, Aerojet-General Report No. 8800-37, 30 December 1965.

(3) Beer, R., Fabrication Technology of Lightweight Turbine Components Using the Electron-Beam Welding Process to Fabricate Sheet Metal Blades and Join the Blades to Disc or Support Structure, Aerojet-General Report No. 8800-49, 1 April 1966.

DESIGN PROPERTIES	
- MATERIALS ENGINEERING DEPARTMENT, LRO	
Inconel 718 Elastic Properties	Issue: No. 1
Date: 1-23-65	

Young's Modulus, Torsional Modulus, and Poisson's Ratio vs Temperature



DESIGN PROPERTIES MATERIALS ENGINEERING DEPARTMENT, LRO	Inconel 718 Tensile Properties
MATERIAL: Inconel 718	Issue No. 1 Date: 1-21-65

Ultimate Tensile Stress, 0.2% Yield Stress, and Elongation
vs Temperature

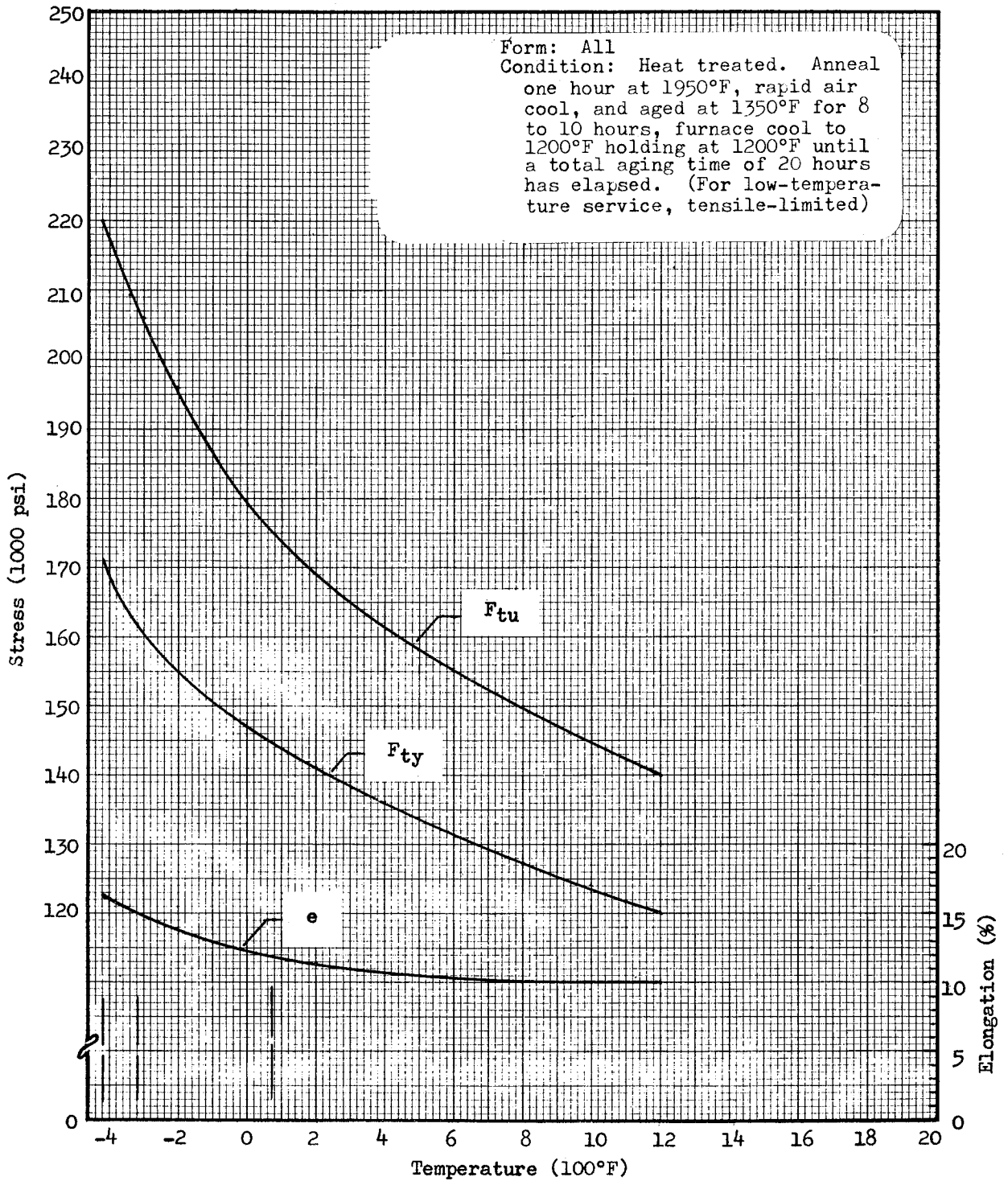


Figure 8

Gas tungsten arc welding was used primarily in the fabrication of the turbine inlet manifold, which is also made from 718 material. The fabrication of this difficult composite weldment is described in Appendix D of this report.

B. DESIGN DESCRIPTION

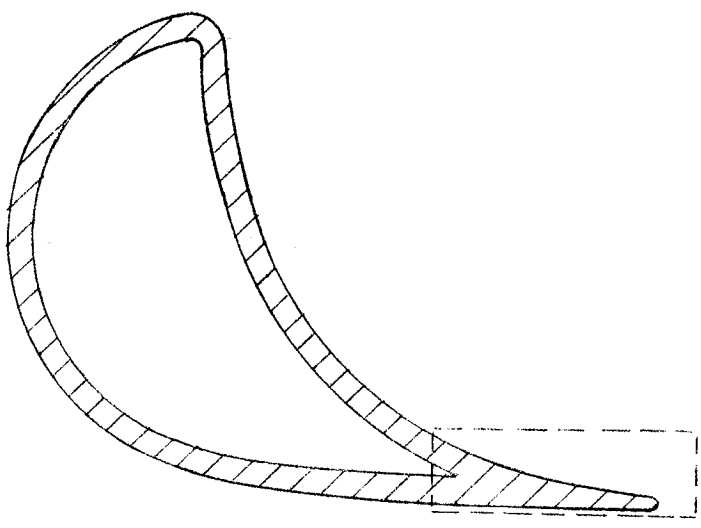
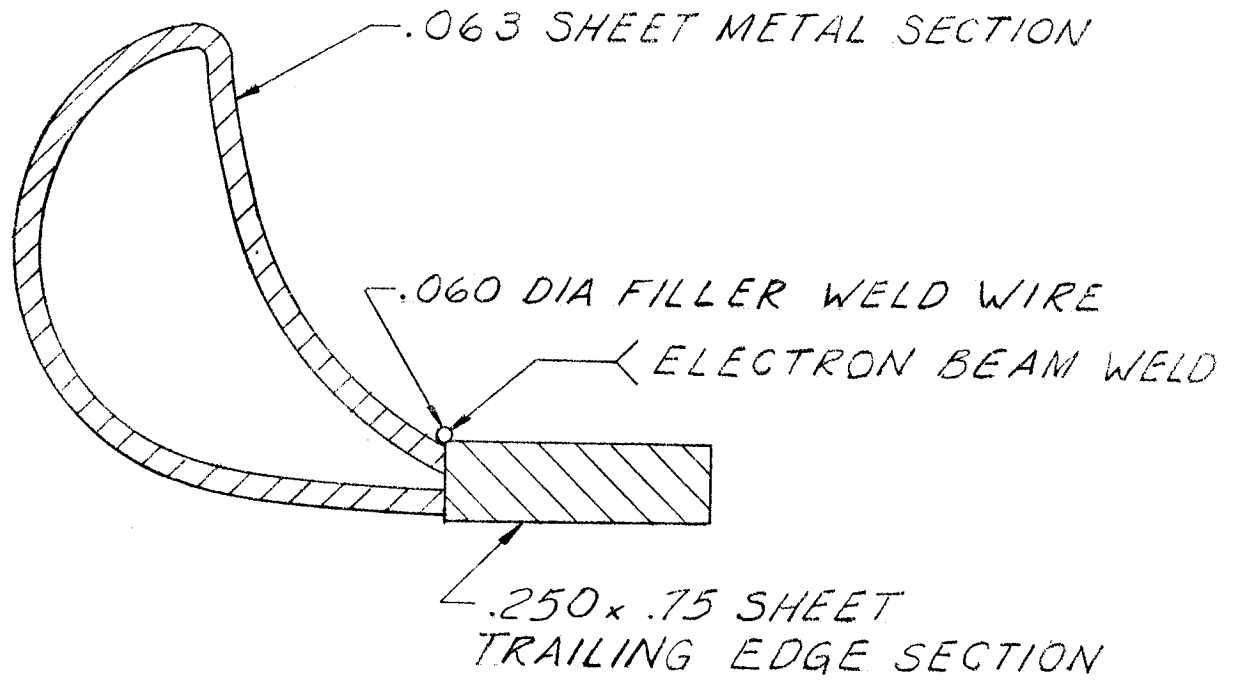
1. Rotor Assembly

a. General Design Philosophy

The selection of the rotor configuration was principally centered around the design criterion of minimum weight. Taking advantage of the relatively low tip speed, it was envisioned that the blade loads could be carried by an individual rim for the first and second row, respectively. Structurally, these rims were to function as "free rings." In this way, the turbine discs, which join the bladed rims with a center hub, are not affected by turbine blade radial forces and serve only for the transmission of the driving torque. This permits thin wall construction, but a thin disc or membrane, although structurally sound for steady-state loading, is very susceptible to disc vibration. This problem was overcome by making the two membranes conical and arranging them to form a rigid box section when they were mechanically-joined in the rotor assembly (see Figure No. 10). This box section structure is formed by face contact of the circular flanges at the major extremities of the two discs and adjoinment to the common center hub by coupling lugs and a bolted connection. The rotor assembly center hub connection to the power transmission shaft is assured by diametral pilots for concentric alignment and squareness, splines for transmission of driving torque, and a center bolt for axial retention. Specific design features are discussed in the following paragraphs.

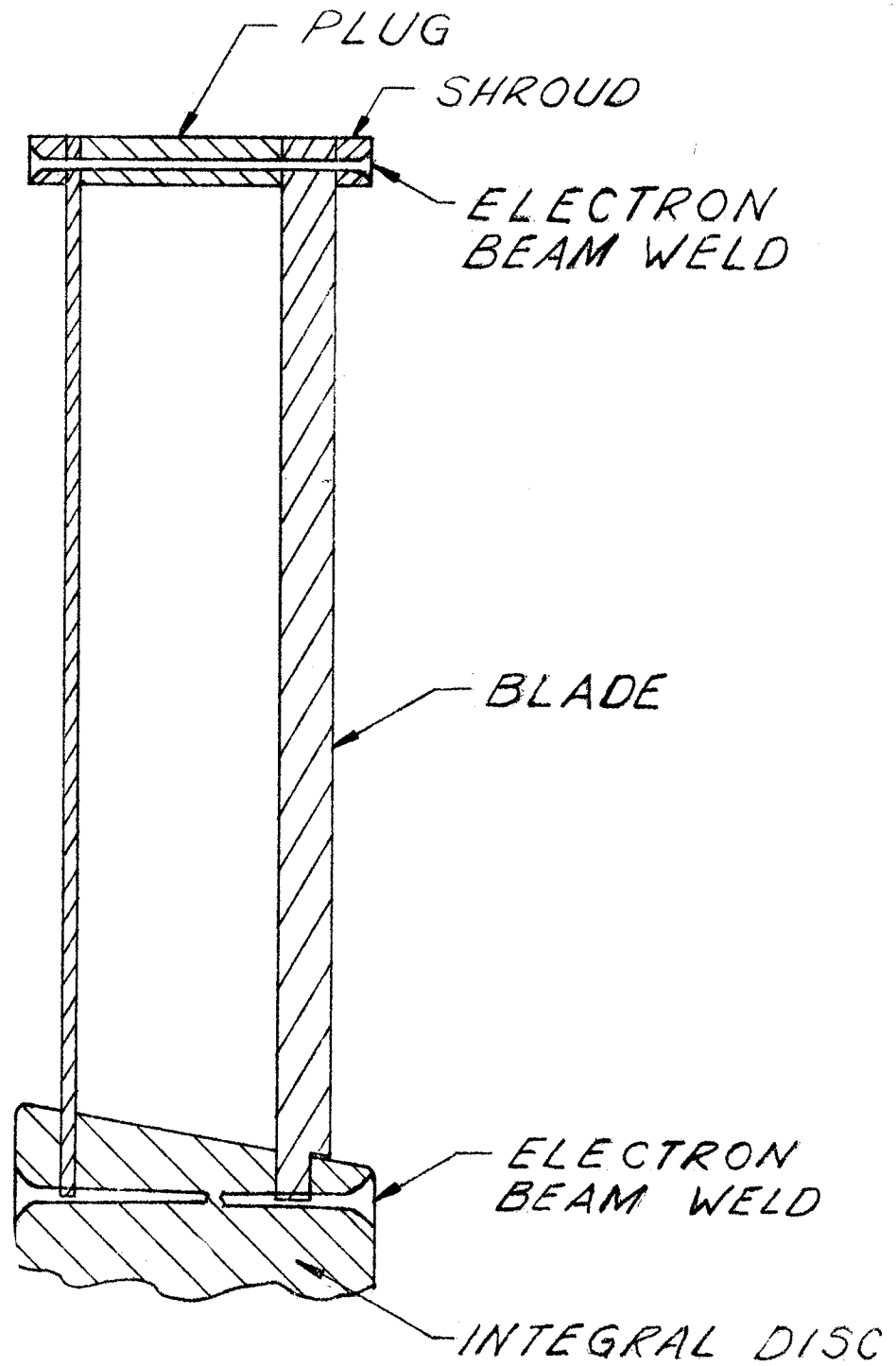
b. Turbine Rotor Blading

The general concept described above requires rotor blades of minimum mass to minimize centrifugal blade load and to conform to the over-all design objective of minimizing component weight. This suggests a hollow structure for the blades of the aerodynamic profile as in Figure No. 3, with 98 blades for the first-row wheel, and 94 blades for the second-row wheel. Hollow blades were formed from 0.063-in. thick Inconel 718 sheet, as illustrated in Figure No. 11, and electron-beam welded to the disc and shroud of the first and second-row wheel, respectively. Figure No. 12 shows the weld joint design and was developed through considerable application engineering effort for utilizing the recently-introduced welding process. The calculated blade centrifugal stress is on the order of 16,000 psi and the blade bending stress is 11,000 psi. It is notable that the blade profile is identical for the first and second row wheel. However, the blades for the second wheel are longer, to accommodate the increase in volumetric flow of the gas, and the blade positioning is adjusted to the difference in gas exit angle between the first and second row.



ROTOR BLADE CONFIGURATION IN AS WELDED AND AS FINAL MACHINED CONFIGURATION

Figure 11



Typical Electron Beam Weld Configuration

The above described design solution was analytically compared with the more conventional solid blade construction and blade root attachment by dove-tail, T-slot, or fir-tree. Solid blades are not only heavier but cause greater root-stresses because of the correspondingly larger centrifugal force. Therefore, they require a heavier rim for fastening the blades and a heavier disc profile corresponding to the added radial stresses. Such a course, although more customary, would have resulted in a rotor assembly that is approximately 250 lb heavier than the selected design.

c. Turbine Wheel, First Row

The turbine wheel is a weldment consisting of a forged disc, formed sheet metal blades, and the shroud. All parts of the weldment are of Inconel 718 material. The disc shape is conical to provide structural stiffness in a thin-wall member, and also to prevent buckling caused by thermal-gradient-induced stresses. The shroud is a rolled ring fabrication, which is segmented into a pattern, as shown in Figure No. 13, which permits radial growth of the blades but retains alignment and vibration dampening qualities. Connection to the center hub is provided by coupling lugs; these are discussed in greater detail in Paragraph III,B,1,e, of this report.

d. Turbine Wheel, Second Row

The mechanical design of this wheel is shown in Figure No. 14. Although this wheel is larger than the first row wheel, the design principle, material, and method of manufacture is identical.

e. Rotor Hub

The two turbine wheels are attached to a common center hub which serves as the connection to the power transmission shaft. The design criterion for the wheel-to-hub interface is a radially unrestrained joint, allowing the growth of the rotor as a result of thermal and centrifugal effects while maintaining alignment concentricity. This is provided by means of a multi-lug, parallel face coupling connection. Load-sharing for the probability of less than 100% lug contact was carefully studied and sufficient safety margin was assured for a minimum of three lugs in full contact. A nine lug coupling was incorporated into the final coupling design for the wheel-to-hub joint. Concentric interface of this rotor hub with the power transmission shaft is assured by cylindrical pilots; a 47 tooth involute spline of 12/24 diametral pitch is used for torque transmission. The rotor hub design is illustrated in Figure No. 15. This configuration is conventional in the turbo-machinery field and selection for this application was based upon the operational reliability experienced by Aerojet-General Corporation with similar applications.

f. Turbine Wheel Fasteners

The rotor assembly shown in Figure No. 10 has an arrangement of nine equally-spaced bolt and nut joints securing the turbine wheels to the rotor

hub. The bolts are of 3/8-in. nominal size with relieved shank for improved impact fatigue strength properties. Clearance holes in the wheels and in the hub assure that the fastener is not affected by radial growth of the wheels relative to the hub. Bolt torque values are controlled for uniform tightening, repeatable safety margin, and maintenance of an unrestrained joint. A special locking plate secures the bolt head and nut against rotation after torquing. The materials include Inconel 718 for the bolts, 303 stainless steel for the nuts, and 321 stainless steel for the locking plates.

The fastener approach for this important joint was selected with emphasis upon simplicity and reliability. It was carefully compared with alternative solutions (i.e., the use of body-fitted bolts was initially intended, but the idea was discarded to isolate the rotor torque load, eliminate transverse shear stresses, and assure an unrestrained joint). Bolt size was selected to minimize the size of the holes through the turbine wheels.

g. Stress Analysis Summary

Detailed stress and vibration analyses of this rotor were made. (4)(5) The structural integrity of this rotor for an operational start and shutdown life of 3200 cycles was substantiated.

2. Inlet Nozzle

a. General Design Philosophy

The selected configuration is a full-admission nozzle and is designed for manufacture by electron-beam weld fabrication techniques using Inconel 718 material throughout. Flow passages are converging and produce subsonic (Mach 0.80) nozzle exit flow. Forty-three blades are used in the nozzle block. The blade profile is detailed in Figure No. 3. A rigid flange around the outer shroud is used to bolt the nozzle block to the inlet manifold. The connection of the inner shroud to the inlet manifold is formed by a relatively thin (0.040-in.) membrane, which is an integral part of the nozzle weldment and secured to the inlet manifold by bolting. The membrane serves as a flexible joint capable of tolerating a thermal gradient as well as axial and radial tolerance accumulations. It also provides the separator (seal) between the gas in the inlet manifold and the cavity downstream of the inlet nozzle. Figure No. 6 shows the nozzle orientation and interface in the turbopump.

(4) Mod II Turbine Rotor, Aerojet-General Report No. SA-OTPA-242, 8 November 1965
 (5) Chinn, T. and Severud, L. K., Analytical and Experimental Vibration Analysis of the Turbine Buckets for the M-1 Liquid Oxygen Turbopump, NASA CR-54830, 30 June 1966

b. Nozzle Block Weldment

The design of the nozzle block is illustrated in Figure No. 16. This configuration is a weldment consisting of the outer bolting flange, outer shroud, vanes, inner shroud, membrane (seal cone), and inner bolting flange. All parts of this composite weldment are made from Inconel 718 material and are joined by electron-beam welding and brazing. The weld joint alone is sufficient to carry all mechanical loads. The braze fillet around the profile is expected to serve as a vibration dampener. The blades are hollow, sheet-metal-formed airfoils. The fabrication technology for this nozzle weldment is principally the same as that for the rotor (wheel and blades).⁽⁶⁾

Conceptwise, the rigid attachment of the unslotted nozzle block to the manifold is a departure of usual design practice. The configuration was analyzed for thermal gradients and insignificant temperature differences were found to exist between the nozzle outer shroud and the support cone of the manifold. Therefore, the design shown on Figure No. 16 was selected to minimize leakage problems.

c. Stress Analysis Summary

A detailed stress analysis was made⁽⁷⁾. It presents positive margins of safety and proves the structural integrity of the design.

3. Reversing Row Assembly

a. General Design Philosophy

The reversing row (stator) concept, Figure No. 17, is designed to minimize distortions caused by temperature gradients. This is done by cutting the vane assembly into six segments. Within each segment, the blades are free to grow radially inward while the outer and inner shrouds can grow tangentially and axially. Figure No. 18 illustrates the arrangement selected. Axially, each stator segment is held by two tongues engaged in annular grooves in the support ring. Two pins secure each segment to the support ring and fix the direction in which the nozzle segments are free to grow axially. In this arrangement, tangential and axial flexibility (floatability) is provided to prevent thermal distortion during operation.

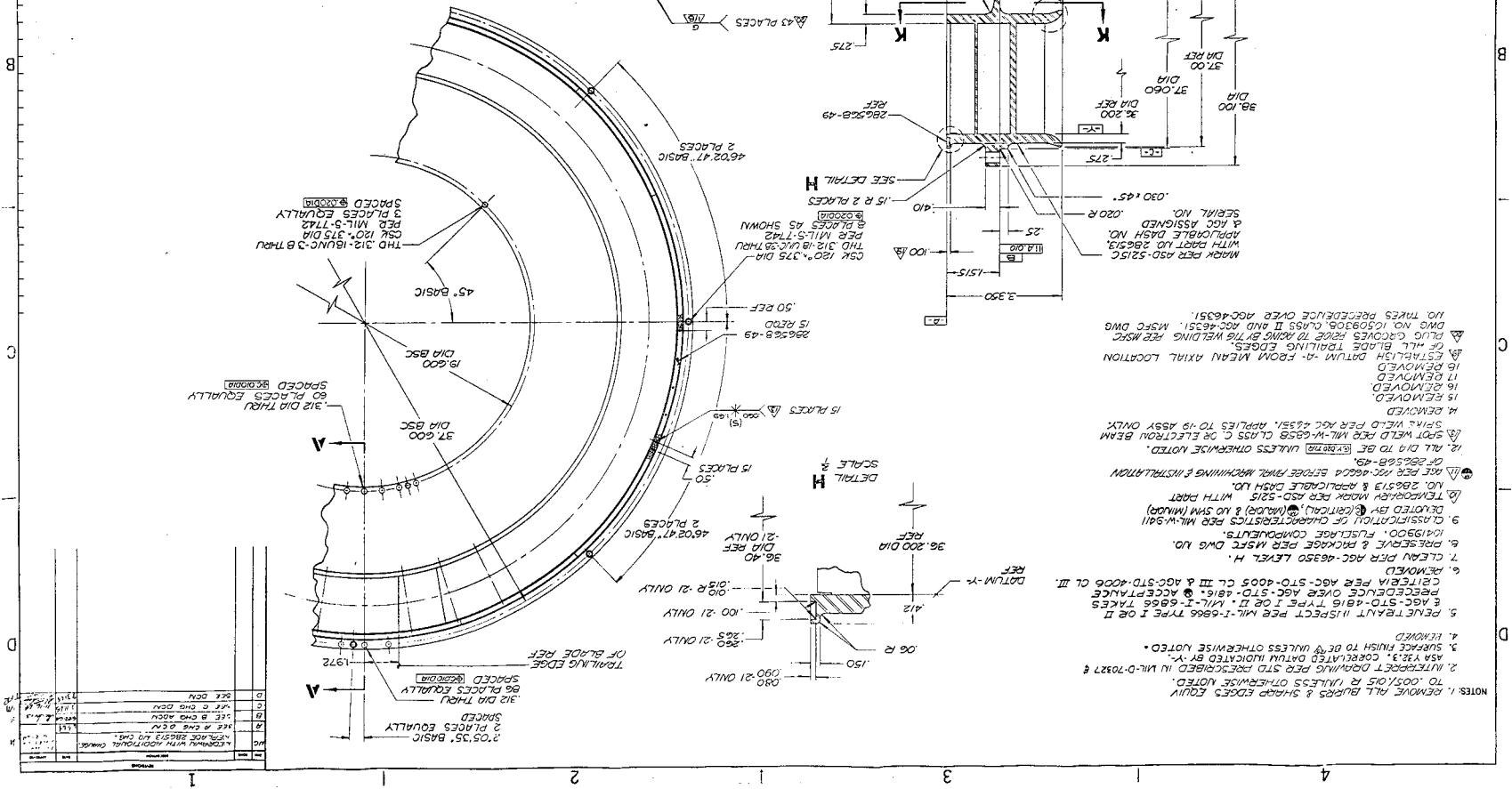
b. Weldment - Stator Vanes

The profiles of the stationary vanes for the reversing row is identical to the profile of the two rows of moving blades in the rotor. The

(6) Beer, R., Aerojet-General Report No. 8800-49, op. cit.

(7) Mod II Nozzle, Aerojet-General Report No. SA-OTPA-243, 1 December 1965

NO.	DESCRIPTION	DATE	BY	CHECKED
1	REMOVED			
2	REMOVED			
3	REMOVED			
4	REMOVED			
5	REMOVED			
6	REMOVED			
7	REMOVED			
8	REMOVED			
9	REMOVED			
10	REMOVED			
11	REMOVED			
12	REMOVED			
13	REMOVED			
14	REMOVED			
15	REMOVED			
16	REMOVED			
17	REMOVED			
18	REMOVED			
19	REMOVED			
20	REMOVED			
21	WELD ROD			
22	WELD ROD			
23	WELD ROD			
24	WELD ROD			
25	WELD ROD			
26	WELD ROD			
27	WELD ROD			
28	WELD ROD			
29	WELD ROD			
30	WELD ROD			
31	WELD ROD			
32	WELD ROD			
33	WELD ROD			
34	WELD ROD			
35	WELD ROD			
36	WELD ROD			
37	WELD ROD			
38	WELD ROD			
39	WELD ROD			
40	WELD ROD			
41	WELD ROD			
42	WELD ROD			
43	WELD ROD			
44	WELD ROD			
45	WELD ROD			
46	WELD ROD			
47	WELD ROD			
48	WELD ROD			
49	WELD ROD			
50	WELD ROD			
51	WELD ROD			
52	WELD ROD			
53	WELD ROD			
54	WELD ROD			
55	WELD ROD			
56	WELD ROD			
57	WELD ROD			
58	WELD ROD			
59	WELD ROD			
60	WELD ROD			
61	WELD ROD			
62	WELD ROD			
63	WELD ROD			
64	WELD ROD			
65	WELD ROD			
66	WELD ROD			
67	WELD ROD			
68	WELD ROD			
69	WELD ROD			
70	WELD ROD			
71	WELD ROD			
72	WELD ROD			
73	WELD ROD			
74	WELD ROD			
75	WELD ROD			
76	WELD ROD			
77	WELD ROD			
78	WELD ROD			
79	WELD ROD			
80	WELD ROD			
81	WELD ROD			
82	WELD ROD			
83	WELD ROD			
84	WELD ROD			
85	WELD ROD			
86	WELD ROD			
87	WELD ROD			
88	WELD ROD			
89	WELD ROD			
90	WELD ROD			
91	WELD ROD			
92	WELD ROD			
93	WELD ROD			
94	WELD ROD			
95	WELD ROD			
96	WELD ROD			
97	WELD ROD			
98	WELD ROD			
99	WELD ROD			
100	WELD ROD			



NOTES:

1. REMOVE ALL BURRS & SHARP EDGES EQUALLY
2. INTERFERE DOWNSIDE STG TO BE REMOVED IN MIL-D-70327 & ASH 153. CORRELATED DATUM INDICATED BY "X".
3. SURFACE FINISH TO BE "R" UNLESS OTHERWISE NOTED.
4. REMOVE
5. PENETRANT INSPECT PER MIL-I-6866 TYPE I OR II & AGC-STD-416 TYPE I OR II. MIL-I-6866 TAKES ACCEPTANCE & AGC-STD-416.
6. CRITERIA PER AGC-STD-4005 CL III & AGC-STD-4006 CL III.
7. REMOVE
8. REMOVE
9. CLEAN PER AGC-46350 LEVEL H.
10. REMOVE
11. REMOVE
12. REMOVE
13. REMOVE
14. REMOVE
15. REMOVE
16. REMOVE
17. REMOVE
18. REMOVE
19. REMOVE
20. REMOVE
21. REMOVE
22. REMOVE
23. REMOVE
24. REMOVE
25. REMOVE
26. REMOVE
27. REMOVE
28. REMOVE
29. REMOVE
30. REMOVE
31. REMOVE
32. REMOVE
33. REMOVE
34. REMOVE
35. REMOVE
36. REMOVE
37. REMOVE
38. REMOVE
39. REMOVE
40. REMOVE
41. REMOVE
42. REMOVE
43. REMOVE
44. REMOVE
45. REMOVE
46. REMOVE
47. REMOVE
48. REMOVE
49. REMOVE
50. REMOVE
51. REMOVE
52. REMOVE
53. REMOVE
54. REMOVE
55. REMOVE
56. REMOVE
57. REMOVE
58. REMOVE
59. REMOVE
60. REMOVE
61. REMOVE
62. REMOVE
63. REMOVE
64. REMOVE
65. REMOVE
66. REMOVE
67. REMOVE
68. REMOVE
69. REMOVE
70. REMOVE
71. REMOVE
72. REMOVE
73. REMOVE
74. REMOVE
75. REMOVE
76. REMOVE
77. REMOVE
78. REMOVE
79. REMOVE
80. REMOVE
81. REMOVE
82. REMOVE
83. REMOVE
84. REMOVE
85. REMOVE
86. REMOVE
87. REMOVE
88. REMOVE
89. REMOVE
90. REMOVE
91. REMOVE
92. REMOVE
93. REMOVE
94. REMOVE
95. REMOVE
96. REMOVE
97. REMOVE
98. REMOVE
99. REMOVE
100. REMOVE

Figure 16

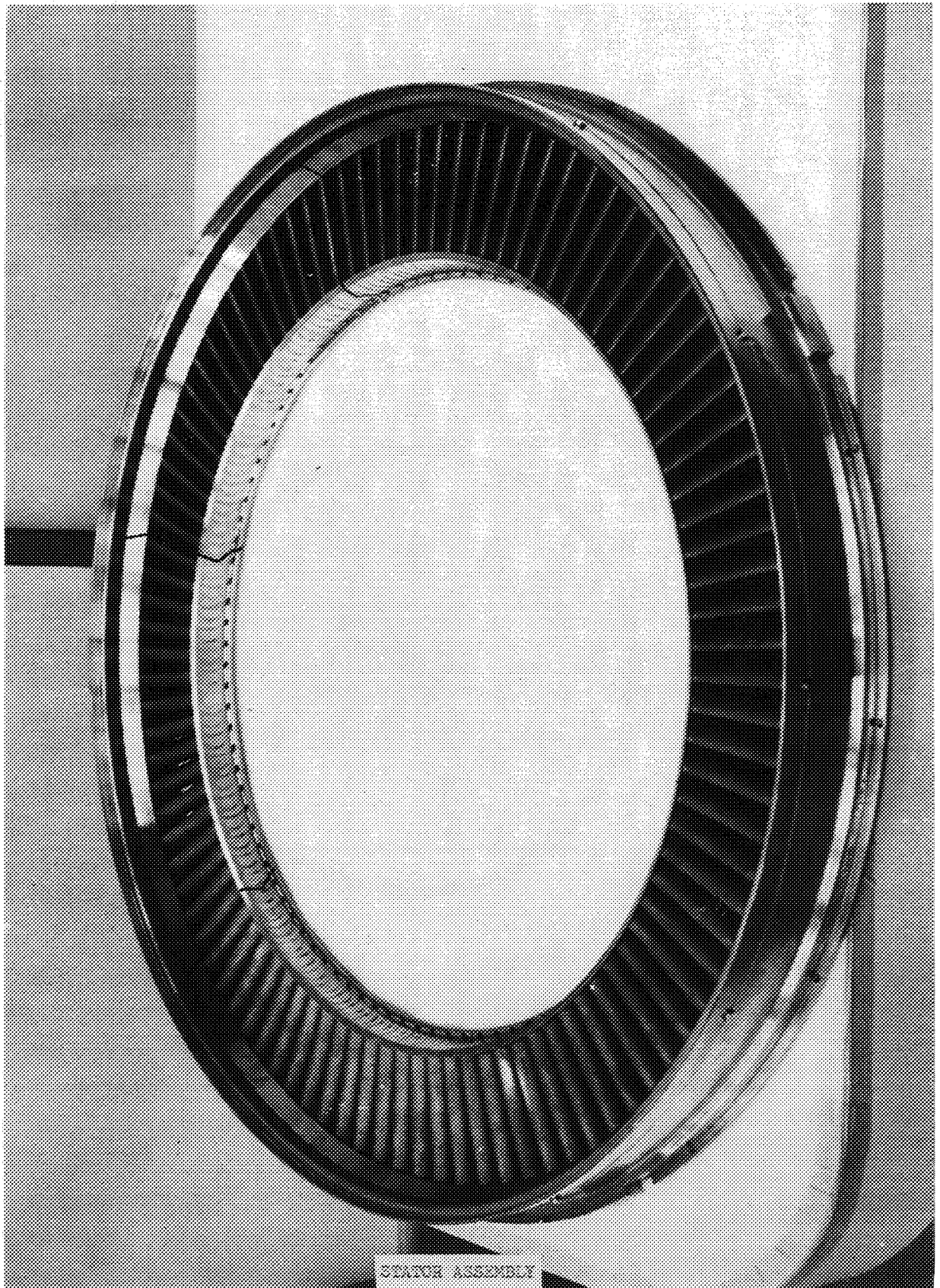


Figure 17

aerodynamic flow requirement is satisfied by the respective stagger angle and blade length, shown pictorially in Figures No. 3 and No. 4. Ninety-seven vanes are used in the stator. The vane attachment to the inner and outer shroud is by electron-beam welding. Fabrication details are discussed in a separate report⁽⁸⁾. Figure No. 19 shows the weldment of vanes and shrouds, cut into six segments.

c. Support Ring and Assembly

The six stator segments are assembled in a support ring and retained by connecting pins as shown in Figure No. 18. The support ring forms the interface with the turbine inlet housing and exhaust manifold. An annular tongue and groove joint allows for relative axial movement between the reversing row assembly and the turbine inlet manifold. This is illustrated in Figure No. 20, which also shows a set screw adjustment for axial positioning of the reversing row relative to the rotor during assembly. Retention of the reversing row assembly is secured by the annular welded casing joint connecting the inlet manifold to the exhaust manifold. The support ring is tangentially restrained by four anti-rotation lugs.

d. Stress Analysis Summary

A detailed stress analysis was made⁽⁹⁾ indicating positive margins of safety.

4. Inlet Manifold and Support Structure

a. General Design Philosophy

A primary influence in the configuration of the inlet manifold is the turbopump minimum weight requirement because the inlet manifold is of large proportions. Large parts are generally considered good candidates for applying weight reduction practices effectively. It was believed that a manifold, while basically a pressure vessel, can conceivably also have the necessary structural characteristics to carry externally applied loads in addition to internal pressure forces. The practical application of this concept resulted in combining the turbine inlet manifold, the pump backplate, and the turbine support structure into a unitized component. In this design, a single separator wall replaces the otherwise adjacent closure walls of the manifold and the backplate. For maximum strength to weight ratio, a sphere was selected as the basic geometry of the unitized component, with deviations as dictated by interface matching.

The concept of unitized component design not only has weight saving advantages, but also eliminates interfaces and thereby, external static seal problems. The casing joint forming the connection between the inlet manifold and the exhaust manifold is made by means of an assembly weld. This

⁽⁸⁾ Beer, R., Aerojet-General Report No. 8800-49, op. cit.

⁽⁹⁾ Mod II OTPA Stator (Reversing), Aerojet-General Report No. SA-OTPA-245, 10 December 1965

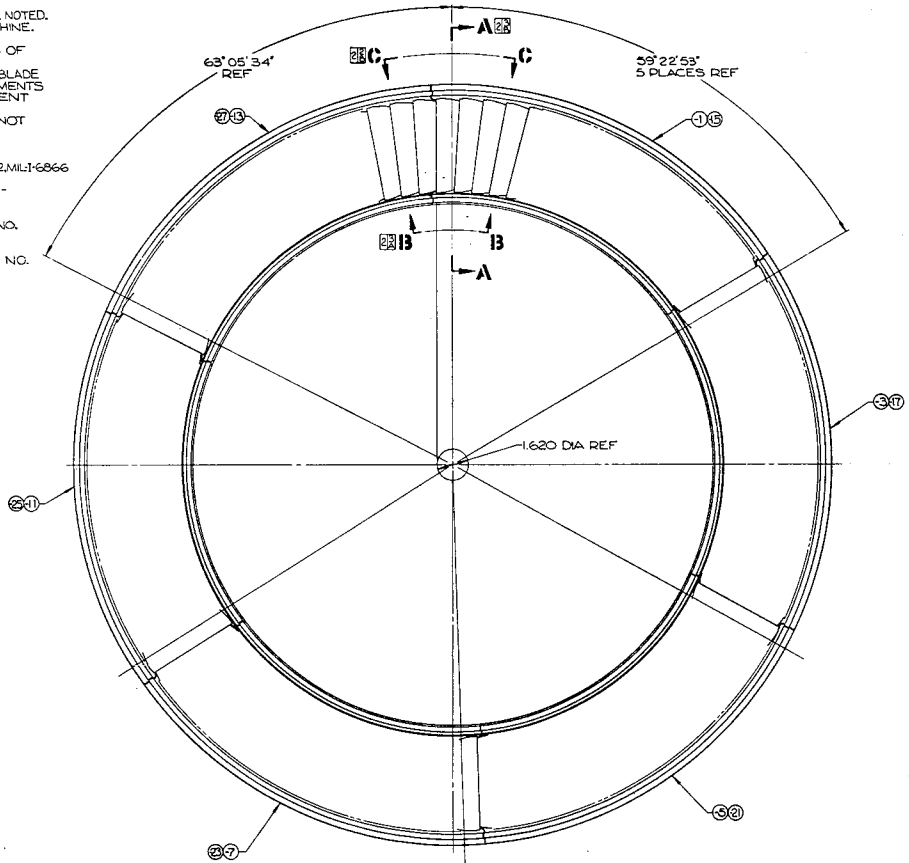
4 3 2 1

REV	DESCRIPTION	DATE	BY	CHKD
A	SEE INCORP ADCN	1/24/54	J. J. JONES	
B	SEE DCN	5/14/54	J. J. JONES	

REMOVE ALL BURRS & SHARP EDGES
 EQUIV TO .003/0.5 R.
 INTERPRET DWG PER STD PRESCRIBED
 IN MIL-D-70327 CORRELATED DATUM INDICATED BY: X
 CLASSIFICATION OF CHARACTERISTICS
 PER MIL-W-9411, DENOTED BY (C) CRITICAL,
 (M) MAJOR AND (N) SYMBOL MINOR.
 SURFACE ROUGHNES TO BE 125.
 ALL DIA TO BE (A.001) UNLESS OTHERWISE NOTED.
 AGE PER AGC-46604 BEFORE FINAL MACHINE.
 ESTABLISH DATUM-B FROM THE MEAN
 AXIAL LOCATION OF THE TRAILING EDGES OF
 THE 97 BLADES.
 MACHINED RING TO BE CUT PARALLEL TO BLADE
 TRAILING EDGE INTO 6 SEGMENTS, (5 SEGMENTS
 CONTAINING 16 BLADES EACH AND 1 SEGMENT
 CONTAINING 17 BLADES)
 MATCHED SET - INDIVIDUAL PIECES ARE NOT
 INTERCHANGEABLE - MAINTAIN AS SET

1. PENETRANT INSPECT PER MIL-I-6866
 TYPE I, AND AGC-STD-4816 TYPE I, CLASS 2, MIL-I-6866
 TAKES PRECEDENCE, ACCEPTANCE
 CRITERIA PER AGC-STD-4005 & AGC-STD-
 4006, CLASS III

1. CLEAN PER AGC-46350, LEVEL H.
 2. PRESERVE & PACKAGE PER MSFC DWG NO.
 10419900, FUSELAGE COMPONENTS.
 3. MARK CONTAINED PER ASD5215N WITH
 PART NO. 286556, APPLICABLE DASH NO.
 & AGC ASSIGNED SERIAL NO.

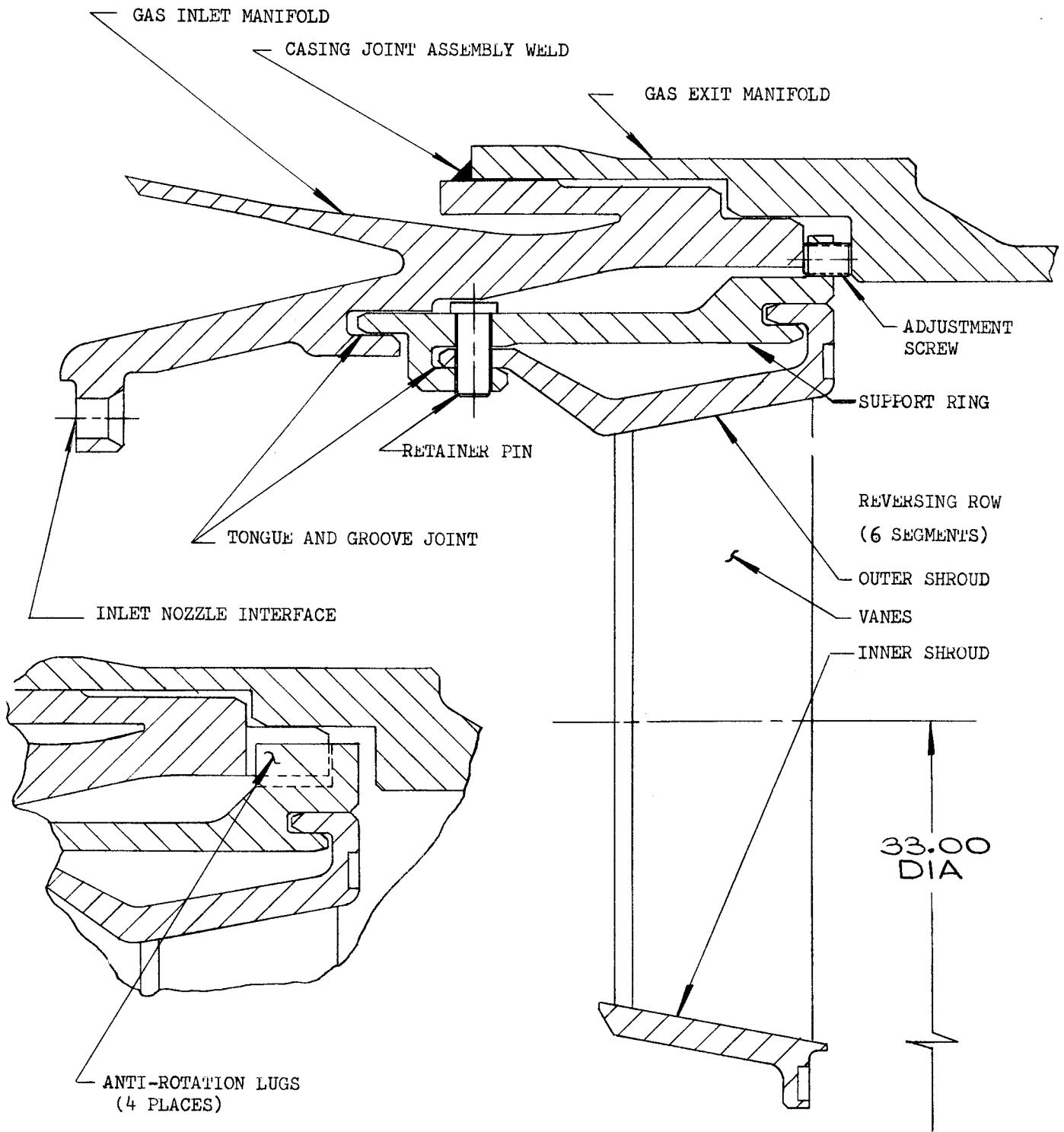


1	-27	MAKE FROM 286555-9	1	1
1	-25		1	1
1	-23		1	1
1	-21		1	1
1	-17		1	1
1	-15		1	1
1	-13	MAKE FROM 286555-9	1	1
1	-11		1	1
1	-7		1	1
1	-5		1	1
1	-3		1	1
1	-1	MAKE FROM 286555-9	1	1

UNLESS OTHERWISE SPECIFIED		MATERIAL SPECIFICATION	
FINISH	AS SHOWN	STAINLESS STEEL	304
SCALE	AS SHOWN	QUANTITY	1
DATE	1/24/54	DESIGNED BY	J. J. JONES
APPROVED BY		CHECKED BY	
PART NO. 286556		VANE, STATOR-TURBINE, OXIDIZER	
REV. 05824		286556	

Figure 19, Sheet 1 of 2

4 3 2 1



Stator and Casing Joint

Figure 20

eliminates both the thermal stress problems of a heavy bolted flange and a mechanical seal at this location. Dual Conoseals are used on the gas inlet flange connections and the pump housing and power transmission housing interfaces.

It is recognized that the benefits to be obtained by the unitized component concept require solutions of unusual fabrication engineering and insulation problems. Furthermore, the success of this solution is subject to considerable detail design work and analytical considerations, in particular heat transfer studies and stress analysis, to be followed by development experimentation and testing.

b. Composite Weldment

The turbine inlet manifold, the pump backplate, and the turbine support structure are fabricated as a unitized, composite weldment. It is a light-weight structure, consisting of Inconel 718 forgings and formed plate and tubing materials, joined by the gas tungsten arc welding method. The turbine inlet nozzle is attached to this weldment by bolting and completes the geometry of the gas inlet torus. The interface with the 11-1/2-in. diameter turbine-gas supply lines is accomplished by means of two connecting flanges. An annular groove forms the means for joining the reversing row assembly. Provision for the final casing joint, which connects the exhaust manifold to the turbopump, is accomplished by means of a weld flange designed for assembly welding. The weld carries the structural load and serves as the gas seal.

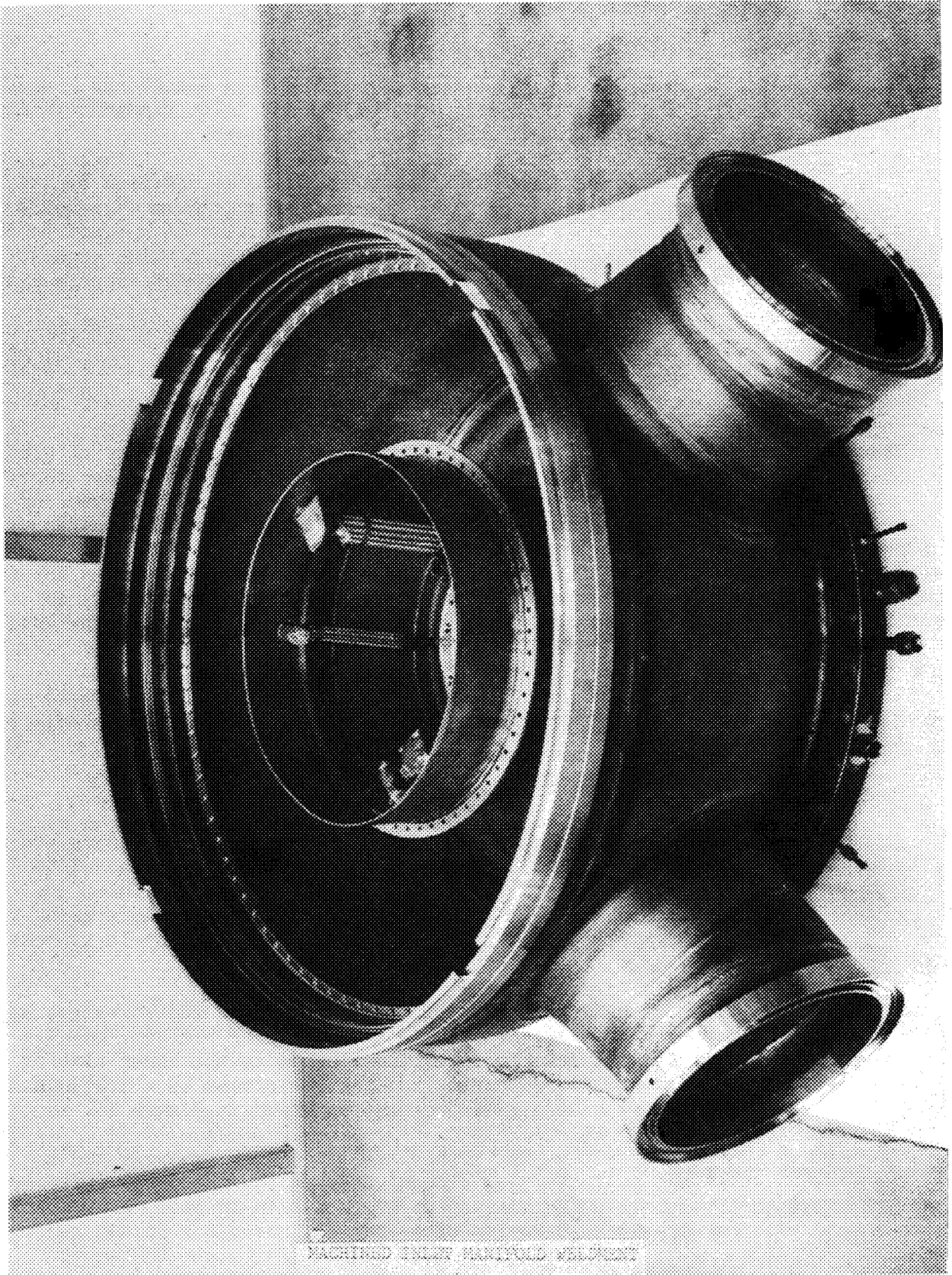
The mechanical design of this component is illustrated in Figures No. 6 and No. 21. The fabrication technology is detailed in Appendix D of this report.

c. Insulation

The unitized component is subjected to a large temperature difference existing between the turbine inlet manifold and the pump backplate structure at the points of abutment. This results from the turbine inlet gas temperature being approximately 1050°F and the adjoining pump backplate being at -297°F liquid oxygen temperature. The resulting thermal gradient is extremely steep and consequently, large thermal stresses are caused.

To lessen the degree of thermal gradient and stresses, an insulation was incorporated into the design. A ceramic fiber blanket, manufactured by Johns-Manville, was selected. It is attached to the inner side of the turbine inlet manifold and is protected from the gas stream by a 0.063-in. thick Hastelloy-C liner. The assembly arrangement is shown in Figure No. 6.

The effectiveness of the insulation was analyzed and the heat transfer calculations indicate that without insulation, the outer periphery of the manifold torus assumes a temperature of 900°F within 10 sec. When insulated, the same wall will be at -230°F at 20 sec of operation, and 650°F at 400 sec,



MACHINED THREE MANIFOLD FLANGES

Figure 21

approximately the length of a full duration run. From this and the corresponding stress levels, it was concluded that for long durations, the insulation is essential, but for short tests of 10 sec or less, the turbopump could be operated without this insulation. Details of the heat transfer study are presented in Appendix B.

d. Stress Analysis Summary

A detailed stress analysis is presented in Appendix C. It substantiates the structural integrity of this design.

5. Exhaust Manifold

a. General Design Philosophy

The purposes of the exhaust manifold are to collect the rotor exit flow and provide the turbine interface to the gas exit lines. This is to be accomplished with a minimum weight configuration. A hemispherical shape (20.25-in. radius) was selected as the basic geometry. Two 15-in. diameter gas exit flanges are spaced 180 degrees apart to meet the engine line connections. A 11.10-in. inside diameter flange, oriented axially, permits shaft access during development for such requirements as torque check, while providing for a 500 horsepower auxiliary power take-off from the turbopump shaft for possible engine application. The mechanical configuration of the exhaust manifold and its assembly relationship to the turbopump is shown in Figure No. 6.

b. Weldment

The exhaust manifold is weld fabricated, using Inconel 718 material throughout. The nominal wall thickness of the hemisphere is 0.250-in. Details of this weldment are illustrated in Figure No. 22. The part as shown does not include a turbine exit flow straightener; however, such a device is anticipated to be needed in the final design to minimize the exit losses of the gas leaving the rotor.

c. Casing Joint

The connection between the inlet manifold and exhaust manifold forms the casing joint of the turbine. This interface consists of a cylindrical pilot and of weld flanges that are joined at assembly by an annular fillet weld. This weld carries the structural load, serves as a static seal, and serves as a retainer for the reversing vane assembly, which is axially positioned by adjustment screws. Figures No. 6 and No. 20 show the details of this connection.

d. Stress Analysis Summary

A detailed stress analysis was made.⁽¹⁰⁾ This analysis substantiates the structural integrity of the design.

(10) Mod II OTPA Weld Joint - Turbine Manifold - Exhaust Housing, Aerojet-General Report No. SA-OTPA-240, 14 July 1965

IV. CONCLUSIONS

From the technical discussion, it is evident that the requirement for minimizing weight was practiced with rigid discipline in the mechanical design of the turbine components. The primary criterion, flight weight design, was achieved by venturing into concepts and configurations of unusual complication and that are not customary in turbine design practice. Consequently, the design has a high risk factor and the need for considerable test development improvements must be anticipated before operational reliability can be assured. Unfortunately, for reasons of the directed early program termination, there was no opportunity for development and hardware improvement. Nevertheless, the ability to cope with unusual requirements was demonstrated and design as well as analysis experience was gained. The design highlights, categorized by individual components, are:

A. ROTOR ASSEMBLY

The outstanding feature is the blade design and the blade attachment by means of electron-beam welding. It is believed to be the first of the Electron-Beam Welding Process for turbine rotors made from Inconel 718 material. The conical turbine disc concept represents an interesting and promising departure from the more conventional turbine disc profiles.

B. INLET NOZZLE

Nozzle blading design and fabrication technology using the electron beam welding techniques and Inconel 718 material are the significant features. The whole nozzle block is weld-fabricated. The possible shortcomings of a rigidly-welded nozzle block are recognized and action was taken for alternative back-up design solutions.

C. REVERSING ROW ASSEMBLY

The reversing row assembly features an excellent design solution for tangential, radial, and axial flexibility (floatability) to guard against thermal distortion during operation. This was accomplished by the use of tongue and groove joints as well as pin connections in the assembly of the stator parts, which principally consist of six segments and a support ring. The material is Inconel 718 and the electron-beam welding technology is utilized.

D. INLET MANIFOLD AND SUPPORT STRUCTURE

The design of this part is unusual because it combines the functions of the pump backplate, the turbine inlet manifold, and the turbine support structure although there is some sacrifice in development flexibility. The single weldment configuration is complicated and the part is highly-stressed because of large thermal gradients. Assurance of structural integrity hinges upon a complicated analytical model permitting plastic deformation and is subject to many variables. The disadvantages and the risks are well recognized. However, the concept was deemed worthy of pursuit because of the weight savings indicated.

IV. EXHAUST MANIFOLD

E. EXHAUST MANIFOLD

A significant feature is the design of the casing joint, which connects the exhaust manifold to the inlet manifold and also serves as a retainer for the reversing vane stator. The part is weld-fabricated from Inconel 718 material. It is recognized that the design requires the addition of a vane system to minimize gas exit losses.

BIBLIOGRAPHY

1. Beer, R., Aerodynamic Design and Estimated Performance of a Two-Stage Curtis Turbine For the Liquid Oxygen Turbopump of the M-1 Engine, NASA CR 54764, 19 November 1965
2. Beer, R., Fabrication Technology of Lightweight Turbine Components using the Electron-Beam Welding Process to Fabricate Sheet Metal Blades and Join the Blades to Disc or Support Structure. Aerojet-General Report No. 8800-49, 1 April 1966
3. Chinn, T. and Severud, L. K., Analytical and Experimental Vibration Analysis of the Turbine Buckets for the M-1 Liquid Oxygen Turbopump, NASA CR 54830, 30 June 1966
4. Inouye, F. T., Hunt, V., Jansen, G. R., and Frick, V., Summary of Experience using Inconel 718 on the M-1 Engine, Aerojet-General Report No. 8800-37, 30 December 1965
5. Salisbury, J. K., Power Volume, Kent's Mechanical Engineers' Handbook, John Wiley & Sons, Inc., N.Y.
6. Mod II OTPA Weld Joint-Turbine Manifold-Exhaust Housing, Aerojet-General Report No. SA-OTPA-240, 14 July 1965
7. Mod II Turbine Rotor, Aerojet-General Report No. SA-OTPA-242, 8 November 1965
8. Mod II Nozzle, Aerojet-General Report No. SA-OTPA-243, 1 December 1965
9. Mod II OTPA Stator (Reversing), Aerojet-General Report No. SA-OTPA-245, 10 December 1965

APPENDICES

APPENDIX A

STRUCTURAL DESIGN CRITERIA

TABLE OF CONTENTS

	<u>Page</u>
I. General	A-2
II. Definition of Pressure Terms	A-2
III. Definition of Inertia, Thrust, and Line Loads	A-2
IV. Shock and/or Dynamic Load Criteria	A-2
V. Temperature Design Criteria	A-2
VI. Definition of Stress Categories	A-3
A. Primary Stress	A-3
B. Secondary Stress	A-3
C. Peak Stress	A-3
VII. Cyclic Loading and Fatigue Analysis	A-3
VIII. Margin of Safety	A-5
A. Margin of Safety Based Upon Yield	A-5
B. Margin of Safety Based Upon Ultimate	A-5
C. Compound or Combined Stress	A-5
IX. Deformation Criteria	A-7
X. Additional Criteria for Rotating Discs	A-7
XI. Additional Criteria for Pump Impeller Vanes and Turbine Buckets	A-7

APPENDIX A

STRUCTURAL DESIGN CRITERIA

Compiled by F. D. Ronkovich and L. K. Severud

I. GENERAL

All components shall be capable of withstanding limit and proof loads without undergoing excessive permanent deformation and without deflections which will adversely affect the performance characteristics of the turbopump assembly. All components shall be capable of 21 re-uses and a total operating duration of 10,500 sec. Adequate structural integrity and high reliability is to be a primary design objective.

The ability of all components to meet the strength and deformation requirements shall be substantiated analytically. Experimental substantiation of structural integrity shall be performed in cases for which the reliability of the stress analysis is questionable.

II. DEFINITION OF PRESSURE TERMS

M.E.O.P.---The maximum expected operating pressure

Proof-----1.2 M.E.O.P.---design to yield

Burst-----1.6 M.E.O.P.---design to ultimate

III. DEFINITION OF INERTIA, THRUST, AND LINE LOADS

Limit Load---The critical load or combination of loads and environment, the occurrence of which is expected at least once during the life of the component

Design to yield---1.0 x limit load

Design to ultimate---1.5 x limit load

IV. SHOCK AND/OR DYNAMIC LOAD CRITERIA

Equivalent static loads derived from dynamic analyses are to be used and these equivalent static loads are subjected to the same factors as given in Section III of this Appendix.

V. TEMPERATURE DESIGN CRITERIA

Components will be designed for the critical operating conditions created by the combination of pressure and temperature gradients existing during turbopump assembly transient and steady-state operation. Metal temperature shall be based upon heat transfer analysis. Experimental data obtained from test programs for similar hardware shall be factored into the analysis whenever such data are available.

VI. DEFINITION OF STRESS CATEGORIES⁽¹⁾

A. PRIMARY STRESS

A stress developed by the imposed loading which is necessary to satisfy the laws of equilibrium between external and internal forces and moments. The basic characteristics of a primary stress is that it is not self-limiting. If a primary stress exceeds the yield strength of the material through the entire thickness, the prevention of failure is entirely dependent upon the strain-hardening properties of the material.

B. SECONDARY STRESS

A stress developed by the self-constraint of a structure. It must satisfy an imposed strain rather than being in equilibrium with an external load. The basic characteristic of a secondary stress is that it is self-limiting because minor distortions can satisfy the discontinuity conditions or thermal expansions which causes the stress to occur.

C. PEAK STRESS

The highest localized stress in the region under consideration. The basic characteristic of a peak stress is that it does not cause any significant distortion and is objectionable mostly as a possible source of fatigue failure. Examples of peak stress are:

1. The thermal stress in the wall of a vessel caused by a rapid change in temperature or a large temperature gradient.
2. The stress at a local structural discontinuity.

VII. CYCLIC LOADING AND FATIGUE ANALYSIS

All components shall be capable of withstanding cyclic loading associated with 21 turbopump assembly re-uses and 10500 sec operation.

Consideration of a stress which fluctuates about a non-zero value shall be accomplished by use of a modified Goodman diagram. The mean value of the stress used shall be an adjusted value, defined as follows⁽²⁾

Let S'_{mean} = Basic value of mean stress (calculated directly from loading cycle) including stress concentration effects.

S_{mean} = Adjusted value of mean stress

(1) Criteria of Section III of the ASME Boiler and Pressure Vessel Code for Nuclear Vessels, ASME Publication, 1964

(2) *ibid.*

VII, Chapter B, Part 1; Stress Analysis (cont.)

S_{alt} = Amplitude (half range) of stress fluctuation including stress concentration effects

S_y = Yield strength

If $S_{alt} + S'_{mean} \leq S_y$, $S_{mean} = S'_{mean}$

If $S_{alt} + S'_{mean} > S_y$ and $S_{alt} < S_y$, $S_{mean} = S_y - S_{alt}$

If $S_{alt} \geq S_y$, $S_{mean} = 0$

For determination of the allowable number of cycles, an equivalent alternating stress component, S_{eq} , is used in entering the fatigue S-N curve. This value is defined as

$$S_{eq} = \frac{S_{alt}}{1 - \frac{S_{mean}}{S_u}}$$

where S_u = The smaller of the tensile strength or the 50 hr. stress rupture strength.

When a complete S-N curve is not available, the relationship between S and N can be taken as follows (3) (4):

$$S = \frac{E}{4 \sqrt{N}} \ln \frac{100}{100 - RA} + S_e$$

where E = Elastic modulus (psi)

RA = Percent reduction of area in tensile test

S_e = Endurance limit (psi) for 10^8 cycles

S = Strain amplitude times Young's Modulus

Low cycles fatigue (4) (5) (6) which occurs in less than 10^4 cycles, caused by large plastic strain fluctuations characteristic of thermal stress fatigue may be evaluated using the above formula where

S_e = Yield strength, 0.2% offset

S = Strain amplitude x Young's Modulus

(3) ibid.

(4) Langer, B. F., Design of Pressure Vessels for Low-Cycle Fatigue, ASME Trans. Journ. of Basic Engineering, September 1962, pp. 389 - 402

(5) Coffin, L. F. Thermal Stress Fatigue, Product Engineering, June 1957, pp. 175 - 179.

(6) Manson, S. S., Thermal Stresses in Design, Part 3 - Basic Concepts of Fatigue in Ductile Materials, Machine Design, August 7, 1958, pp. 100 - 107.

The calculation of S is based upon the assumption of elastic behavior. However, if instability such as plastic hinges or other forms of non-linearity exist, plastic analysis is required to obtain the strain amplitude.

When a component is subjected to a variety of stress cycles during its lifetime, failure will be taken as when the cumulative usage factor, which is the sum

$$\frac{\eta_1}{N_1} + \frac{\eta_2}{N_2} + \frac{\eta_3}{N_3} + \dots \text{ is equal to } 1.0$$

N_1 = Cycles to cause failure at stress level S_1

η_1 = Cycles of stress level S_1 applied

VIII. MARGIN OF SAFETY

The margin of safety is equal to $\frac{\text{allowable stress}}{\text{calculated stress}} - 1$

For Primary, Secondary, and Peak Stress Levels in Brittle Materials (elongation $\leq 5\%$), and Primary Stress Levels in Ductile Materials (elongation $> 5\%$):

A. MARGIN OF SAFETY BASED UPON YIELD

Allowable stress is minimum yield tensile, compressive or shear stress; yield bending modulus or yield torsional modulus at operating temperature. For welded joints, use 85% of tensile and shear values unless test data justifies otherwise. Calculated stress is derived from proof pressure or design yield load.

B. MARGIN OF SAFETY BASED UPON ULTIMATE

Allowable stress is minimum ultimate tensile, compressive or shear stress, ultimate bending modulus, ultimate torsional modulus, endurance limit, 10 hour stress rupture or critical column stress at operating temperature. For welded joints, use 85% of tensile and shear values unless test data justifies otherwise. Calculated stress is stress derived from burst pressure or design ultimate load.

C. COMPOUND OR COMBINED STRESS

When compound stresses and, in some cases, combined stresses are present, stress ratios may be used in the calculation of margin of safety. For particulars, see MIL-HDBK-5.

For Combined Primary, Secondary and Peak Stress Levels in Ductile Material:

The margin of safety is based upon fatigue life, and is the minimum of

$$M.S. = \frac{E.S.}{1.4 S_{eq}} - 1$$

$$M.S. = \frac{N}{2n} - 1$$

where E.S. = Endurance Strength for N cycles

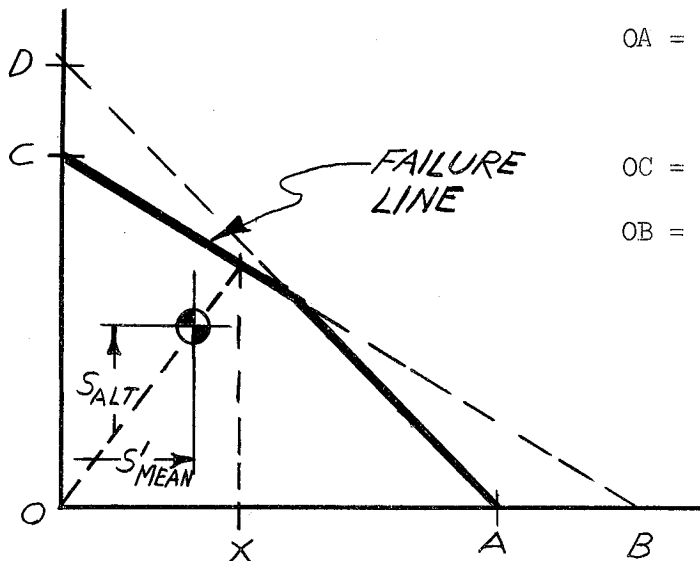
S_{eq} = Alternating Stress Amplitude

N = Cycles of Life for S_{eq}

n = Cycles of S_{eq} Applied

Fluctuating Primary Stress Levels in Ductile Materials:

The margin of safety is determined as follows (7)(8)(9)(10):



OA = OD = yield strength, 0.2% offset, or 10 hr stress rupture strength

OC = Endurance strength for N cycles

OB = Tensile ultimate

For definition of S_{alt} and S'_{mean} , see VII.

The margin of safety is:

$$M.S. = \frac{Ox}{1.25 S'_{Mean}} - 1$$

- (7) Section III, ASME Boiler and Pressure Vessel Code, op. cit.
 (8) Grover, H. J., Gordon, S. A., and Jackson, L. R., The Fatigue of Metals and Structures, Battelle Memorial Institute, Prepared for Bureau of Navy Weapons, Dept. of the Navy, 1954, Revised June 1960, NAVVEPS 00-25-534, pp 127 - 130
 (9) Benham, P. P. and Hoyle, R., Thermal Stress, London, Sir Isaac Pitman & Sons Ltd., 1964, pp 285 - 293
 (10) Horger, O. J., Editor, Metals Engineering Design, ASME Handbook, Second Edition, New York, McGraw-Hill, 1965, Sec. 7.2, pp 192 - 198.

When stress-range curves determined experimentally are available, they may be used in place of the failure lines constructed per the above technique.

IX. DEFORMATION CRITERIA

All deformation which could adversely affect the performance characteristics of a component (i.e. turbine wheel tip growth, etc.) are to be evaluated with particular attention given to creep. Acceptability of deformation magnitudes will be based upon the effects such as performance and clearances.

X. ADDITIONAL CRITERIA FOR ROTATING DISCS

Burst speeds are to be 1.4 times greater than the nominal operating speed. The average tangential stress of the disc, which is a measure of burst speed margin, shall not exceed 50% of the average ultimate material tensile strength.

XI. ADDITIONAL CRITERIA FOR PUMP IMPELLER VANES AND TURBINE BUCKETS

Operating vane and bucket natural frequencies in the range of possible stimuli (i.e. nozzle passing excitation, low order rotational speed excitation, etc.) shall be determined and evaluated for potential fatigue failure. The margin of safety against fatigue failure shall be determined as set forth in Section IX considering the following:

$$\begin{array}{l} \text{Alternating} \\ \text{Stress} \\ \text{Amplitude} \end{array} = .3 \text{ (Fluid Bending) (Dynamic Magnification)}$$

where, Fluid bending stress includes a stress concentration factor appropriate to the article geometry, and

Dynamic magnification includes effects of closeness to resonance, receptiveness of vibration mode to excitation, and damping if appropriate.

Mean Stress = Maximum combined stress level caused by centrifugal loading at shaft design speed, fluid bending loading, and the steady-state thermal stresses.

APPENDIX B

TEMPERATURE ANALYSIS

MOD II OXIDIZER TURBINE

INLET MANIFOLD - BACKPLATE ASSEMBLY

TABLE OF CONTENTS

	<u>Page</u>
I. Summary and Introduction	B-3
II. Discussion	B-3
A. Description of Configuration	B-3
B. Selection of Insulation	B-3
C. Thermal Conductivity	B-4
D. Heat Transfer Analysis for Insulated Configuration	B-5
E. Heat Transfer Analysis for the Configuration without Insulation	B-7
F. Heat Transfer Analysis of Main Joint and Nozzle Shroud	B-7

LIST OF FIGURES

<u>No.</u>	<u>Title</u>	
B-1	Backplate - Inlet Manifold	B-8
B-2	Mod II Turbine Manifold, Conductivity of Insulation	B-9
B-3	Oxidizer Turbine Mod II Inlet Manifold Wall Temperature vs. Time	B-10
B-4	Mod II OTPA Turbine Manifold - Backplate Assembly, Outer Joint	B-11
B-5	Oxidizer Turbine Mod II Inlet Manifold Outer Corner Temperature vs. Time	B-12
B-6	Mod II OTPA Turbine Inlet Manifold, Inner Joint Backplate - Manifold	B-13
B-7	Oxidizer Turbine Mod II Inlet Manifold Inner Corner Temperature vs. Time	B-14
B-8	Oxidizer Turbine Mod II Inlet Manifold Outer Corner Temperature vs. Time	B-15
B-9	Mod II OTPA Turbine Inlet Manifold, Redesign of Outer Manifold-to-Backplate Joint	B-16
B-10	Oxidizer Turbine Mod II Inlet Manifold Outer Corner Redesign Temperature vs. Time	B-17

TABLE OF CONTENTS (CONT.)

<u>No.</u>	<u>Title</u>	<u>Page</u>
B-11	Mod II Oxidizer Turbine Inlet Manifold Heat Transfer	B-18
B-12	Mod II Oxidizer Turbine Inlet Manifold Heat Transfer without Insulation	B-19
B-13	Mod II Oxidizer Turbine Inlet Manifold Heat Transfer without Insulation	B-20
B-14	Mod II Oxidizer Turbine Inlet Manifold Heat Transfer without Insulation, 2 sec	B-21
B-15	Mod II Oxidizer Turbine Inlet Manifold Heat Transfer without Insulation, 4 sec	B-22
B-16	Mod II Oxidizer Turbine Inlet Manifold Heat Transfer without Insulation, 6 sec	B-23
B-17	Mod II Oxidizer Turbine Inlet Manifold Heat Transfer without Insulation, 8 sec	B-24
B-18	Mod II Oxidizer Turbine Inlet Manifold Heat Transfer without Insulation, 10 sec	B-25
B-19	Mod II Oxidizer Turbine Inlet Manifold Heat Transfer without Insulation, 14 sec	B-26
B-20	Mod II Oxidizer Turbine Inlet Manifold Heat Transfer without Insulation, 50 sec	B-27
B-21	Oxidizer Turbine Mod III Main Joint Thermal Analysis	B-28
B-22	Oxidizer Turbine Mod III Main Joint Thermal Analysis, Parts 1-5 and 26-28	B-29
B-23	Oxidizer Turbine Mod III Main Joint Thermal Analysis, Parts 5-13 and 22-24	B-30
B-24	Oxidizer Turbine Mod III Main Joint Thermal Analysis, Parts 14-21	B-31
B-25	Oxidizer Turbine Mod III Main Joint Thermal Analysis, Parts 29-33	B-32
B-26	Oxidizer Turbine Mod III Main Joint Thermal Analysis, Parts 34-39	B-33

APPENDIX B
Prepared by C. E. Klessig

I. SUMMARY AND INTRODUCTION

The inlet manifold-backplate assembly of the Model II oxidizer turbine is exposed to temperature extremes of -320°F to 1000°F . The pump discharge housing and the bearing housing are chilled-down before operation causing the backplate of the assembly to be chilled to -320°F . During operation of the turbine, hot gases of 1000°F pass through the inlet manifold causing it to heat up rapidly.

However, the backplate stays at approximately -320°F resulting in a large thermal gradient in the two short structural members joining the backplate and inlet manifold. To reduce this thermal gradient, the manifold was lined internally with an insulation.

Without insulation, the .100-in. thick spherical manifold wall will reach the gas temperature of 1000°F in 20 sec. Insulated with 1/2-in. Thermoflex insulation, this same wall will reach -230°F in 20 sec and 650°F in 400 sec, the length of a normal run. The insulation not only reduces the final temperature reached by the wall but greatly reduces the rate of temperature rise allowing adjacent areas time to warm up, thereby reducing thermal stresses.

II. DISCUSSION

A. DESCRIPTION OF CONFIGURATION

The backplate is a box-section with one wall common to both backplate and inlet manifold (see Figure B-1). The inlet manifold is internally insulated with a ceramic fiber blanket. A .063-in. thick sheet metal liner is placed over the insulation for retention and to protect the insulation from high velocity gas. In turn, the liner is held in place with a 1/4-in. pin and washer combination.

The areas of thermal interest are the two corners where the hot walls of the inlet manifold join the cold backplate.

B. SELECTION OF INSULATION

Many insulations were investigated. Min-K and Thermoflex were the best two choices. The others were eliminated because of:

1. High conductivity
2. Installation difficulties
3. Ablative - particles pass through turbine
4. Too heavy

5. Not reuseable - good for one run only
6. Not good for required temperature extremes

Min-K has a lower conductivity than Thermoflex under normal atmospheric conditions; however, in a hydrogen-water vapor atmosphere at 200 psia it loses its advantage as the conductivity of the gas controls. Because Min-K must be pre-formed before installation and tends to powder under vibration, Thermoflex was selected for insulating the manifold. Thermoflex is composed of a ceramic fiber matting and is opaque to radiation.

C. THERMAL CONDUCTIVITY

The effective conductivity of the H₂ and H₂O vapor mixture plus Thermoflex ranges from 1.15 to 1.55 BTU/hr Ft²°F/in. depending upon temperature as shown in Figure B-2. The other conductivities shown in Figure B-2 are: Min-K in air, Thermoflex in air, gaseous hydrogen, and H₂ and H₂O vapor.

The conductivity of the H₂ + H₂O vapor and Thermoflex was based upon an equation for porous material.(1)

$$K_a = K_s \frac{1 - b \left(1 - \frac{aK_p}{K_s} \right)}{1 + b(a-1)}$$

K_a - Apparent Conductivity

K_s - Conductivity of H₂ plus H₂O Vapor

K_p - Conductivity of Insulation

a - 3 K_s (2K_s + K_p)

b - Ratio of Insulation Volume to Total Volume

The above equations do not include

1. The conductive heat transfer provided by the insulation shield retaining pins.
2. Allowance for convective heat transfer caused by gas flow between the insulation and the manifold walls or within the insulation.

A thermal conductivity was calculated with pins and insulation in parallel heat flow.

(1) Jakob, M., Heat Transfer, Volume 1, 1949, pp 83 - 85

The result of 2.34 BTU/hr ft²°F/in. was rounded off to 2.7 BTU/hr ft²°F/in. to include convective effects in and about the insulation. All subsequent calculations are based upon an effective thermal conductivity of 2.7 BTU/hr ft²°F/in.

D. HEAT TRANSFER ANALYSES FOR INSULATED CONFIGURATION

To determine the effectiveness of the insulation, heat transfer analyses of the walls and the corners of the inlet manifold were made using the following three assumptions:

1. The insulation liner reaches 1000°F immediately.
2. The insulation has no heat capacity.
3. No heat loss from the uninsulated side of the walls.

A temperature versus time analysis for the three walls of the inlet manifold was made. The walls were considered infinitely long and wide so it may be analyzed as a one dimensional heat transfer. The walls were initially at -320°F. Charts were used to determine the temperature.⁽²⁾ The results of how the temperature varies with time are shown on Figure B-3. These temperatures were used for the end points of the manifold walls, such as M₆ and M₇ of Figure B-4, for the numerical analysis.

The corners were analyzed by numerical techniques. This procedure is to divide the area to be analyzed into sections as shown on Figure B-4. For each section, a heat balance is written.

Example - Figure B-4, Section M₁.

$$M_1 C_p \frac{dT_1}{dt} = \left(\frac{KA}{L}\right)_{2,1} (T_2 - T_1) + \left(\frac{KA}{L}\right)_{4,1} (T_4 - T_1) + (hA)_{g,1} (T_g - T_1) - \left(\frac{KA}{L}\right)_{1,o} (T_1 - T_o)$$

Rearrange

$$\Delta T_1 = \left[\left(\frac{KA}{L}\right)_{2,1} (T_2 - T_1) + \left(\frac{KA}{L}\right)_{4,1} (T_4 - T_1) + (hA)_{g,1} (T_g - T_1) - \left(\frac{KA}{L}\right)_{1,o} (T_1 - T_o) \right] \frac{\Delta t}{M_1 C_p}$$

T = Temperature °F

ΔT = Temperature Increment

Δt = Time Increment

(2) Heisler, M. P., Transactions of the ASME, April 1947, pp 227-236

K = Thermal Conductivity in BTU/SEC in² °F/in.

h = Heat Transfer Coefficient BTU/SEC in²°F

A = Area in²

L = Distance Between, inch

M = Weight Section, lb

C_p = Specific Heat BTU/lb

This same equation can be derived for each section. With the above equation, the change in temperature of a section can be determined for a small increment in time. Using initial temperature as a starting point, a temperature versus time history can be obtained by adding the temperature and time increment to the initial temperature and time, then repeat adding the temperature and time increments to the previous temperatures and times until the desired time is reached.

The inlet manifold outer joint was analyzed starting with an initial temperature of -320°F. The corner was sectioned as shown on Figure B-4. The results, see Figure B-5, show that the insulation greatly reduces the temperature in the corner and walls. Without insulation, the thin spherical wall (point M_7) reaches 1000°F in 20 sec. The insulation not only reduces the temperature but allows the adjacent areas to warm up reducing the thermal gradient.

The inlet manifold inner joint was sectioned as shown on Figure B-6. The corner was analyzed using an initial temperature of -320°F. It can be seen on Figure B-7 that the temperatures in this corner stay under 200°F up to 400 sec, the length of a normal run.

The outer joint was reanalyzed with different initial temperatures. The backplate and backplate closure were left at -320°F, the spherical shell was changed to 70°F and section M_4 has a linear gradient from 70°F to -320°F. It was believed that this was a more realistic initial condition. The thermal conductivity used was from Figure B-2 and the curve for $H_2 + H_2O$ and Thermoflex which is a deviation from the otherwise consistently used $K = 2.7$ Btu/hr ft² °F/in. This resulted in much lower temperatures as seen on Figure B-8. The change is mainly the result of the reduced thermal conductivity.

A configuration change (see Figure B-9) was made to the spherical shell where it joins the corner to ascertain if it would reduce the gradient in this area. The analysis was made under the same conditions as the first analysis for comparison purposes. Comparing Figure B-10 with Figure B-5, it can be seen that the temperature at points M_4 and M_5 have dropped some 200 degrees F. with the new configuration.

The above studies show that the thermal gradient must be taken into consideration when determining the stress in these parts. Should the stress get too high because of thermal stress, configuration changes such as the suggested redesign of the outer corner will help reduce the thermal gradient.

E. HEAT TRANSFER ANALYSIS FOR THE CONFIGURATION WITHOUT INSULATION

Initial Temperature

Backplate and Backplate Closure -320°F

Spherical Shell 70°F with a one-inch section having a linear gradient from 70°F to -320°F.

The analysis without insulation was made to ascertain if short run tests could be made without insulation. The results shown in Figures B-11 through B-20 indicate that even for runs of 10 sec, very steep thermal gradients are obtained.

F. HEAT TRANSFER ANALYSIS OF MAIN JOINT AND NOZZLE SHROUD

An analysis was made of this area to ascertain if any steep temperature gradients exist and how the expansion patterns would affect the stresses in the main joint weld. The analysis set-up is shown on Figure B-21 with the results shown on Figures B-22 through B-26. No steep temperature gradients were found in the main joint and the temperatures obtained did not cause any high stresses.

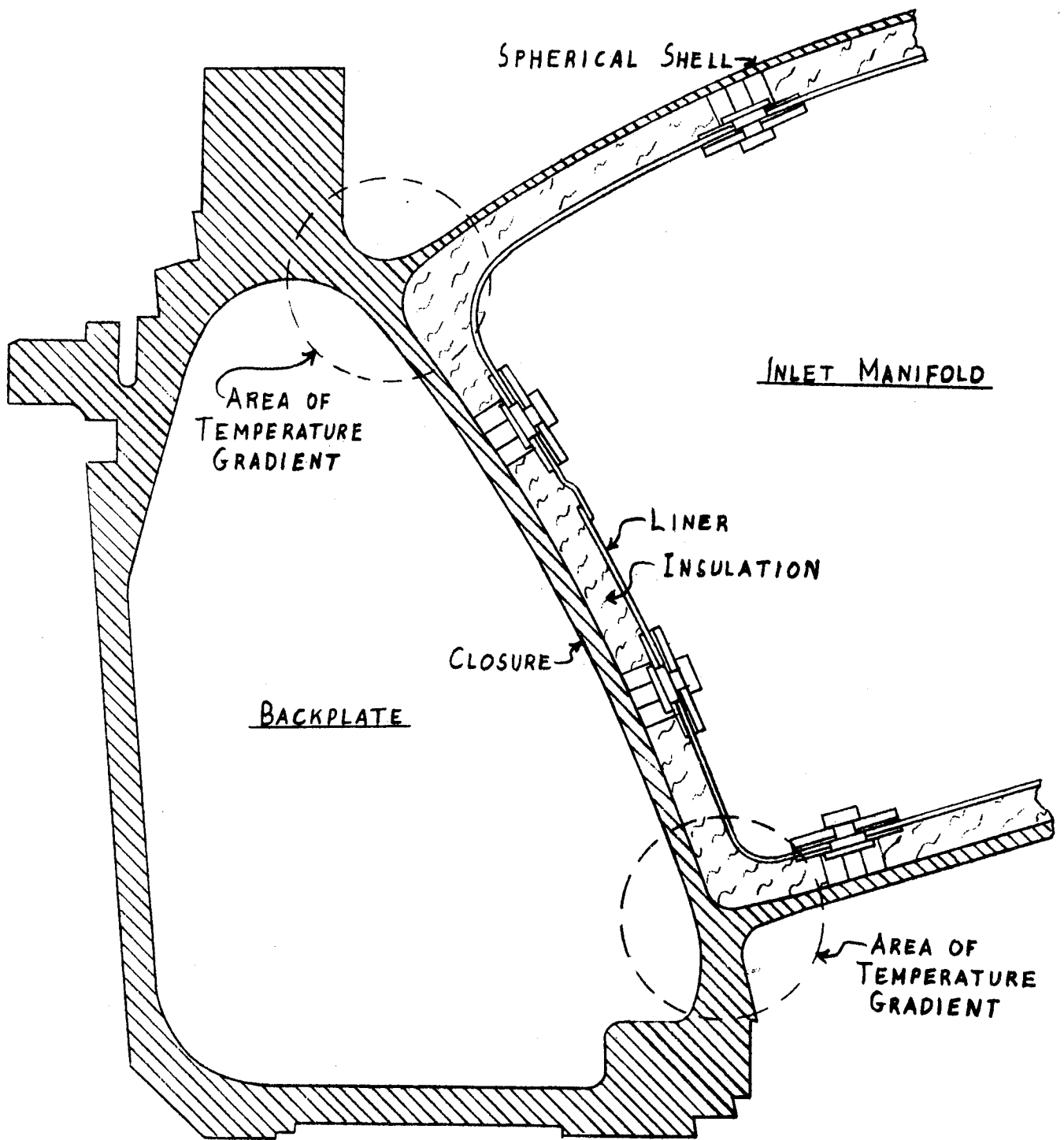
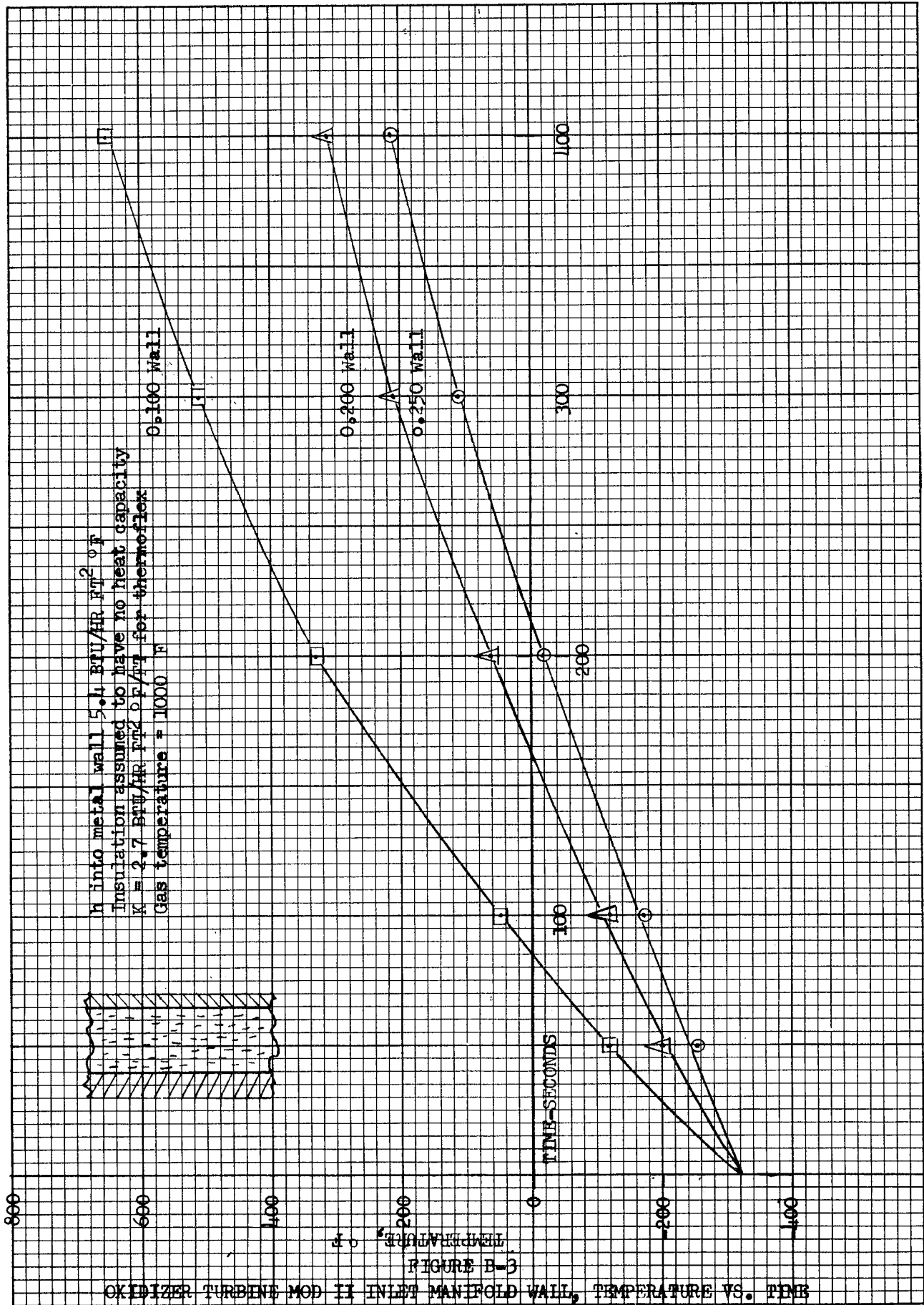


FIGURE B-1
 BACKPLATE - INLET MANIFOLD

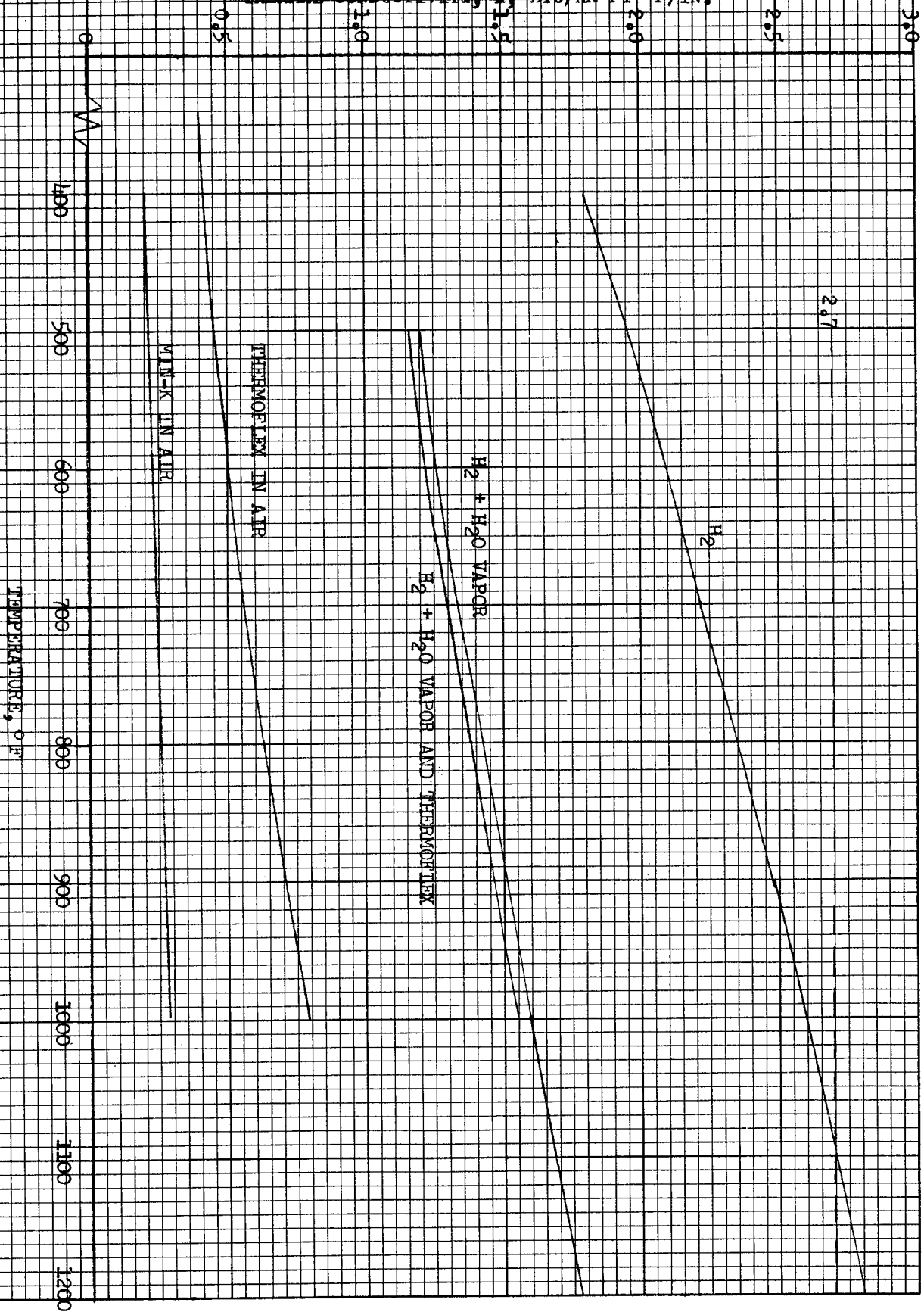


OXIDIZER TURBINE MOD II INLET MANIFOLD WALL, TEMPERATURE VS. TIME

MOD II FURNACE MANIFOLD, CONDUCTIVITY OF INSULATION

FIGURE B-2

THERMAL CONDUCTIVITY, k , BTU/HR FT²OR/IN.



2.7

H₂

H₂ + H₂O VAPOR

H₂ + H₂O VAPOR AND THERMOFLEX

THERMOFLEX IN AIR

MIN-K IN AIR

TEMPERATURE, °F

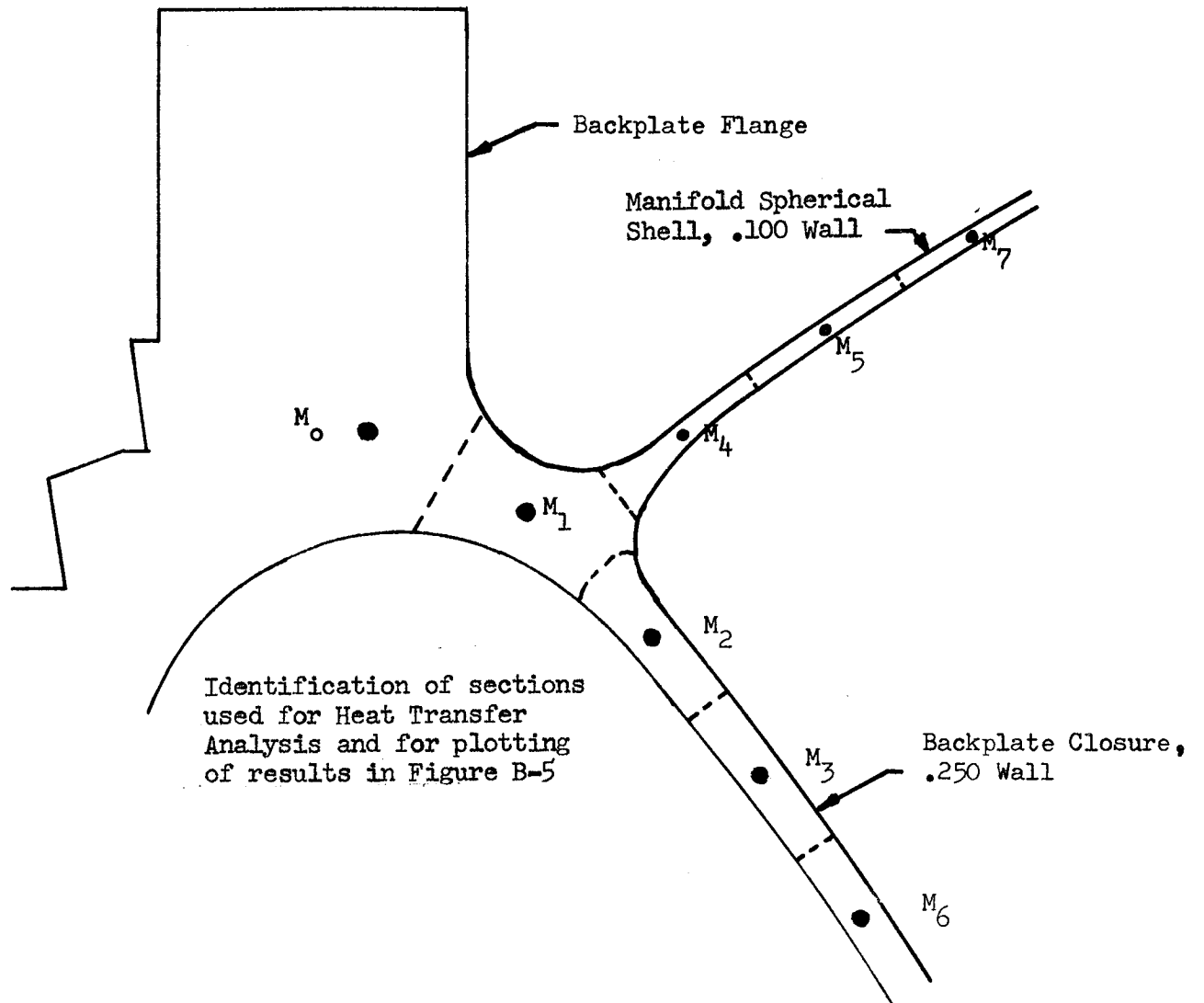


FIGURE B-4

MOD II OTPA TURBINE MANIFOLD-
BACKPLATE ASSEMBLY, OUTER JOINT

h into metal wall $5.4 \text{ BTU/HR FT}^2 \text{ } ^\circ\text{F}$
 Insulation assumed to have no heat capacity
 $K = 2.7 \text{ BTU/HR FT}^2 \text{ } ^\circ\text{F/IN.}$ for thermoflex
 Gas temperature = 1000°F

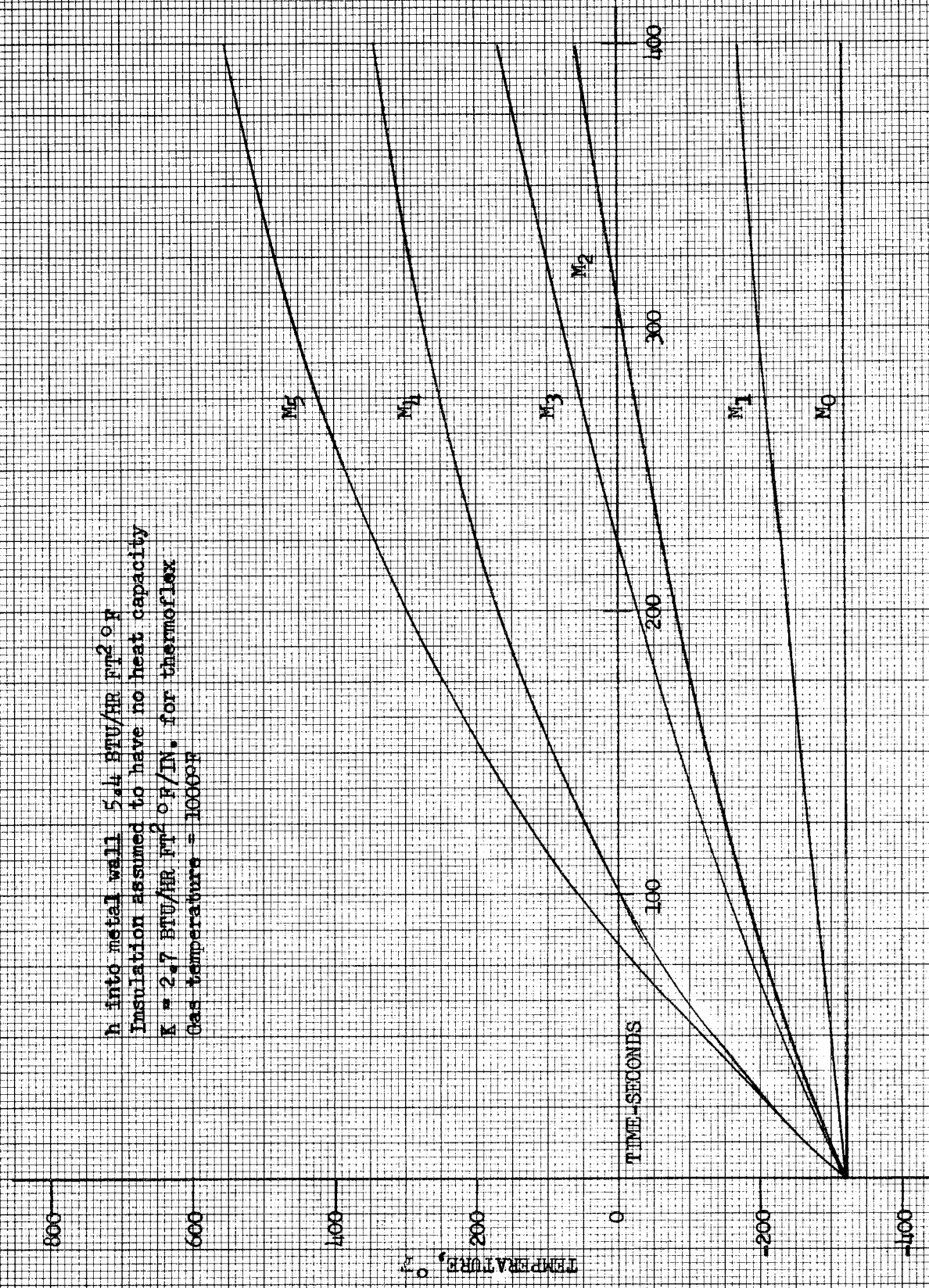


FIGURE B-5

OXIDIZER TURBINE MOD II INLET MANIFOLD OUTER CORNER
TEMPERATURE VS. TIME

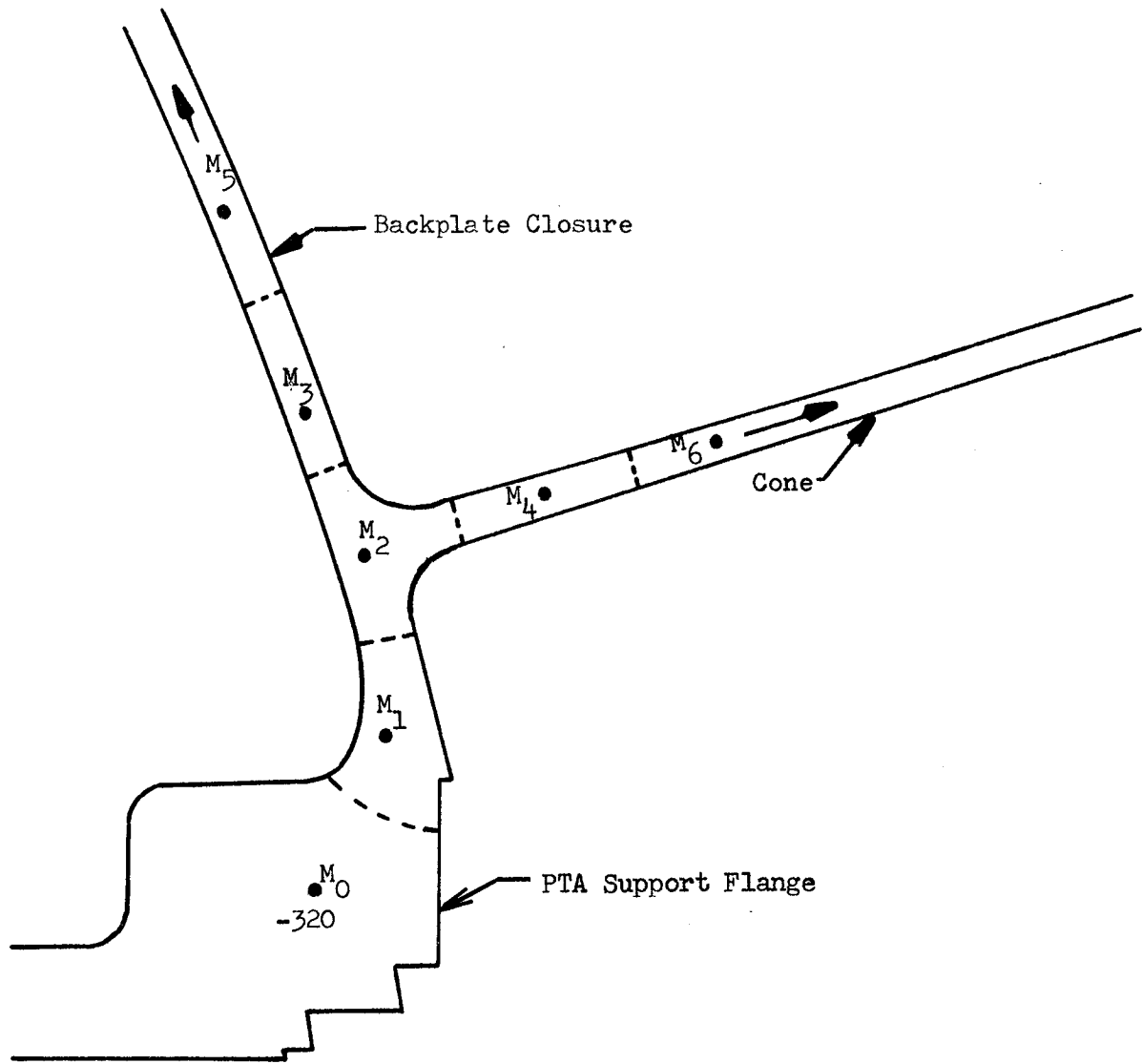
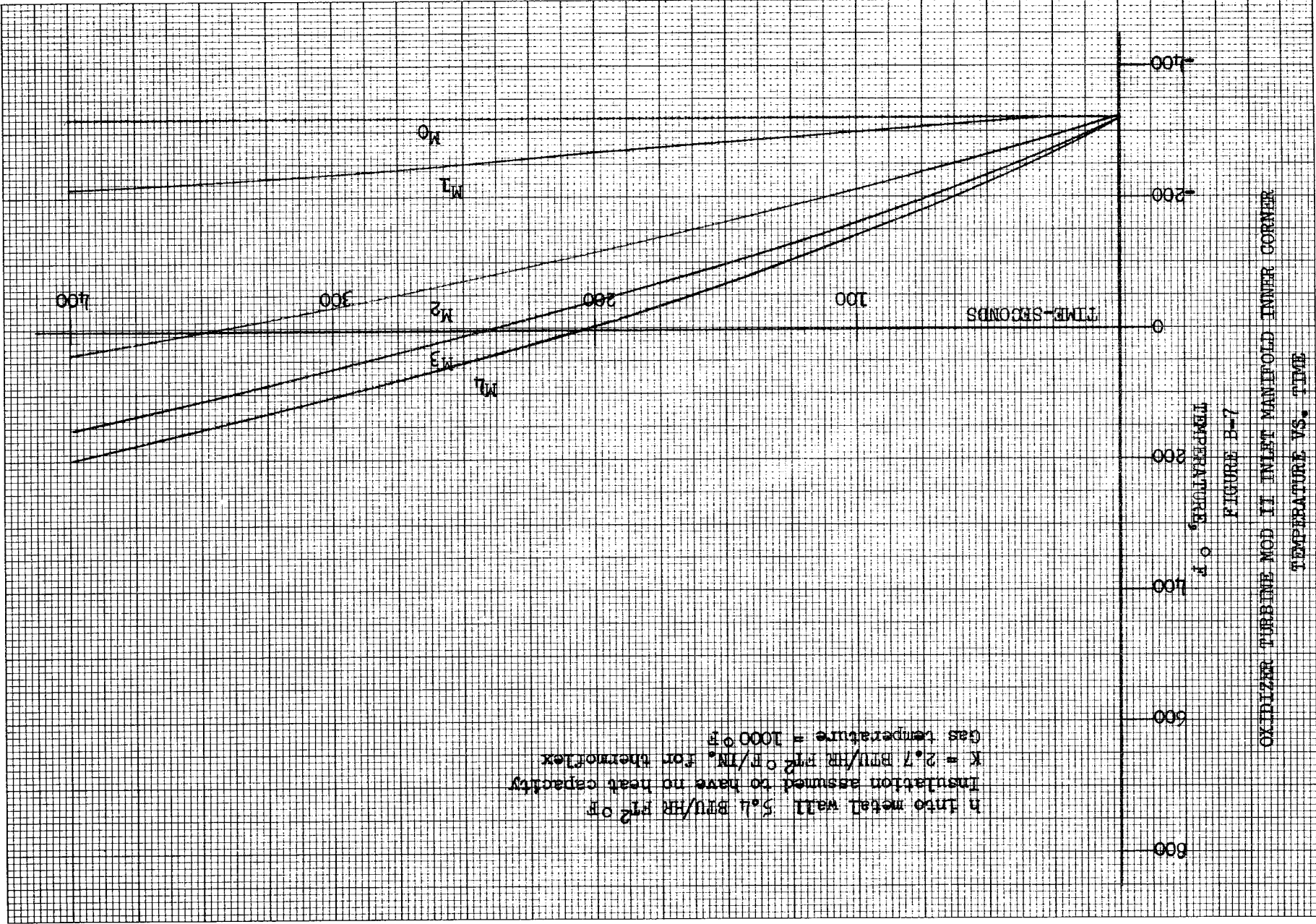


FIGURE B-6

MOD II OTPA TURBINE INLET MANIFOLD
(Inner Joint Backplate - Manifold)



OXIDIZER TURBINE MOD II INLET MANIFOLD INNER CORNER
 FIGURE B-7
 TEMPERATURE, °F
 TEMPERATURE VS. TIME

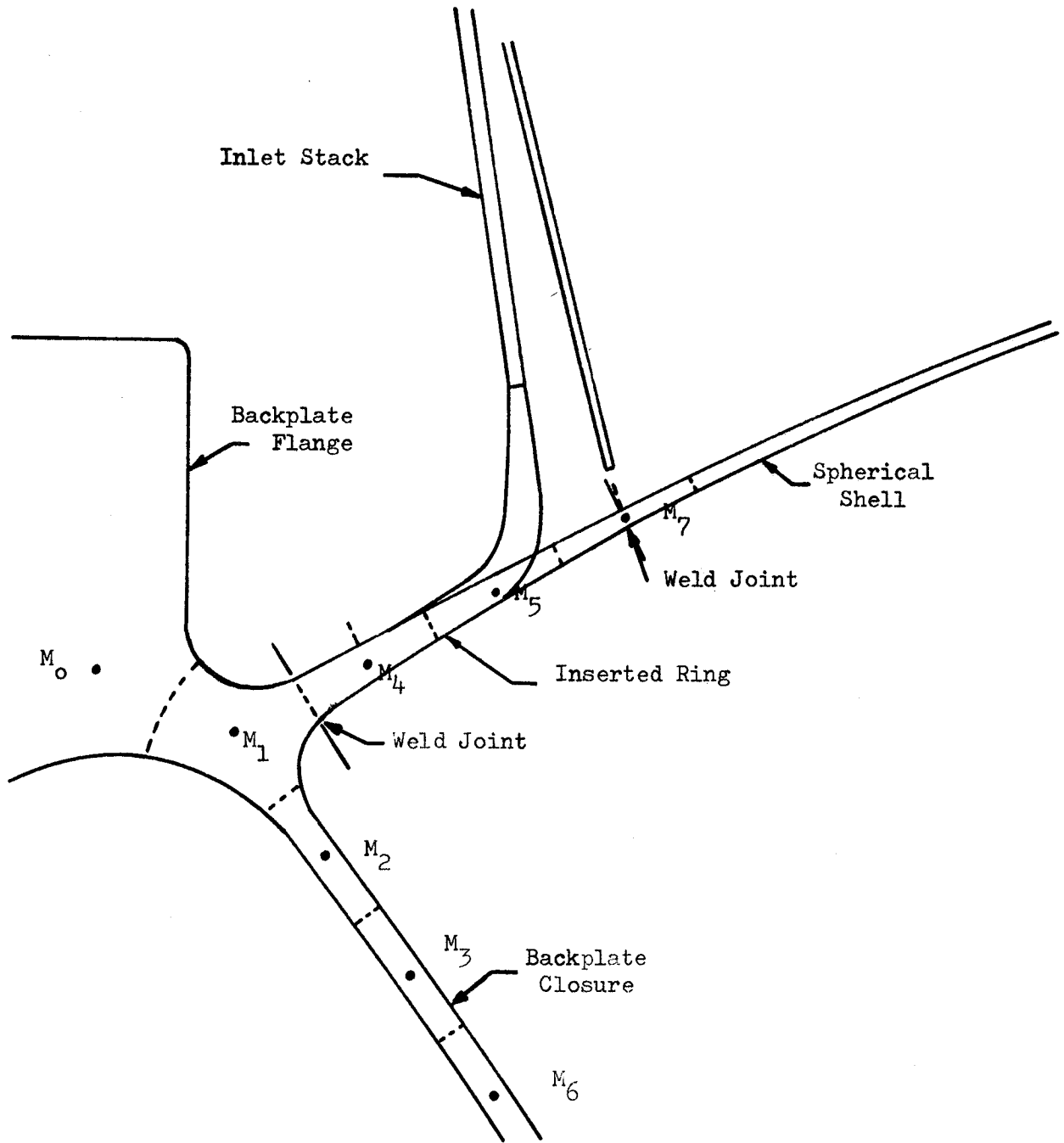


FIGURE B-9

MOD II OPA TURBINE INLET MANIFOLD
 (Redesign of Outer Manifold to Backplate Joint)

h into manifold variable with temperature $h = K/.5\text{-in.}$
 Insulation assumed to have no heat capacity
 K from Figure B-2, Curve H₂ + H₂O vapor and thermoflex
 Gas temperature = 1000°R
 Spherical shell at room temperature away from corner at time -0

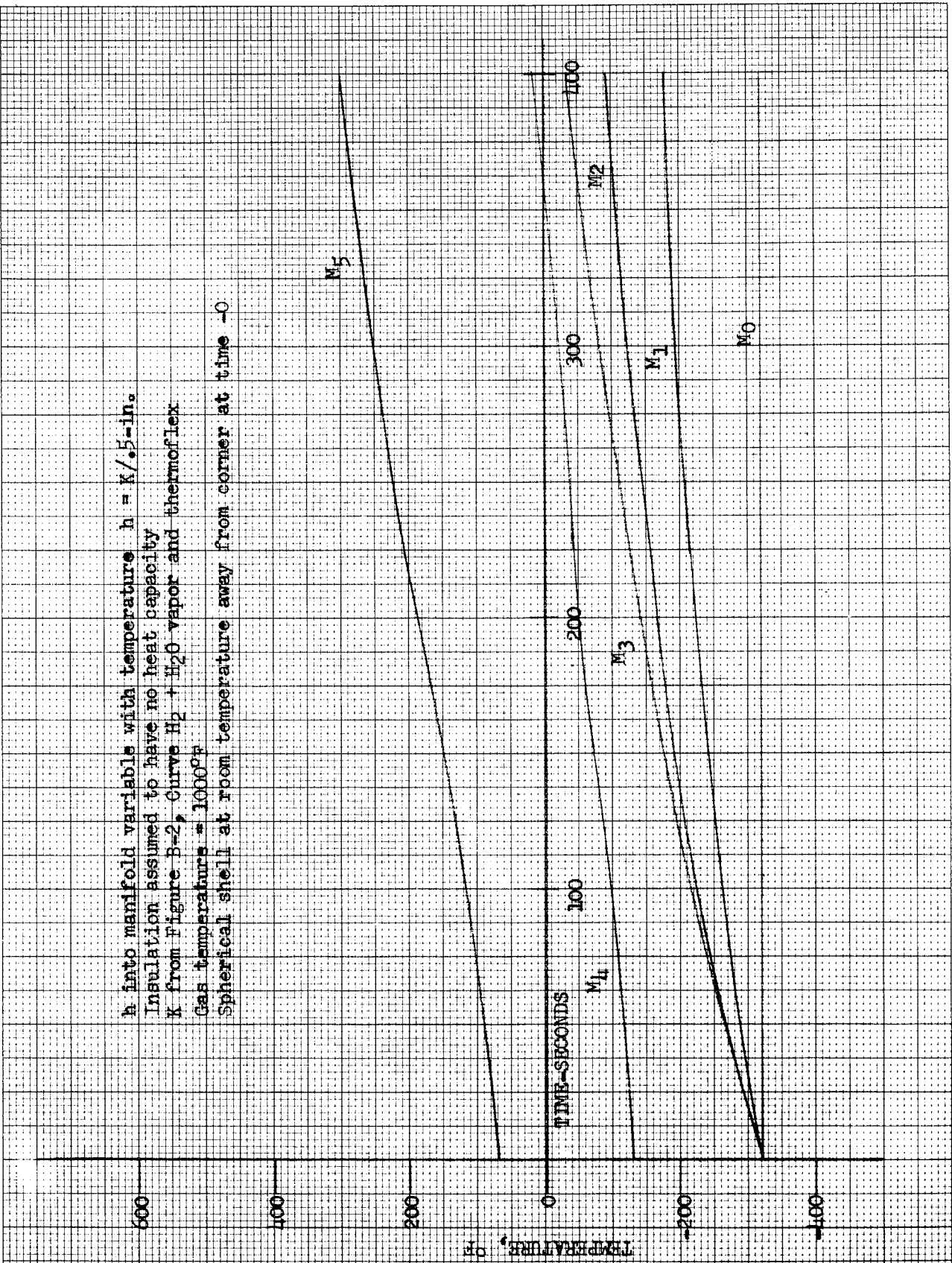


FIGURE B-8

OXIDIZER TURBINE MOD II INLET MANIFOLD OUTER CORNER
 TEMPERATURE VS. TIME

h into metal wall $5.4 \text{ BTU/HR FT}^2 \text{ } ^\circ\text{F}$
 Insulation assumed to have no heat capacity
 $K = 27 \text{ BTU/HR FT}^2 \text{ } ^\circ\text{F/IN.}$ for thermoflex
 Gas temperature = $1000 \text{ } ^\circ\text{F}$

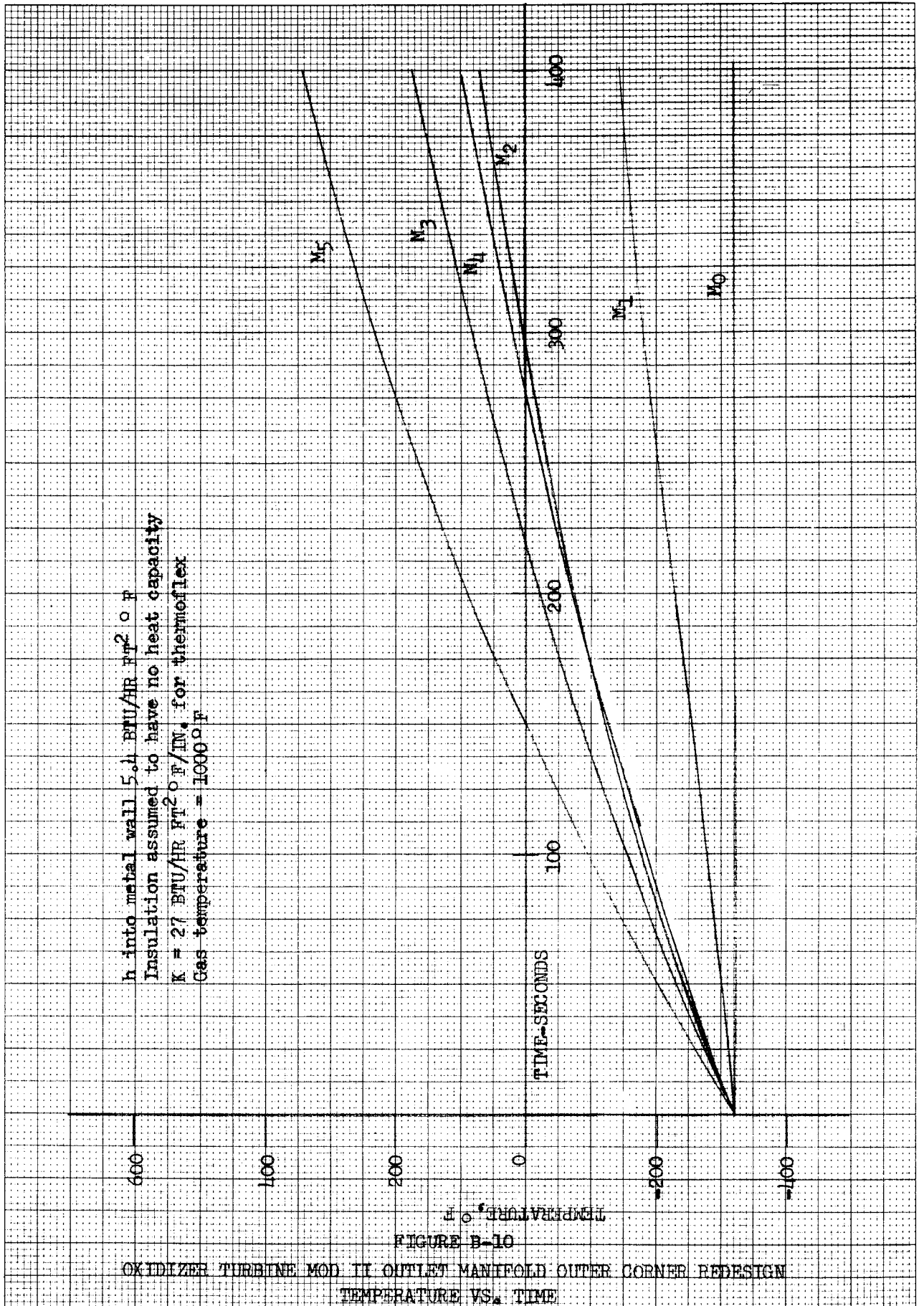


FIGURE B-10
 OXIDIZER TURBINE MOD II OUTLET MANIFOLD OUTER CORNER REDESIGN
 TEMPERATURE VS. TIME

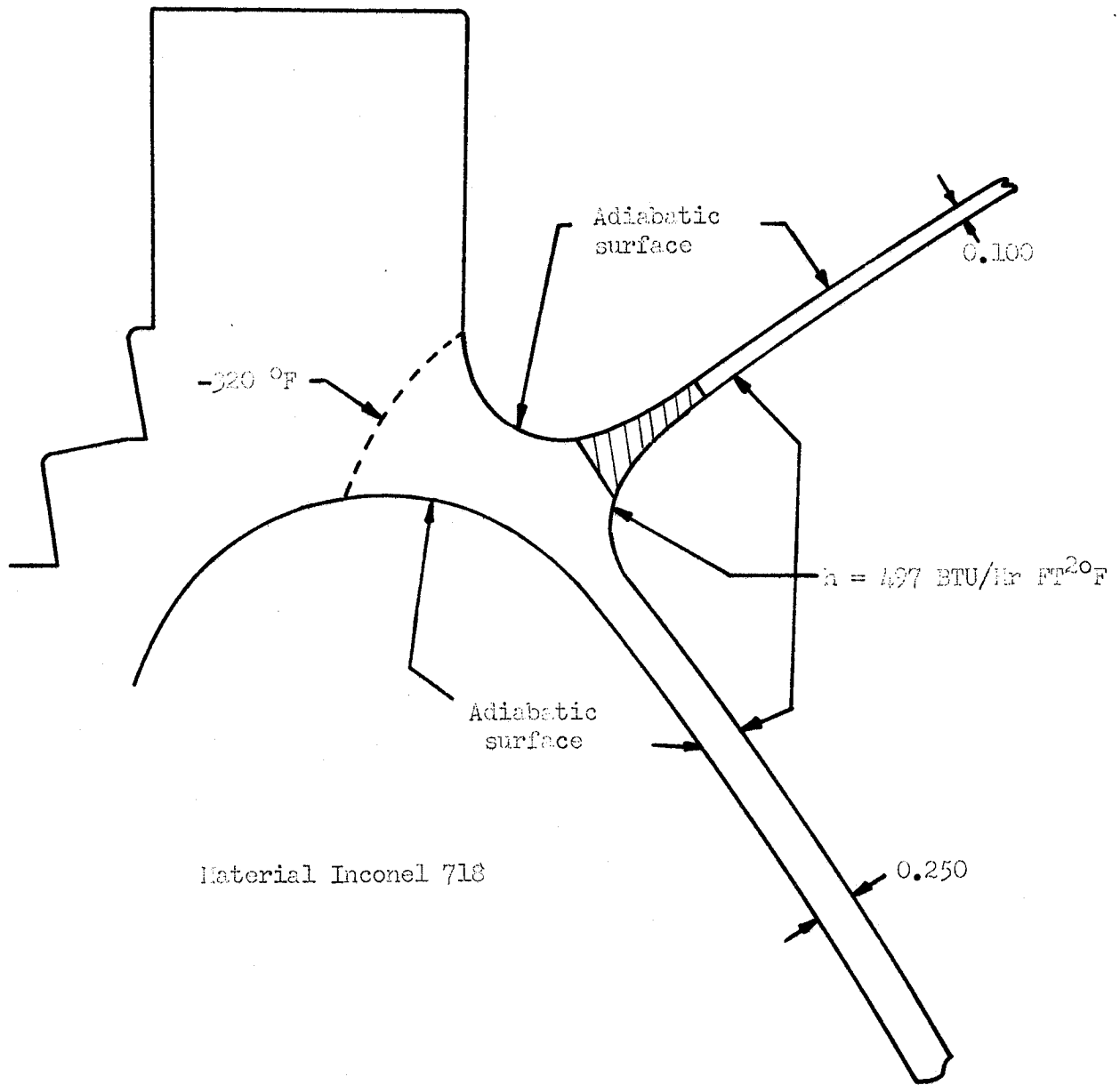


Figure B-11
Model II Oxidizer Turbine Inlet Manifold - Heat Transfer
Page B-18

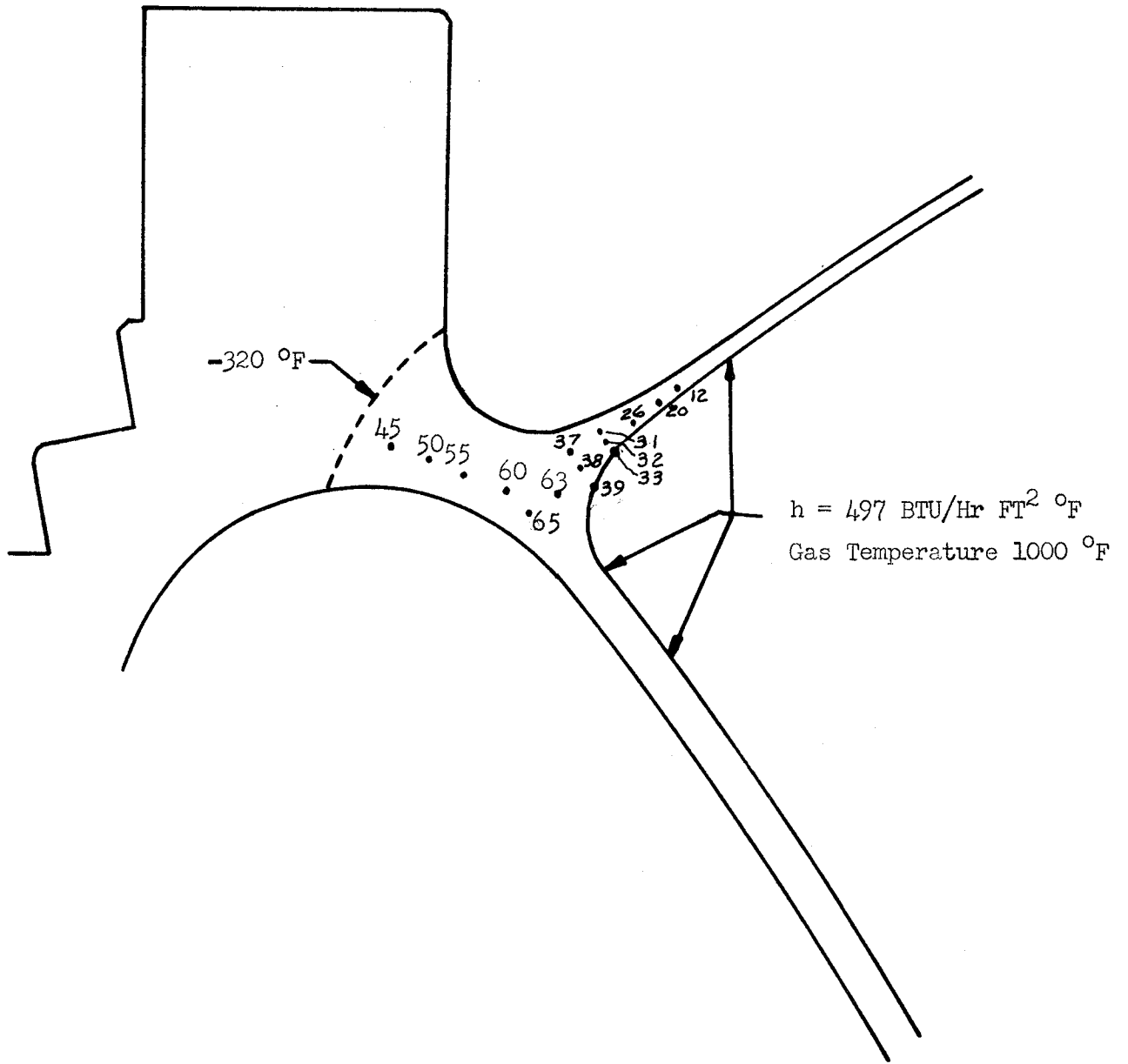


Figure B-12
 Model II Oxidizer Turbine Inlet Manifold-Heat Transfer Without Insulation
 Page B-19

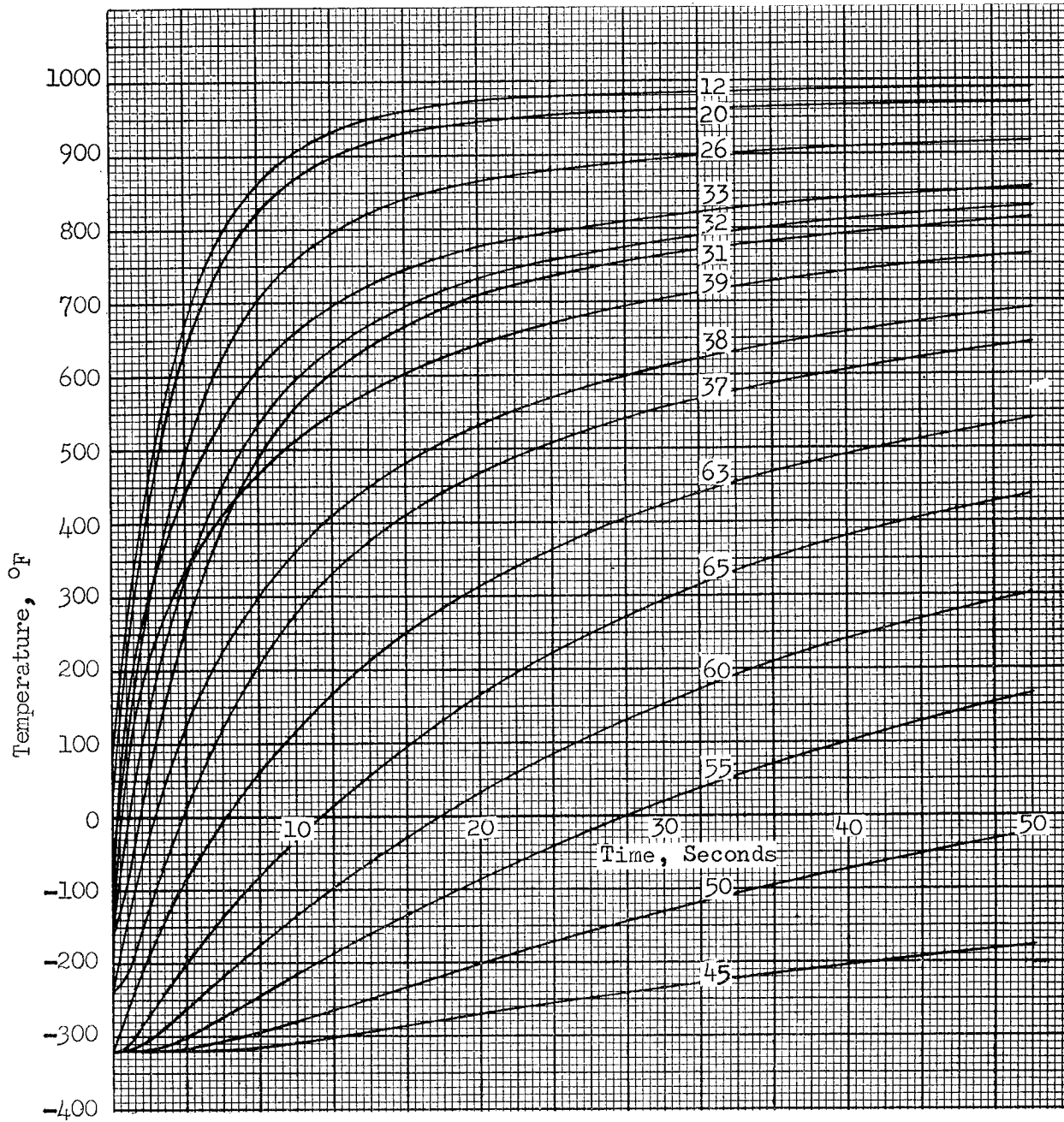


Figure B-13
 Model II Oxidizer Turbine Inlet Manifold - Heat Transfer Without Insulation
 Page B-20

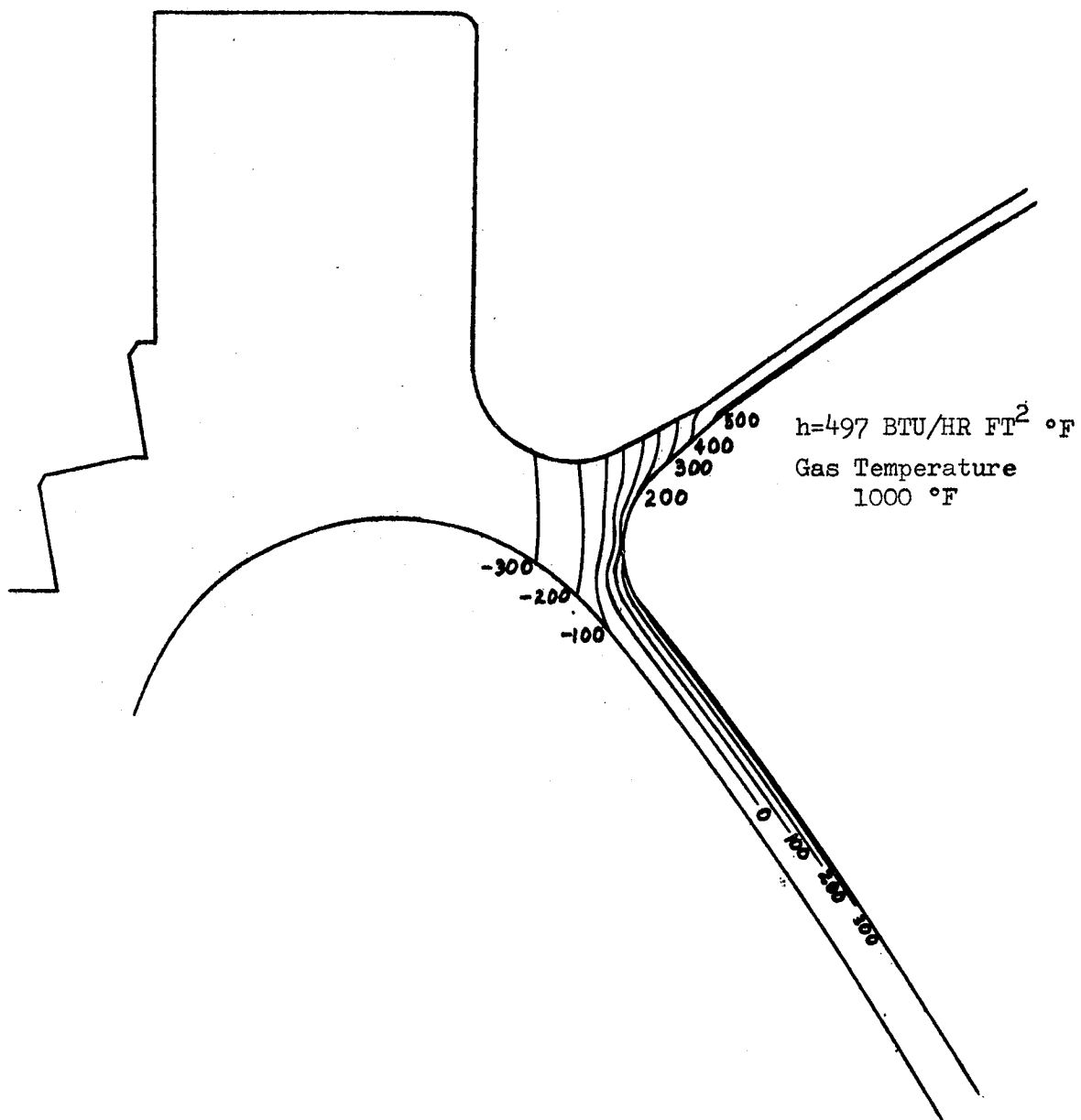


FIGURE B-14
 MOD II OXIDIZER TURBINE
 INLET MANIFOLD
 HEAT TRANSFER WITH-
 OUT INSULATION
 TIME 2 SECONDS

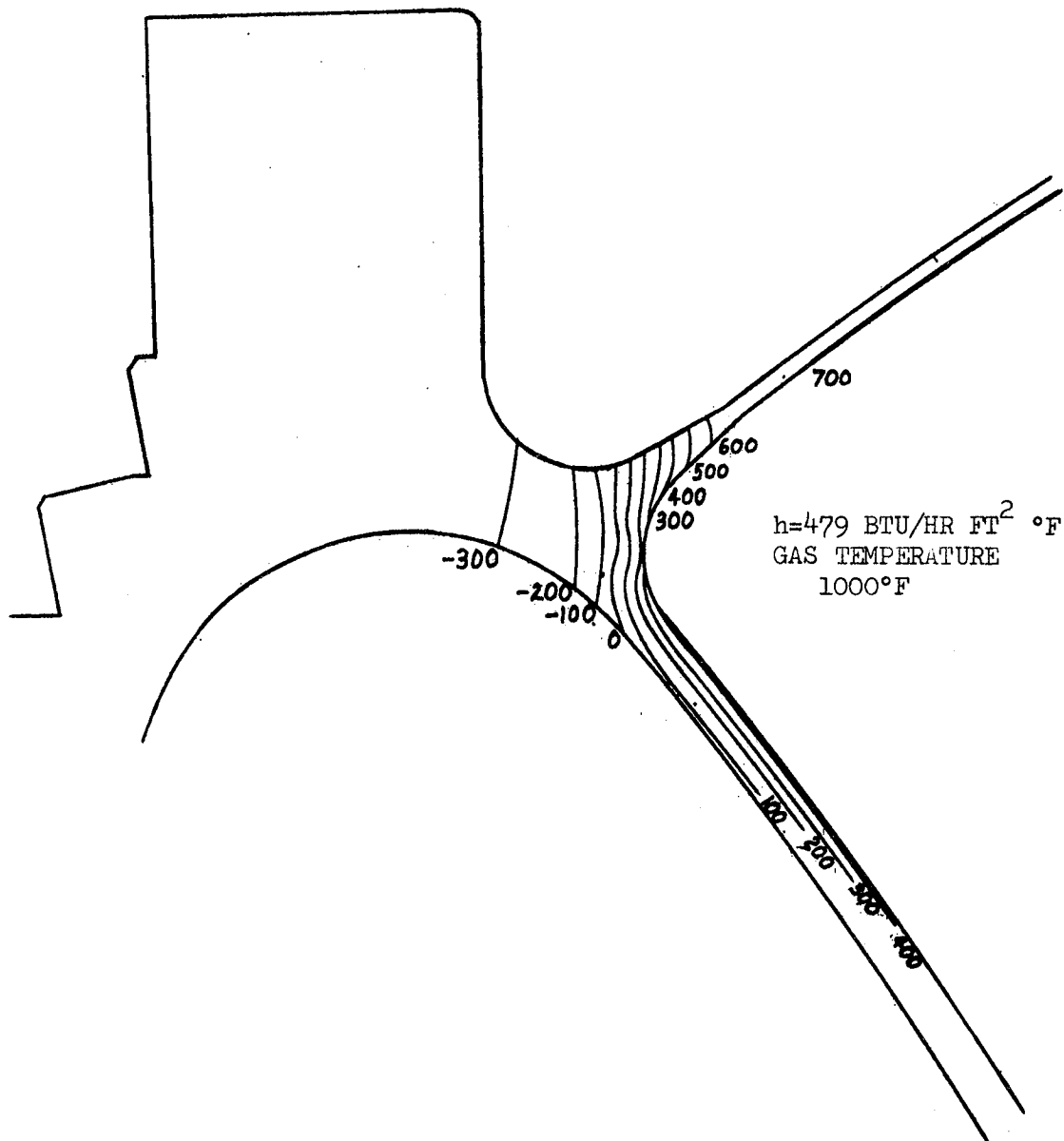


FIGURE B-15

MOD II OXIDIZER TURBINE INLET MANIFOLD
 HEAT TRANSFER WITHOUT INSULATION
 TIME 4 SECONDS

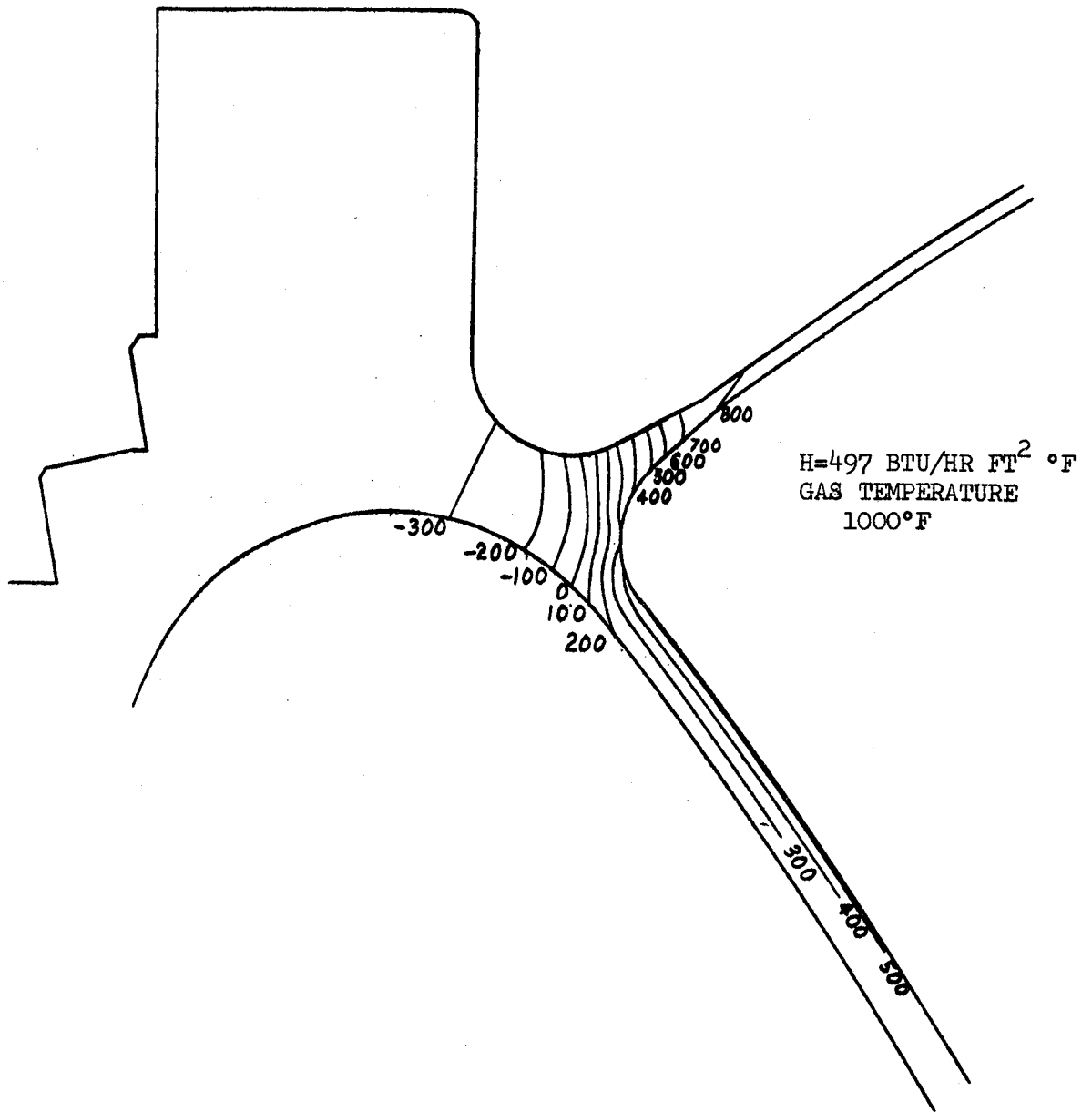


FIGURE B-16
 MOD II OXIDIZER TURBINE
 INLET MANIFOLD
 HEAT TRANSFER WITHOUT INSULATION
 TIME 6 SECONDS

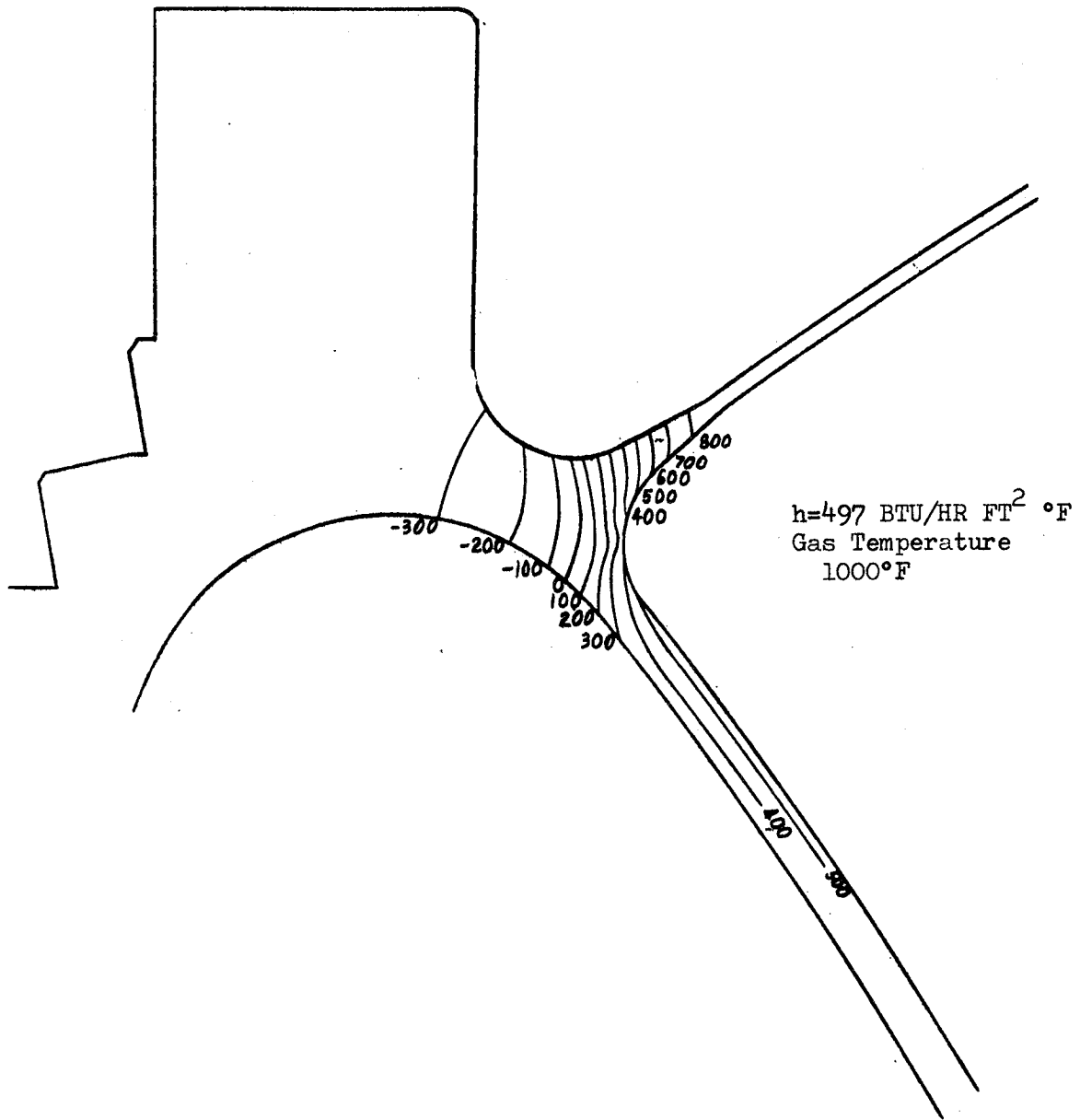


FIGURE B-17
 MOD II OXIDIZER TURBINE INLET MANIFOLD
 HEAT TRANSFER WITHOUT INSULATION
 TIME 8 SECONDS

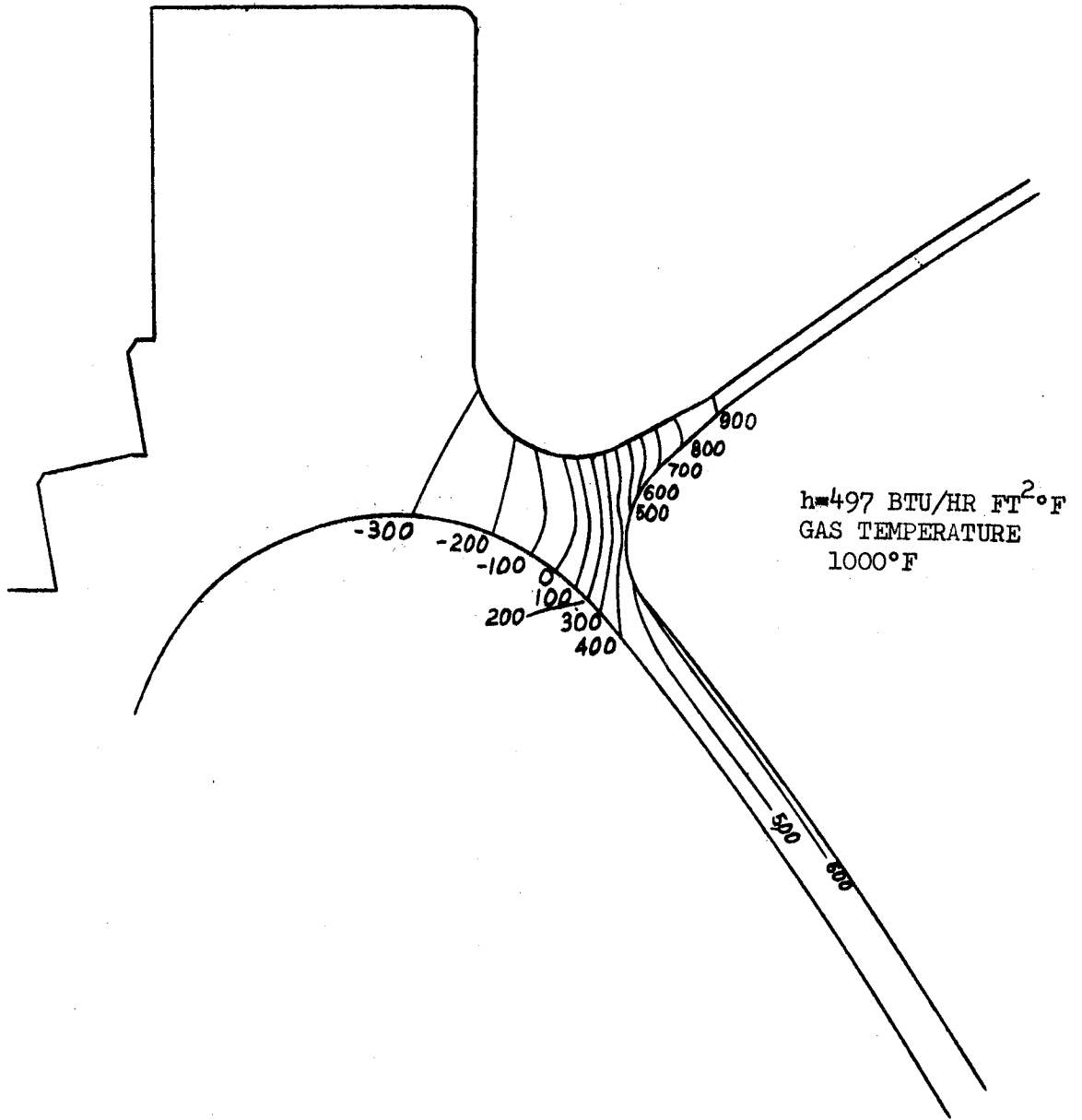


FIGURE B-18

MOD II OXIDIZER TURBINE INLET MANIFOLD
 HEAT TRANSFER WITHOUT INSULATION TIME 10 SECONDS

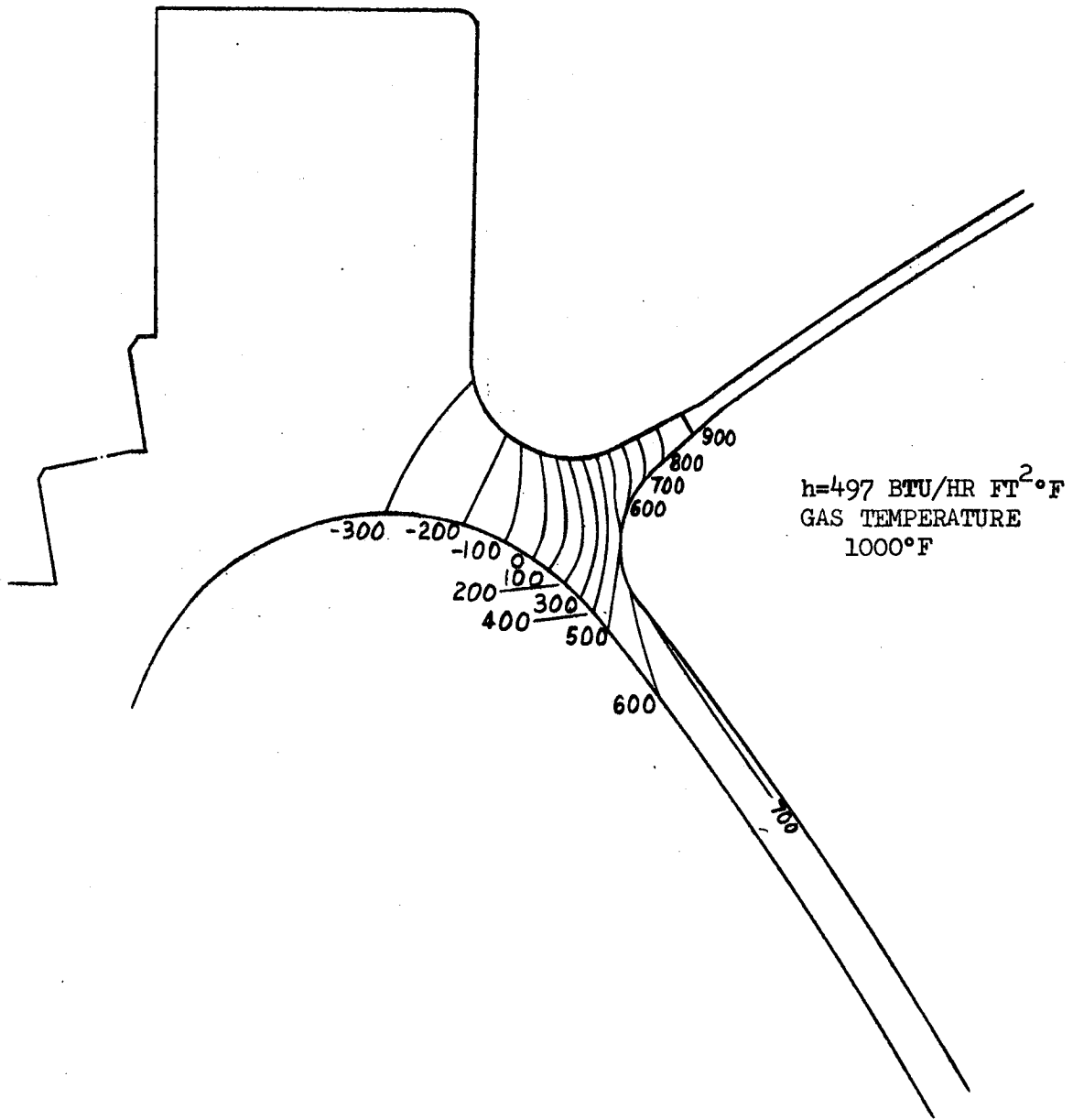


FIGURE B-19
MOD II OXIDIZER TURBINE INLET MANIFOLD
HEAT TRANSFER WITHOUT INSULATION TIME 14 SECONDS

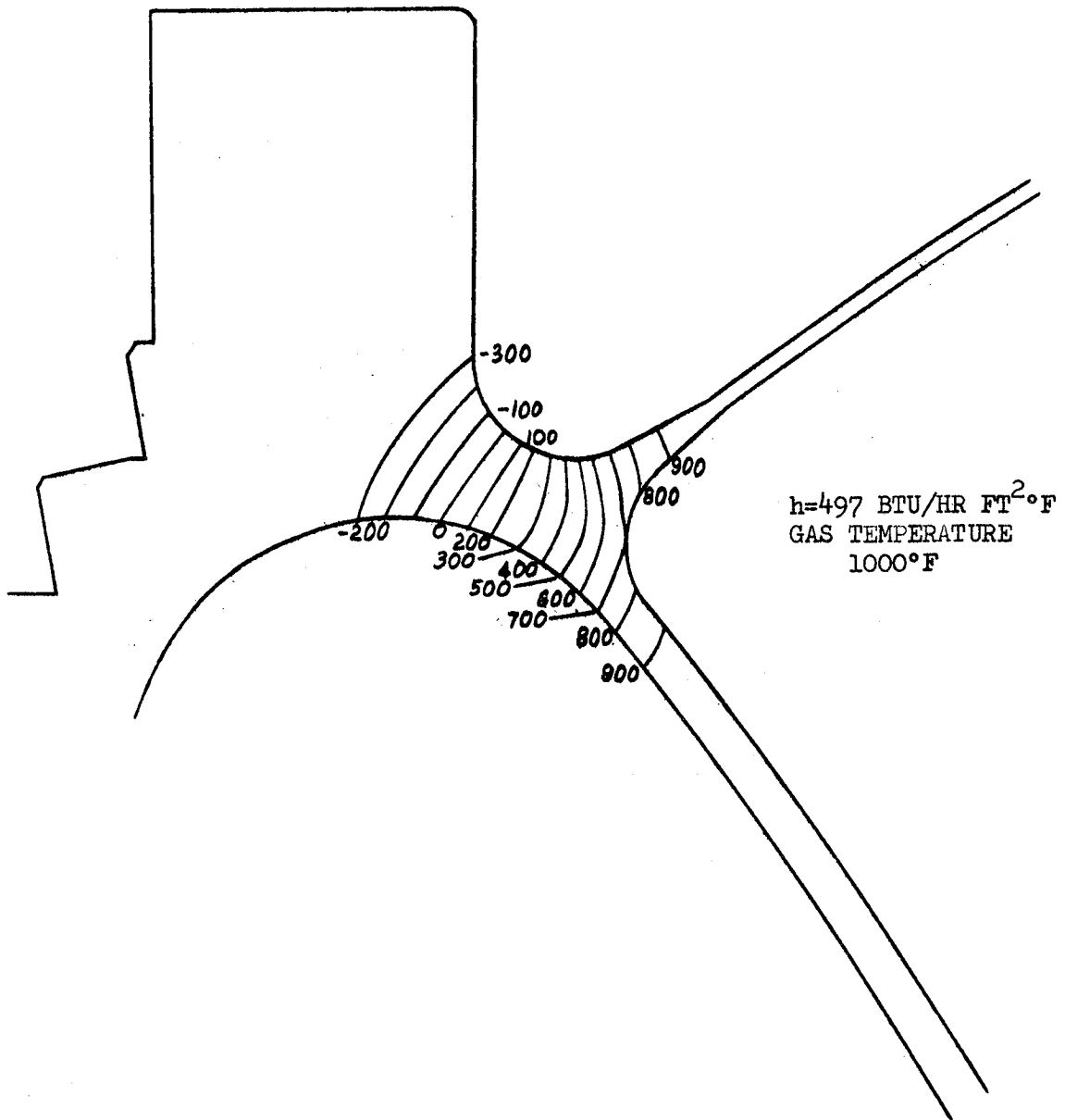


FIGURE B-20
 MOD II OXIDIZER TURBINE INLET MANIFOLD
 HEAT TRANSFER WITHOUT INSULATION TIME 50 SECONDS

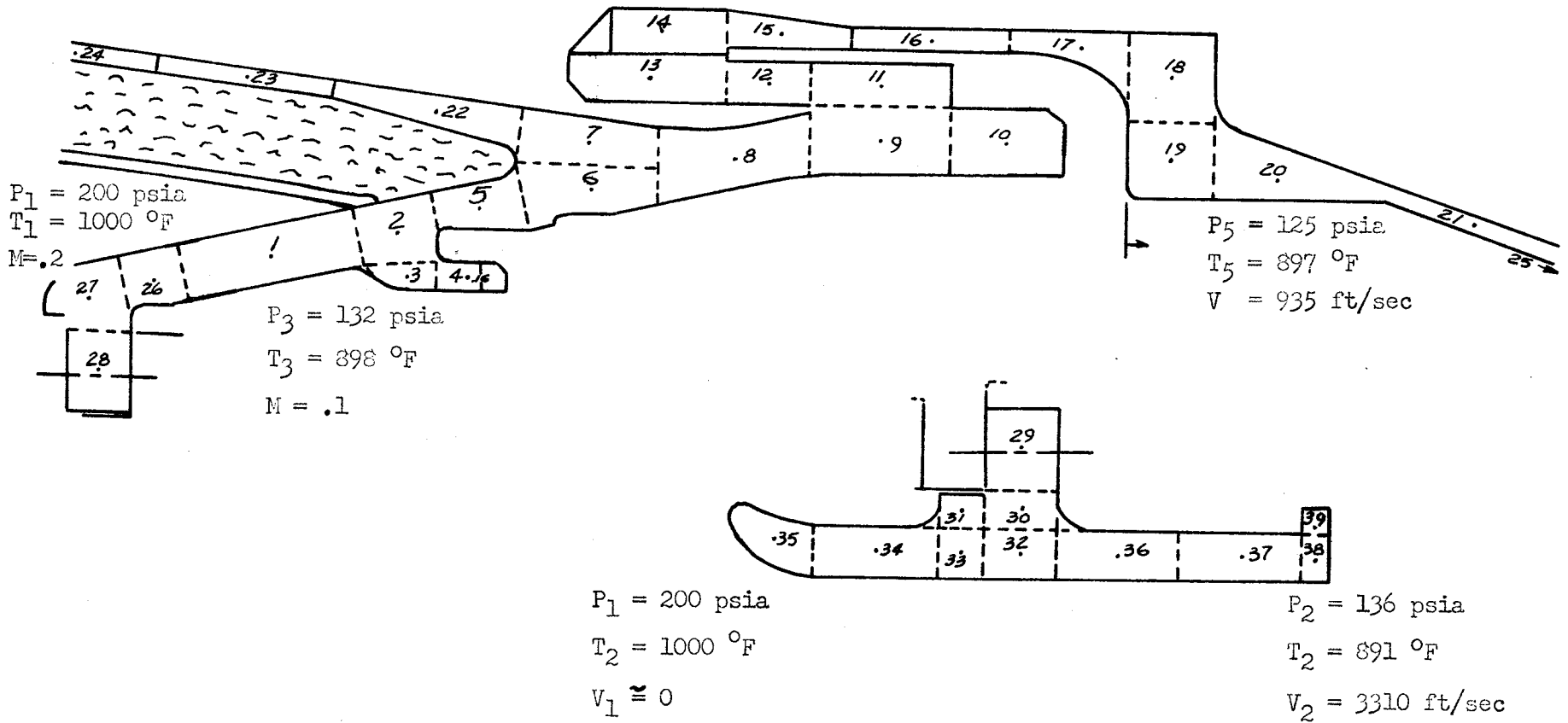
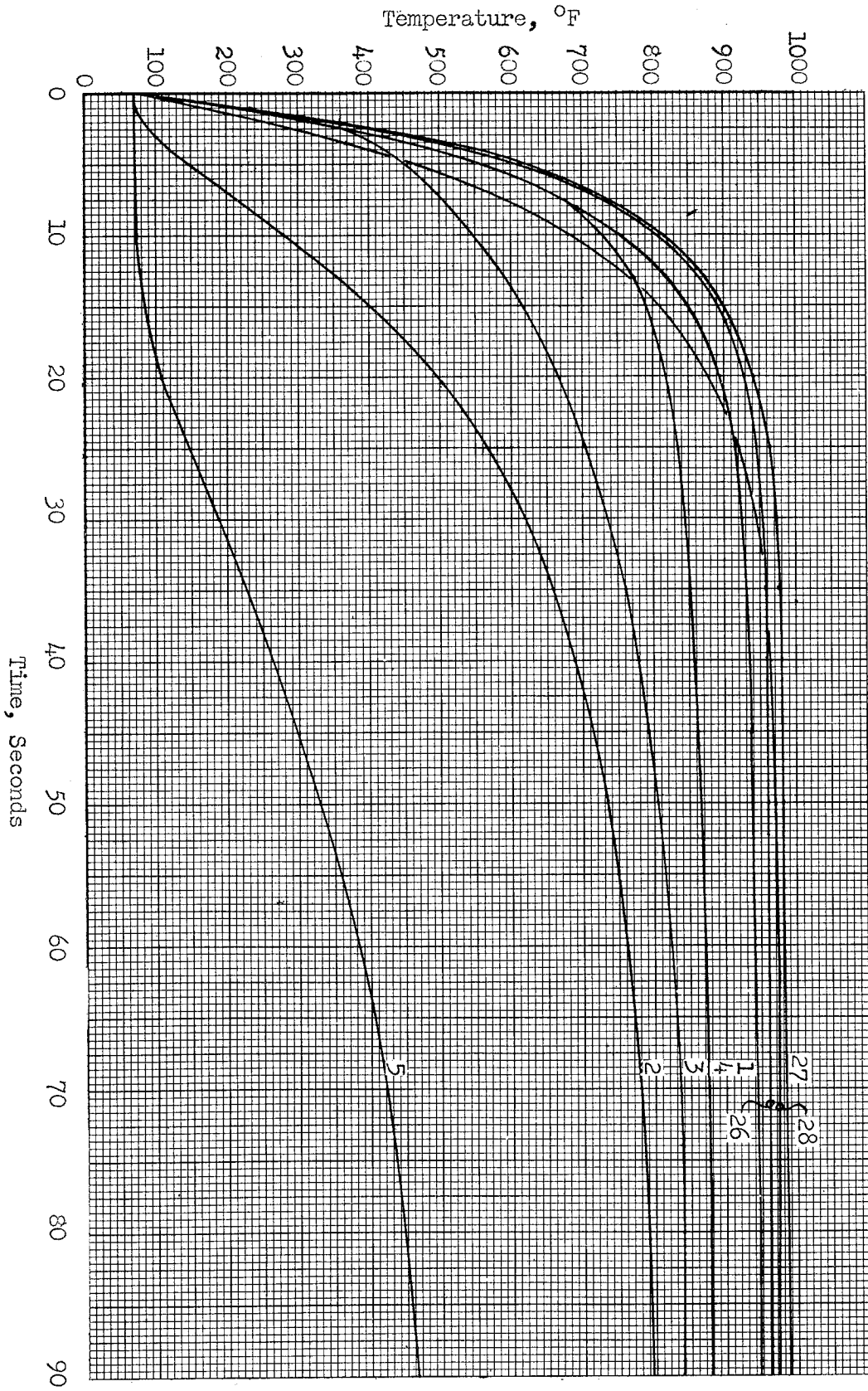


Figure B-22
Oxidizer Turbine Model II Main Joint Thermal Analysis (Points 1-5 & 26-28)



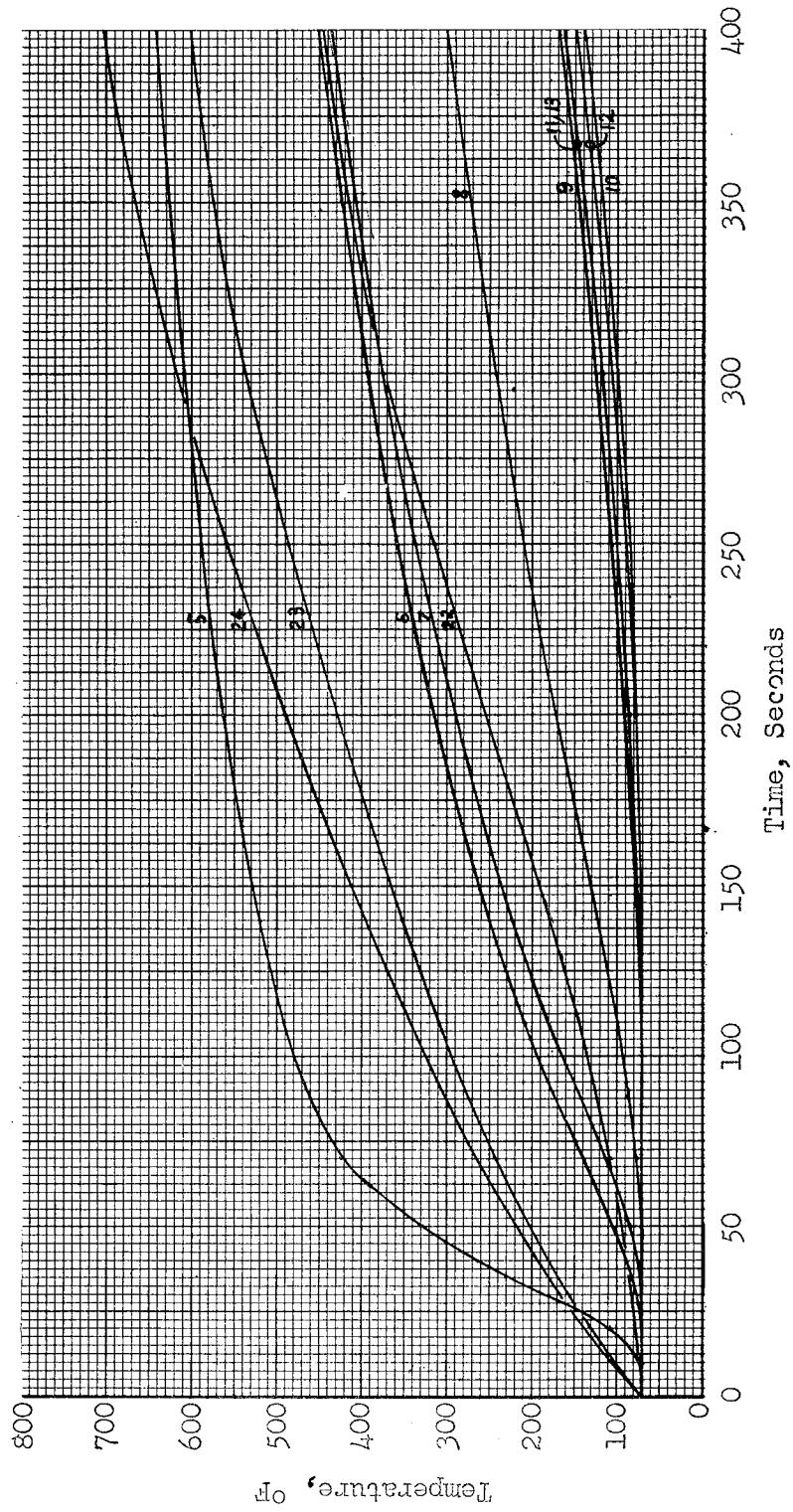
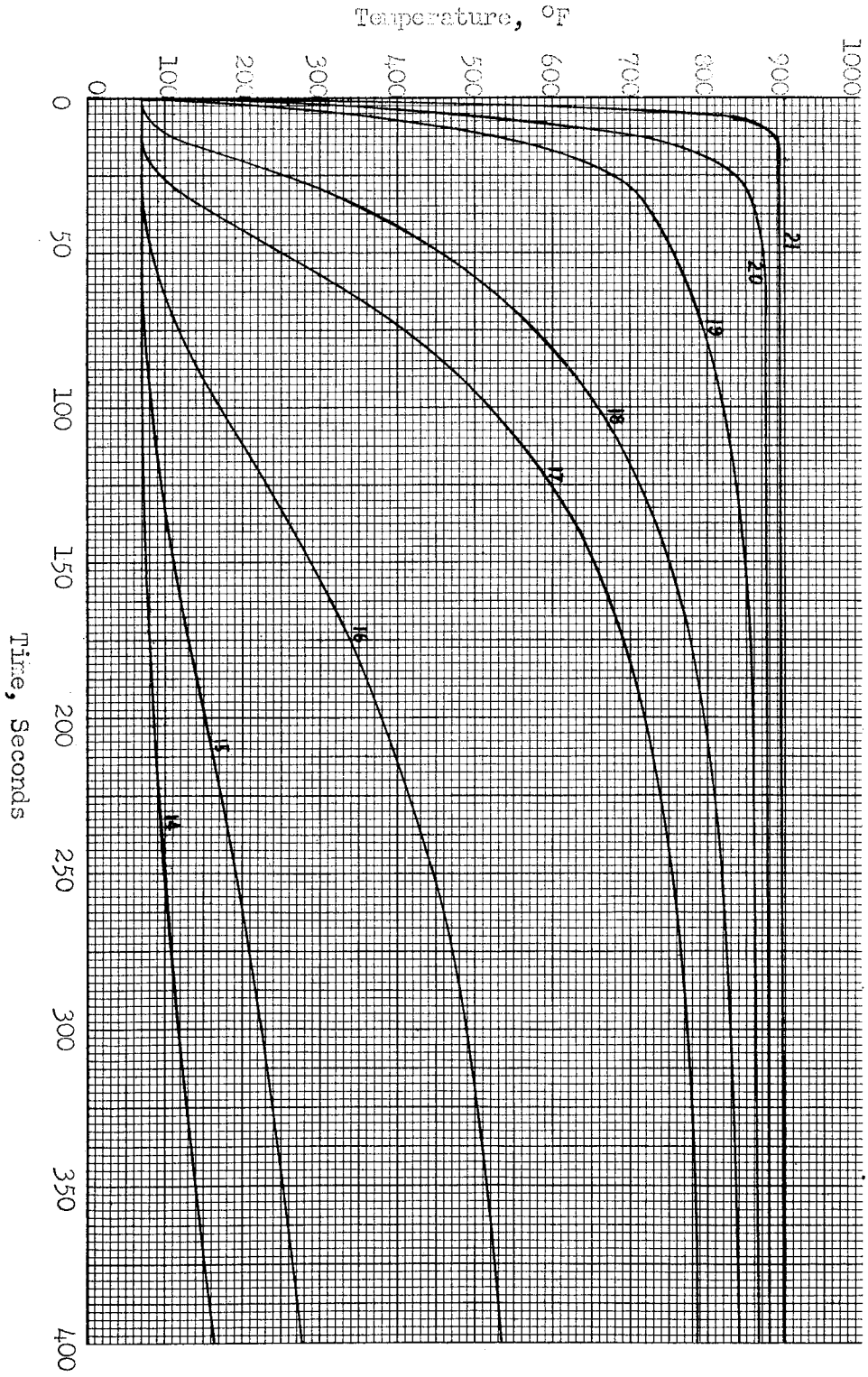
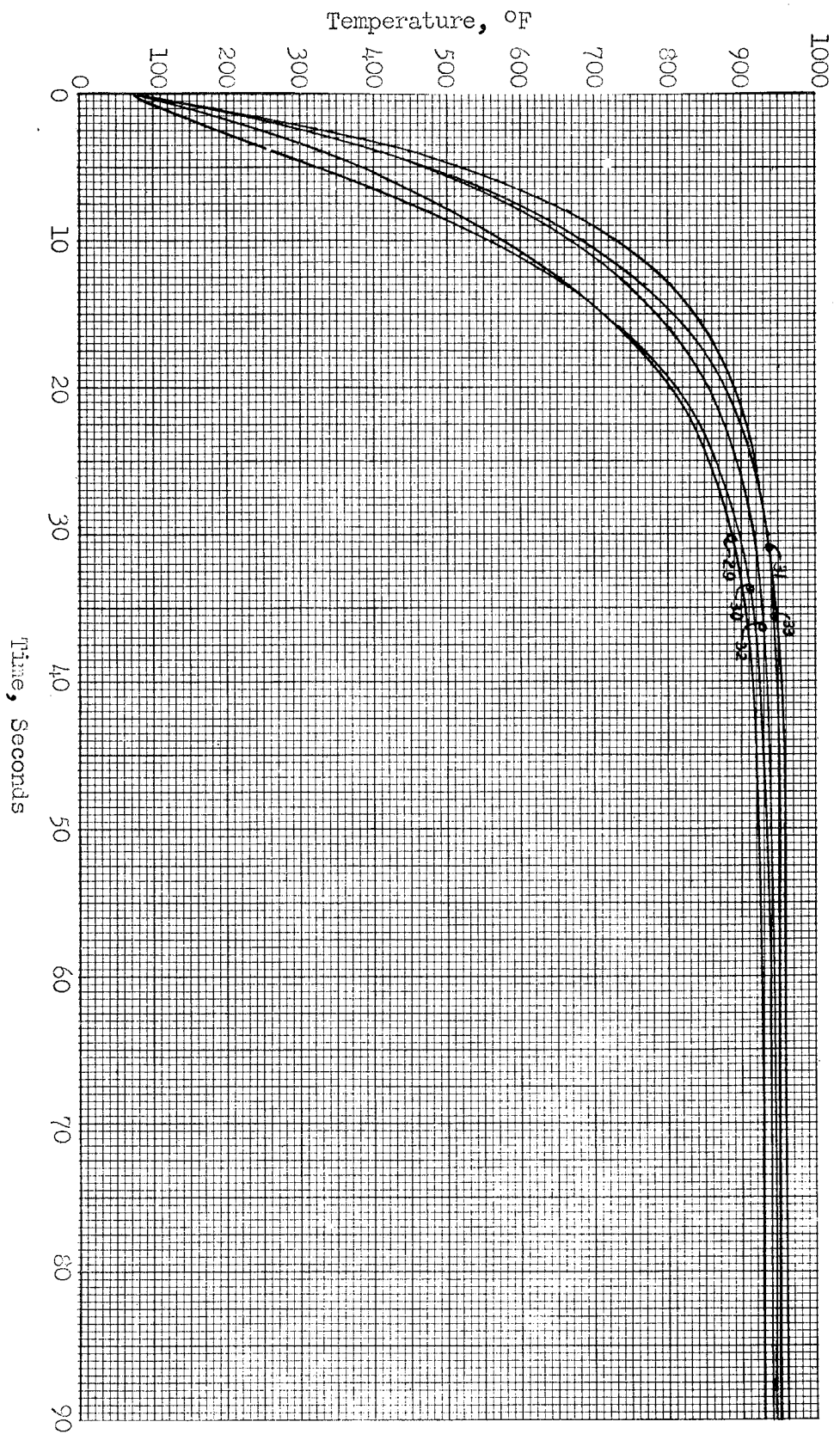


Figure B-23
 Oxidizer Turbine Model II Main Joint Thermal Analysis (Points 5-13 & 22-24)





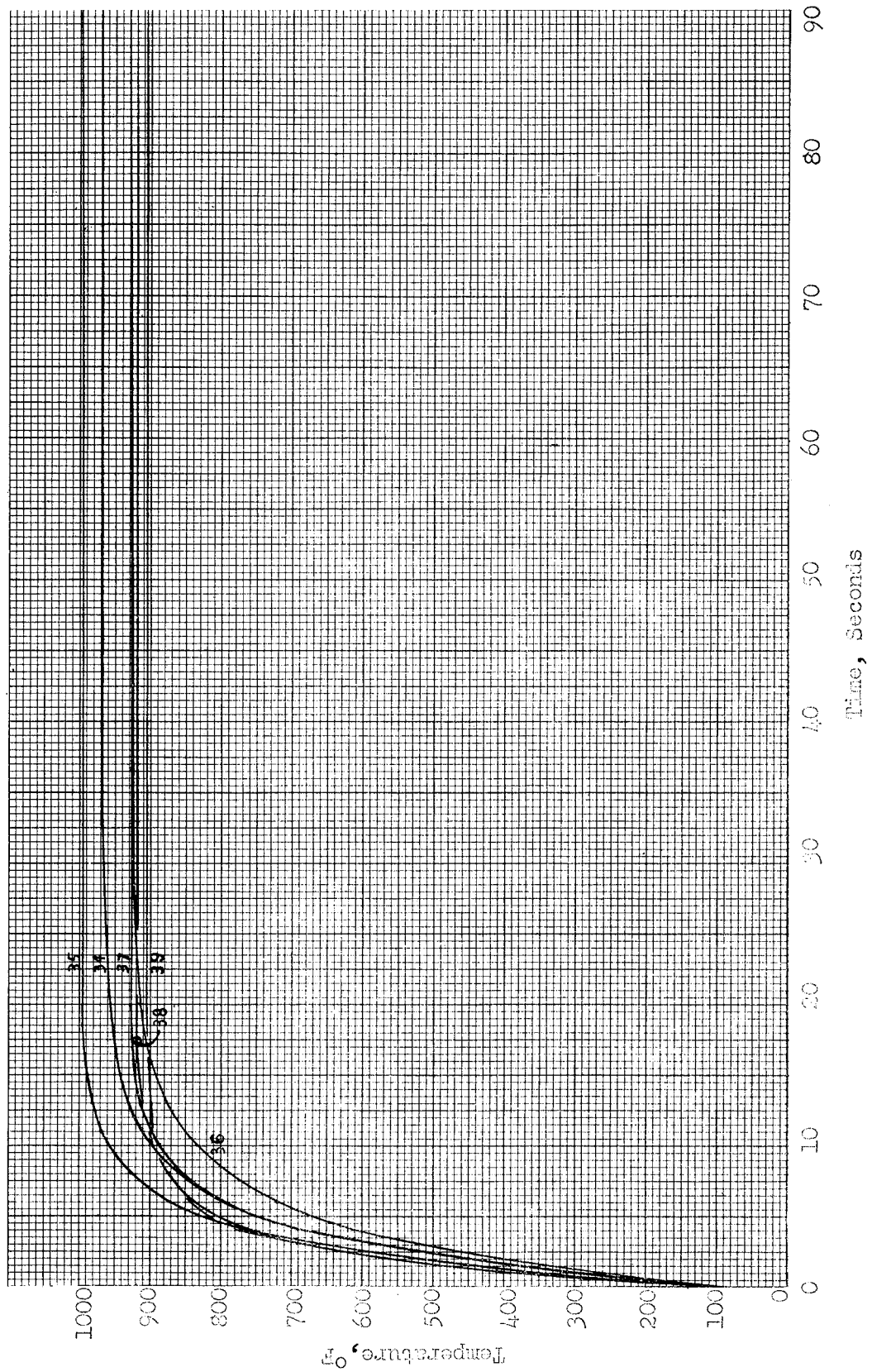


Figure B-26
 Oxidizer Turbine Model III Main Joint Thermal Analysis
 (Points 34-39)

APPENDIX C

STRESS ANALYSIS OF
M-1 MOD II OXIDIZER TURBINE
INLET MANIFOLD AND BACKPLATE
ASSEMBLY

TABLE OF CONTENTS

	<u>Page</u>
I. Introduction	C-1
II. Summary of Results	C-2
III. Design Criteria	C-5
A. Definition of Pressure and Loading Criteria	C-5
B. Definition of Inertia and Thrust Loading Terms and Criteria	C-5
C. Margin of Safety	C-5
D. Calculated Stress	C-5
E. Margin of Safety for Primary Stress	C-6
F. Determining The Margin of Safety for The Combined Primary, Secondary, and Peak Stresses	C-7
G. Low Cycle Fatigue Life	C-8
IV. Material Properties	C-10
V. Method of Analysis and Loading Condition	C-11
A. Backplate Assembly, P/N 286506	C-11
B. Manifold, P/N 286501	C-12
VI. Stress Analysis	C-13
A. Backplate Assembly	C-13
B. Manifold and Inlet Stack	C-13
C. Stress Summary and Margin of Safety	C-14
VII. Conclusion	C-16

LIST OF TABLES

<u>No.</u>	<u>Title</u>	
C-I	Critical Stress in Backplate and Manifold	C-4
C-II	Mod II OTPA Backplate and Manifold Stress Summary	C-14

Table of Contents (cont.)LIST OF FIGURES

<u>No.</u>	<u>Title</u>	<u>Page</u>
C-1	Elastic Range and Plastic Strain	C-8
C-2	Beam Section	C-10
C-3	Mechanical Properties of Inconel 718	C-17
C-4	Mod II Oxidizer Turbine Backplate and Manifold Loading Condition (Limit)	C-18
C-5	Mechanical and Thermal Loads-Backplate Assembly	C-19
C-6(a)	Line Loads at Manifold Inlet	C-20
C-6(b)	Line Load Distribution at Manifold Inlet (Limit Condition)	C-21
C-7	Tangential Stress Distribution-Backplate Assembly	C-22
C-8	Meridional Stress Distribution-Backplate Assembly	C-23
C-9	Manifold Inlet at Section A (Limit Condition)	C-24
C-10	Manifold Inlet at Section A (Ultimate Condition)	C-25
C-11	Manifold Inlet at Section A, Limit Load + Thermal Load (Temperature at 400 sec)	C-26
C-12	Manifold Inlet at Section B, Limit Load + Thermal Load (Temperature at 400 sec)	C-27
C-13	Manifold Inlet at Section B (Ultimate Condition)	C-28
C-14	Manifold at Section C (Limit Condition)	C-29
C-15	Manifold at Section C (Ultimate Condition)	C-30
C-16	Manifold at Section C, Limit Load + Thermal Load (Temperature at 400 sec)	C-31

APPENDIX C

Prepared by T. Chinn, L. W. Bartholf, and L. K. Severud

I. INTRODUCTION

This is a discussion of a structural analysis of the Model II Oxidizer Turbine Inlet Manifold and Backplate Assembly, P/N 286501.

The structures were analyzed for the most critical operating conditions. The loading conditions for the backplate assembly are pump cavity pressure, turbine manifold pressure, bearing load, and temperature gradients between the hot gases in the manifold and the liquid fuel. The turbine inlet manifold loading conditions are manifold pressure, external line loads, and temperature gradients.

The existence of the manifold inlet ducts complicates a simple axisymmetric solution for the manifold housing; therefore an approximate solution was used to predict the stresses at the inlet-to-manifold junction. The approximate method consisted of taking a section of the inlet and treating it as a shell of revolution. Two sections were taken, one along the longitudinal axis and the other in the circumferential direction.

II. SUMMARY OF RESULTS

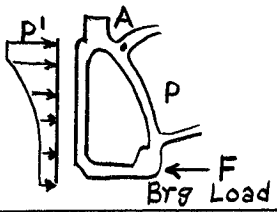
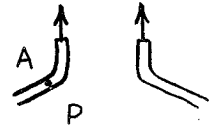
The critical stresses and Margins of Safety (M.S.) for the Oxidizer Turbine Manifold and Backplate assembly are summarized below. The minimum Margin of Safety was determined for two stress conditions: the primary stress condition only, and the primary plus secondary or peak stress condition. The M.S. for the latter takes into account thermal stress cycling.

The critical stress condition for the backplate assembly is the result of a large temperature gradient at the manifold-to-backplate flange. In the manifold section, the critical stress occur at the inlet-to-manifold juncture along the circumferential direction. The resulting stress in this area is largely the result of the inlet line loads.

II. Summary of Results (cont.)

TABLE C-I

CRITICAL STRESS IN BACKPLATE AND MANIFOLD

	Design Condition	Total Stress @ A	Minimum M.S.
Backplate 	Mech Load + Thermal Load p = 375 psi T = 650°F F = ± 70 Kips	120,000 psi	1.5*(1)
Manifold Section B 	Mech Load p = 375 psi	1149,000	0(2)
	Mech Load + Thermal p = 375 psi T = 650°F	146,000	.85*(1)

(1) $M.S. = \frac{2F_{ty}}{\text{Total Stress}} - 1$ (See Section III Design Criteria)

(2) $M.S. = \frac{1}{\frac{\sigma_m}{F_{ty}} + \frac{\sigma_b}{F_{by}}} - 1$

III. DESIGN CRITERIA

The design criteria for the M-1 engine states that all structural components shall be capable of withstanding limit load conditions without suffering excessive permanent deformation and without experiencing deflections which will adversely affect the performance characteristics of the engine.

The design criteria for the Mod II Oxidizer Turbine Manifold and Backplate Assembly as well as the calculated stress are described as follows:

A. DEFINITION OF PRESSURE AND LOADING CRITERIA

Nominal-Maximum pressure to which component is subjected under steady state conditions.

MEOP-The maximum expected operating pressure at any time including engine transient condition.

Proof-1.2 x MEOP

Burst-1.6 x MEOP

B. DEFINITION OF INERTIA AND THRUST LOADING TERMS AND CRITERIA

Limit Load-The critical load or combination of loads and environment the occurrence of which is expected at least once during the life of the component.

Design Yield-1.0 x Limit Load

Design Ultimate 1.5 x Limit Load

C. MARGIN OF SAFETY

The margin of safety is equal to $\frac{\text{allowable stress}}{\text{calculated stress}} - 1$

D. CALCULATED STRESS

The calculated stress can be any, or a combination, of the following:

1. Primary Stress

A stress developed by the imposed loading which is necessary to satisfy the laws of equilibrium between external and internal forces and moment. The basic characteristic of a primary stress is that it is not self-limiting. If a primary stress exceeds the yield strength of the material through the entire thickness, the prevention of failure is entirely dependent upon the strain-hardening properties of the material.

III. D. DESIGN STRESS (cont.)

2. Secondary Stress

A stress developed by the self-constraint of a structure. It must satisfy an imposed strain rather than being in equilibrium with an external load. The basic characteristic of a secondary stress is that it is self-limiting because minor distortions can satisfy the discontinuity conditions or thermal expansions which cause the stress to occur.

3. Peak Stress

The highest stress in the region under consideration. The basic characteristics of a peak stress is that it causes a significant distortion and is objectionable mostly as a possible source of fatigue failure.

E. MARGIN OF SAFETY FOR PRIMARY STRESS

1. Margin of Safety Based Upon Yield

Allowable stress is minimum yield tensile, compressive or shear stress; yield bending modulus; or, yield torsional modulus at operating temperature. Calculated stress is derived from proof pressure or design yield load. The M.S. for the combined membrane and bending stress condition at yield is:

$$\text{M.S.}_{\text{yield}} = \frac{1}{\frac{\sigma_m}{F_{ty}} + \frac{\sigma_b}{F_{by}}} - 1 \quad (1)$$

where: F_{ty} = yield strength at 0.2% offset

F_{by} = yield bending modulus (see Mat'l Property Section for calculated values)

σ_m = calculated membrane stress

σ_b = calculated bending stress

2. Margin of Safety Based Upon Ultimate

Allowable stress is minimum ultimate tensile, compressive or shear stress; ultimate bending modulus; ultimate torsional modulus; or endurance limit at operating temperature. Calculated stress is derived from burst pressure and design ultimate load.

(1) MIL-HDBKS, Strength of Metal Aircraft Elements, ANC-5 Bulletin

III, F, Determining the Margin of Elasticity for the Design
 Primary, Secondary, and Peak Stresses (cont.)

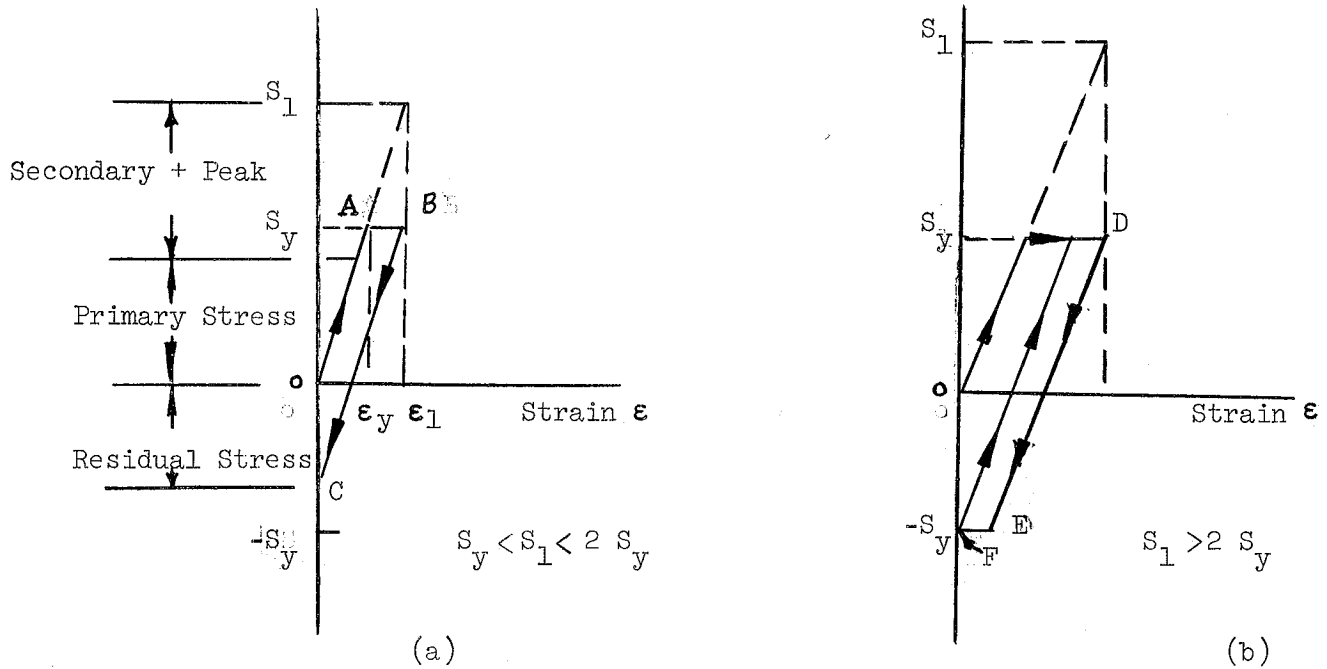


Figure C-1

On subsequent loading, the residual stress must be removed before the stress goes into tension and thus, the elastic range has been increased by the quantity $S_1 - S_y$. If $S_1 = 2S_y$, the elastic range becomes $2S_y$, but if $S_1 > 2S_y$, the fiber yields as shown by 'EF' in Figure C-1 (b) and all subsequent cycles produce plastic strain. Therefore, $2S_y$ is the maximum value of calculated secondary elastic stress which will "shake down" to purely elastic action.

G. LOW CYCLE FATIGUE LIFE

For the condition of plastic strain cycling, the structure must be investigated for fatigue.

The criteria for a low cycle fatigue life under repetitive plastic action is as follows:⁽²⁾

(2) Langer, B. F., Design of Pressure Vessels for Low-Cycle Fatigue, ASME Trans. Journal of Basic Engineering, September 1962, pp 389-402

IV. MATERIAL PROPERTIES

The mechanical properties of INCONEL 718 as a function of temperature are presented in Figure C-3. The minimum yield and ultimate strength properties at room temperature and elevated temperature are specified per AGC 44151, Condition A.

In addition to the tensile strength properties, an allowable bending strength in the plastic range has been determined for INCONEL 718. The strengths were calculated by the following procedure.⁽³⁾

Starting with the basic bending equation for a beam section (see Figure C-2) the allowable bending moment is defined as:

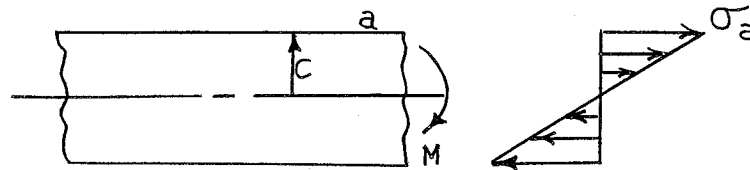


Figure C-2

$$M_a = B_{a,k} (I/c) \quad \text{Eq. (1)}$$

Where: $B_{a,k}$ is the bending modulus of rupture

$$B_a = \frac{Mc}{I} = \sigma_a + (k-1) \sigma_{o,a} \quad \text{Eq. (2)}$$

Thus the bending modulus $B_{u,k}$ for the ultimate condition is:

$$B_{u,k} = \sigma_{t,u} + (k-1) \sigma_{o,u} \quad \text{Eq. (3)}$$

where section factor k is

$$k = \frac{2Qc}{I} \quad \text{Eq. (4)}$$

For a rectangular cross-section, $k = 1.5$, thus the ultimate bending modulus is:

$$B_{u,1.5} = \sigma_{t,u} + 0.5 \sigma_{o,u} \quad \text{Eq. (5)}$$

(3) Gavalis, R., How to Determine Bending Strength in the Plastic Range, Machine Design Data Sheet, July 1964

The yield bending modulus is:

$$B_{y,1.5} = \sigma_{t,y} + 0.5 \sigma_{o,y} \quad \text{Eq. (6)}$$

The stress $\sigma_{o,u}$ and $\sigma_{o,y}$ are plastic limits, and are obtained from Figure 2 of the Machine Design Data Sheet for any material.⁽⁴⁾

A plot of the ultimate and yield bending strength as a function of temperature for INCONEL 718 is shown in Figure C-3.

V. METHOD OF ANALYSIS AND LOADING CONDITION

The Mod II Oxidizer Turbine Manifold and Backplate assembly were analyzed for the following loading conditions: turbine manifold pressure; external inlet line loads; pump cavity pressure; bearing loads; and temperature gradients.

The pressure and line loads for the manifold and backplate assembly are shown in Figure C-4. The line loads at the inlet stack induce a bending moment on the inlet in the circumferential as well as longitudinal direction.

The temperature gradients for the manifold and backplate assembly were obtained from heat transfer data. The temperature gradients at the manifold-to-backplate flange junction were predicted at various operating time intervals up to 400 sec. From the available heat transfer data, the maximum temperature gradient in the manifold juncture occurs at 400 sec. This was assumed to be the most critical thermal condition. A more realistic approach to determine the most critical thermal condition would require a parametric study of the temperature gradient at different operating time; however, because of the lack of time as a result of the M-1 program phaseout, this was not accomplished.

A. BACKPLATE ASSEMBLY, P/N 286506

The stresses in the backplate, under a pressure load, bearing loads, and thermal gradients were predicted using a finite element computer program for axi-symmetrically loaded shells of revolution.

The loading applications for the critical conditions is shown in Figure C-5. The temperature gradient represents the maximum thermal condition. A thrust bearing load of + 70,000 lb acting upon the backplate was applied to the inner external surface of the assembly. In addition, pressures from the impeller induce a pressure distribution on the forward side of the backplate.

⁽⁴⁾ ibid.

7. ANALYSIS OF EXTERNAL LOADING CONDITIONS (cont.)

B. MANIFOLD, P/N 286501

The Mod II Oxidizer Turbine Manifold was analyzed in two parts; the inlet stack-to-manifold area and the manifold housing.

The stress analysis of the inlet stack-to-manifold housing area cannot be accomplished without simplifying assumptions because of the asymmetry of the structure. Therefore, an approximate, but conservative method of analysis was used. This approximate analysis is described in the following paragraphs.

Because the line loads at the inlet are acting primarily in the longitudinal and circumferential directions, it was necessary to investigate two stations on the inlet stack. The two stations (see Section A and B of Figure C-6(a)) were investigated for the external loading conditions as well as internal pressure condition.

The shell section shown in section A must be designed to resist not only internal pressure and thermal gradient but also the longitudinal bending caused by line loads. This section is complicated by the backplate which was assumed to be "fixed" from rotation and deflection.

The shell section of section B was investigated for the circumferential loading as well as pressure and temperature.

The stresses in the two sections were determined by treating the section as an axi-symmetric shell of revolution loaded by internal pressure and axial membrane load caused by the line loads (see Figure C-6(b)). The line loads used in this analysis were the axial and bending loads. The bending load distribution was replaced by a uniform tension load equal to the maximum bending load/in; this is quite conservative. The shear loads were neglected.

A boundary condition for section A was applied at the backplate-to-manifold junction. It was assumed that the stiffness of the backplate was sufficient to resist deflection and rotation; thus, a fixed end boundary condition was used. This condition will provide conservative stress results.

At section B, the membrane section of the manifold was not fixed as in Section A, instead a resultant uniform membrane load is applied.

The stresses in the manifold housing away from the inlet stacks are essentially the result of internal pressure and temperature gradient. Section C of Figure C-6(a) was used to determine the membrane stress and bending stress. The backplate was assumed fixed, whereas a membrane load was applied at the free end.

The membrane, bending, and thermal stresses for the three sections were predicted by utilizing a computer program for analysis of axi-symmetrically loaded shells of revolution. The bending stresses, particularly at the discontinuity, are primarily the result of line loads; however, some secondary stresses are included.

The temperature gradients for the three sections were for an operating time of 400 sec. Their distribution is shown along with their respective loading conditions.

VI. STRESS ANALYSIS

The predicted stress distributions for the Mod II Oxidizer Turbine backplate inlet stack and manifold housing are summarized in Figures C-7 through C-16. The design conditions investigated were limit load, ultimate load, and limit load with thermal gradients.

A. BACKPLATE ASSEMBLY

The tangential (hoop) stress and the meridional stress distribution for the backplate assembly is shown in Figures C-7 and C-8, respectively. The resultant stresses are the result of pressure loads and temperature gradient. The loading condition is shown in Figure C-5.

A maximum peak stress of 120 ksi, which is the meridional stress, occurs at the discontinuity between the manifold and backplate. This area also has the largest thermal gradients. The stresses (both meridional and tangential) throughout the backplate are quite small and therefore, do not present a structural problem.

B. MANIFOLD AND INLET STACK

1. Section A

The inlet stack-to-manifold was analyzed for the limit and ultimate condition as well as limit condition with temperature gradient. In this manner, the primary stress can be separated from the thermal stress. The tangential stresses, which were the most critical, are shown in Figures C-9, C-10 and C-11 for the above loading condition.

At the discontinuity near the backplate, large bending stresses (144,500 psi) resulting from the line loads were developed for the mechanical and thermal loading condition (see Figure C-12). The maximum bending stress includes a thermal hoop stress of 86,000 psi, which is self-limiting and is considered a secondary type of stress. Thus, the primary bending stress at a critical point is not too severe.

V. B. Oxidizer Turbine Backplate (cont.)

2. Section B

The tangential stresses at section B are more critical than in Section A mainly because the line loads are greater. The maximum stress occurs at the discontinuity between the inlet stack and the manifold housing (See Figures C-12 and C-13). The thermal stresses at this section are negligible because the temperature throughout the section is nearly uniform. Thus, the critical condition is the primary bending and membrane stress condition. A high membrane stress of 62,500 psi was the result of the bending caused by the membrane line load.

3. Section C

The critical stress condition at section C is caused by the tangential stress pressure and temperature gradients (see Figure C-16). The maximum tangential stress occurs in the vicinity of the backplate assembly. Because of the large thermal gradient at the discontinuity, large thermal bending stresses (124,000 psi) were developed.

The primary membrane and bending stresses at this section are shown in Figures C-14 and C-15 for the limit and ultimate loading condition.

C. STRESS SUMMARY AND MARGIN OF SAFETY

Table C-II summarizes the critical stress and Margin of Safety for the Mod II Oxidizer Turbine Backplate and Manifold housing. The stresses includes membrane, bending, and thermal stresses. For thermal conditions, the stress includes thermal membrane and bending stress.

TABLE C-II

MOD II OTPA BACKPLATE AND MANIFOLD STRESS SUMMARY

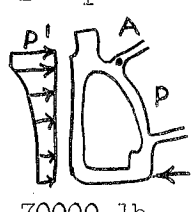
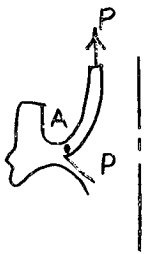
	Design Condition	Stresses @ Point A		Total Stress	Minimum M.S.
		Membrane	Bending		
Backplate  70000 lb	Limit mech + thermal loads p = 375 psi	10,000	110,000	120,000	1.50*

TABLE C-II (cont.)

	Design Condition	Stresses @ Point A		Total Stress	Minimum M.S.
		Membrane	Bending		
Manifold @ Section A 	Limit p = 375 psi p = 900 lb/in.	9,500	58,500	68,000	1.30
	Ultimate p = 495 psi p = 1090 lb/in.	16,500	67,500	84,000	1.66
	Limit and Thermal T = 650°F	1,500	144,500	146,000	.85*
Manifold @ Section B 	Limit p = 375 psi p = 2700 lb/in.	62,500	86,500	149,000	0
	Ultimate p = 495 psi p = 3830 lb/in.	88,000	121,000	209,000	.08
	Limit and Thermal T = 650°F	63,500	82,500	146,000	.85*
Manifold Section C 	Limit p = 375 psi	16,000	54,000	72,000	1.18
	Ultimate p = 495 psi	19,500	72,500	92,000	1.4
	Limit and Thermal T = 650°F	21,000	179,000	200,000	.35*

$$*M.S. = \frac{2 F_{ty}}{\sigma_{Total}} - 1$$

VII. CONCLUSION

The Mod II Oxidizer Turbine Backplate and Manifold housing and inlet has been investigated for the most critical operating condition; that is, mechanical load combined with thermal loads.

Using the design criteria established for the Margin of Safety, two margins of safety were reported herein. One for primary membrane combined with primary bending, and the other for the total stress which includes primary and secondary stress. The secondary stresses in this case is thermal bending.

The most critical section investigated is the inlet stack-to-manifold juncture in the circumferential direction. The M.S. for the primary stress condition is M.S. = 0. The biggest factor affecting the stress is the line loads which in this analysis was quite conservative.

Based upon the analysis presented herein, the M-1 Mod II Oxidizer Turbine Inlet Manifold and Backplate Assembly design has adequate structural integrity to withstand the applied loads and design operating condition.

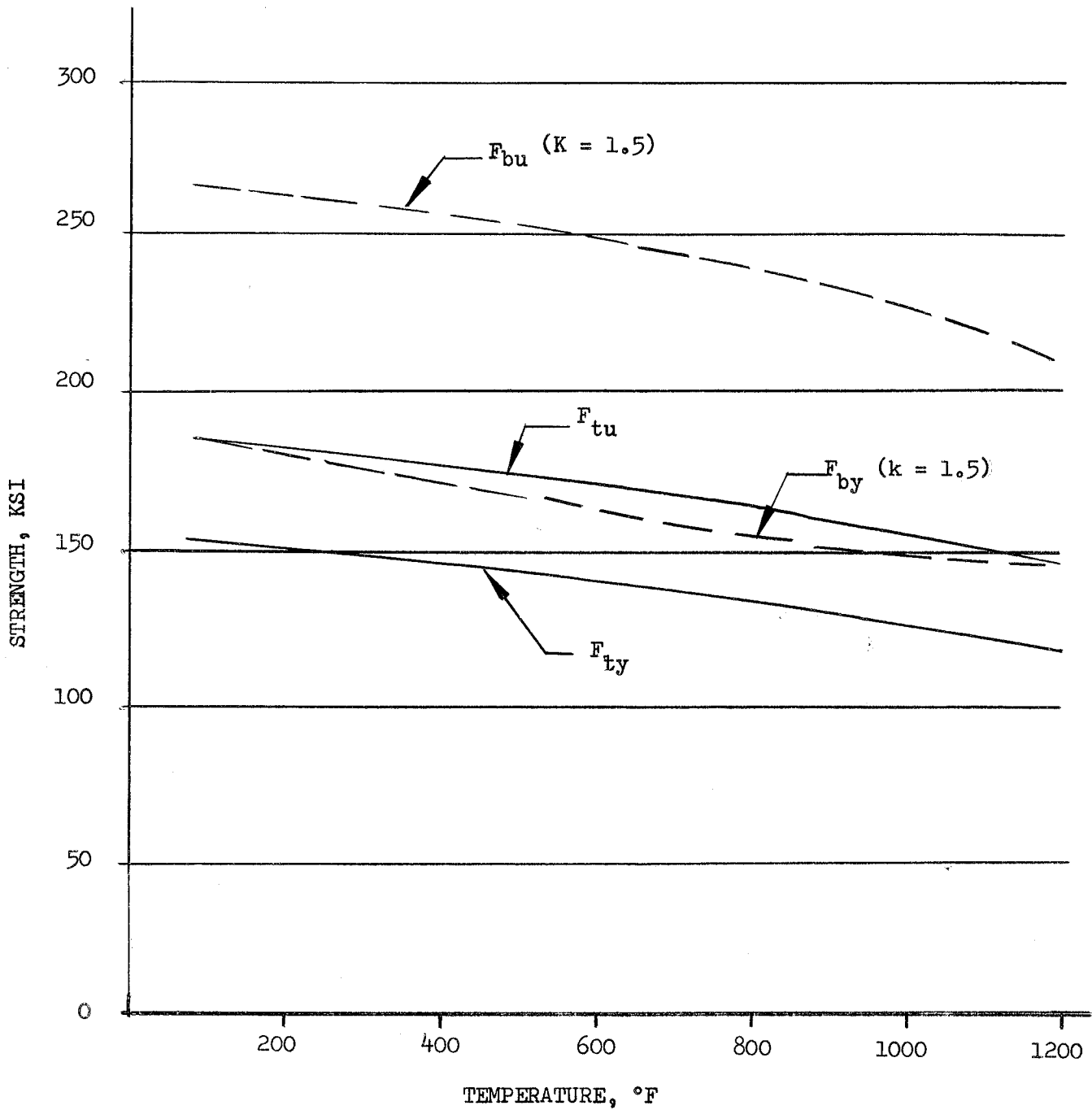
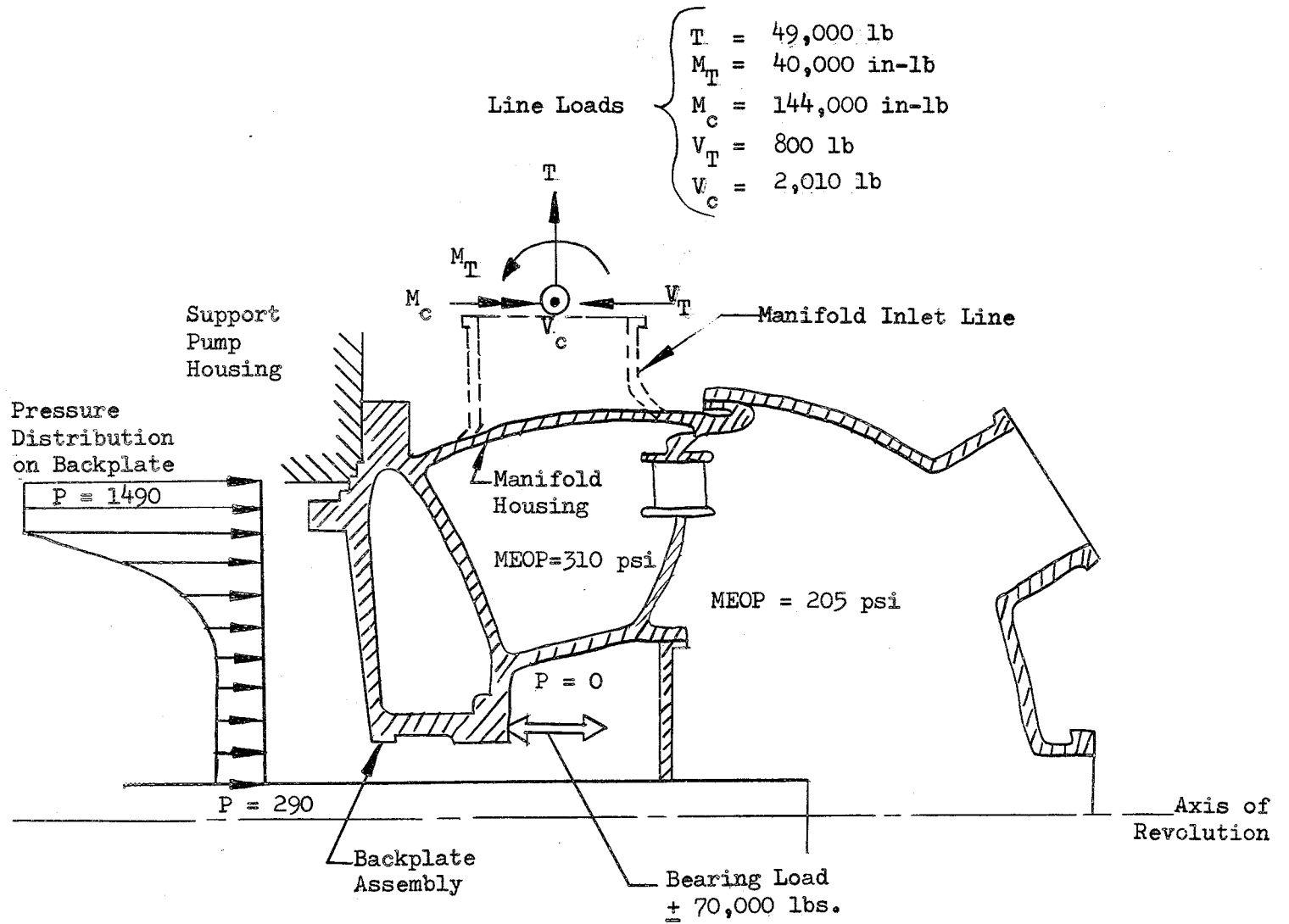


FIGURE C-3
 MECHANICAL PROPERTIES OF INCONEL 718

FIGURE C-4



NOTE: DESIGN PRESS (LIMIT)
 $P = \text{MEOP} \times 1.2$

TEMPERATURE DISTRIBUTION @ 400 SEC.
 (TEMP = °F)

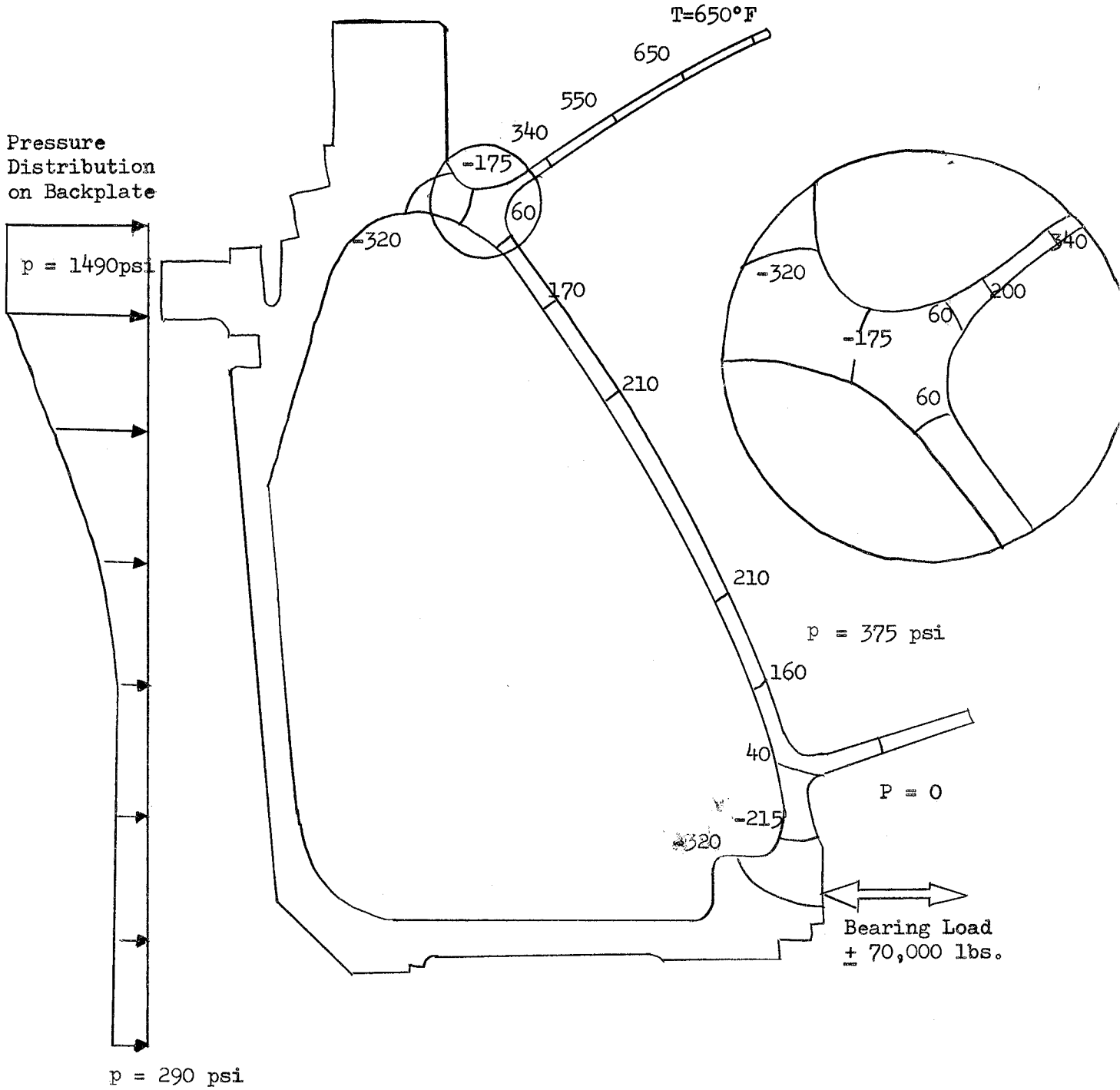


FIGURE C-5

MECHANICAL AND THERMAL LOADS - BACKPLATE ASSEMBLY

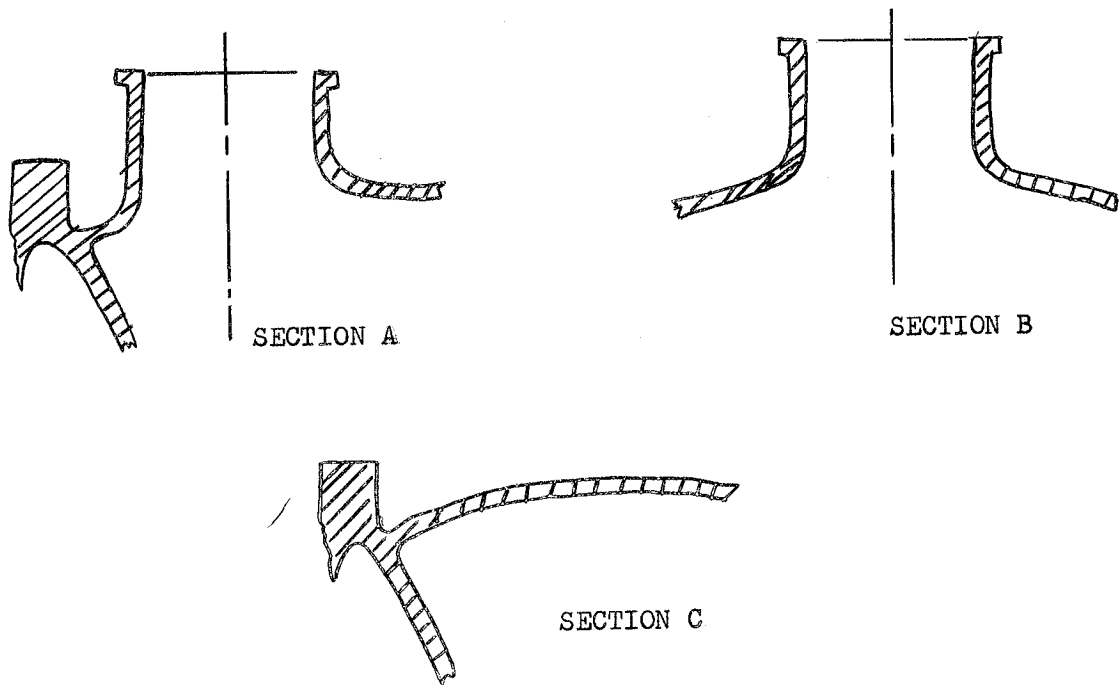
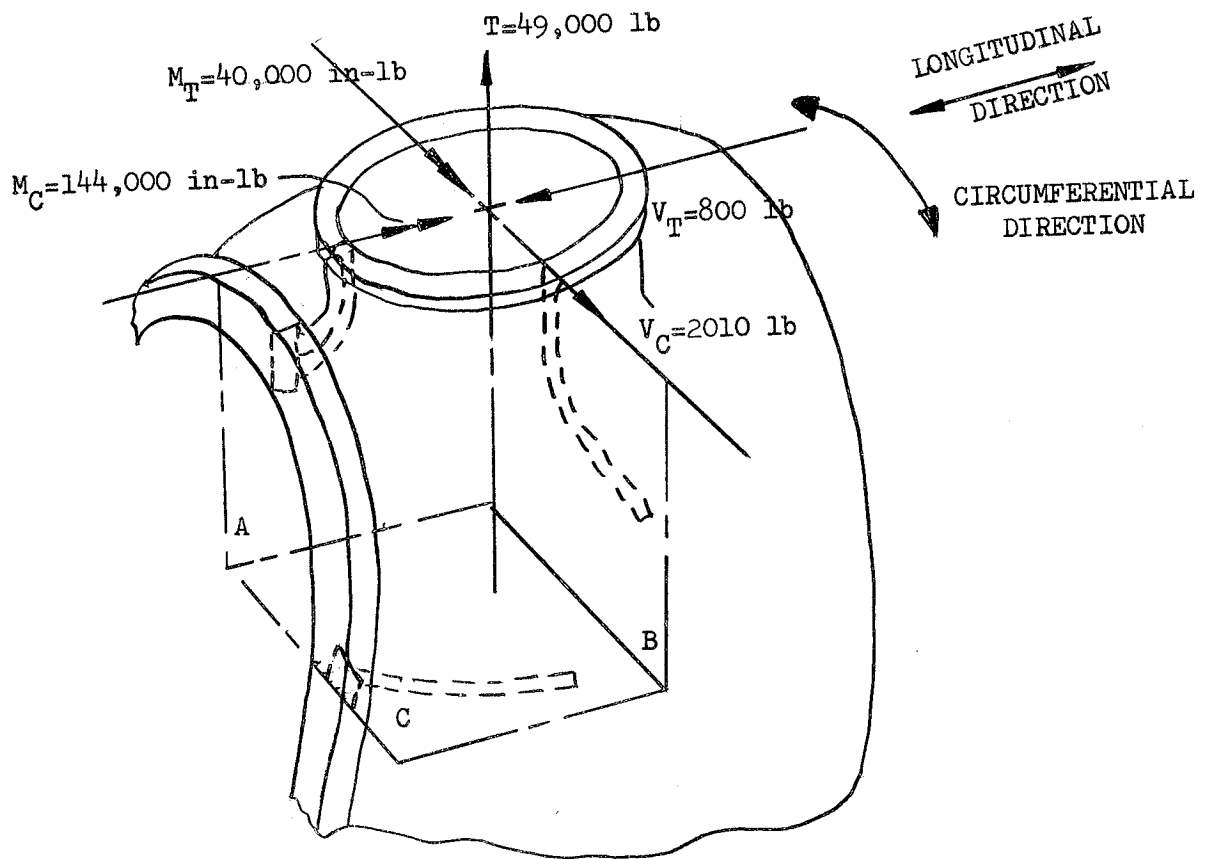


FIGURE C-6a

LINE LOADS AT MANIFOLD INLET

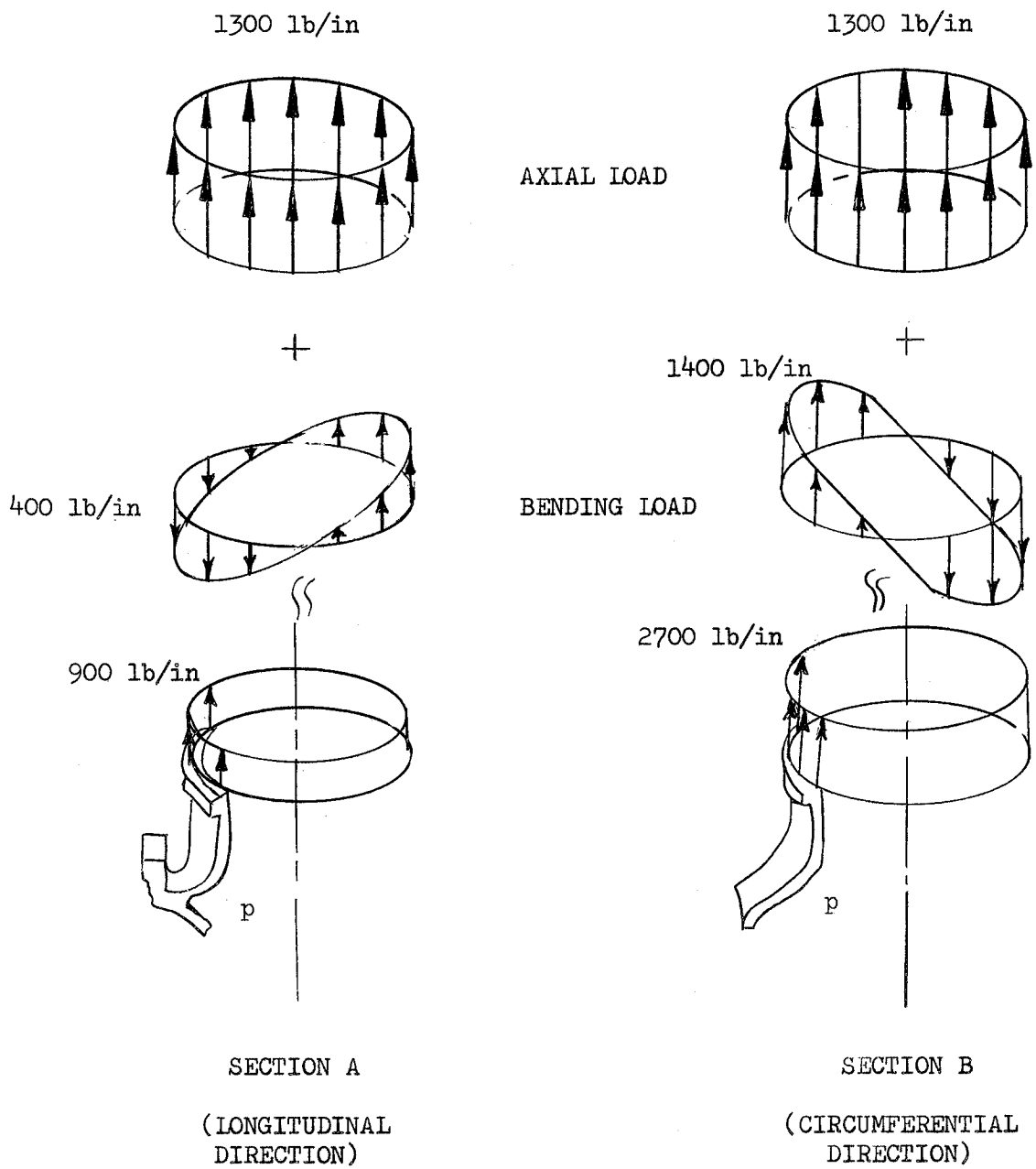


FIGURE C-6b
 LINE LOAD DISTRIBUTION AT MANIFOLD INLET
 (LIMIT CONDITION)

Note: Stress in KSI

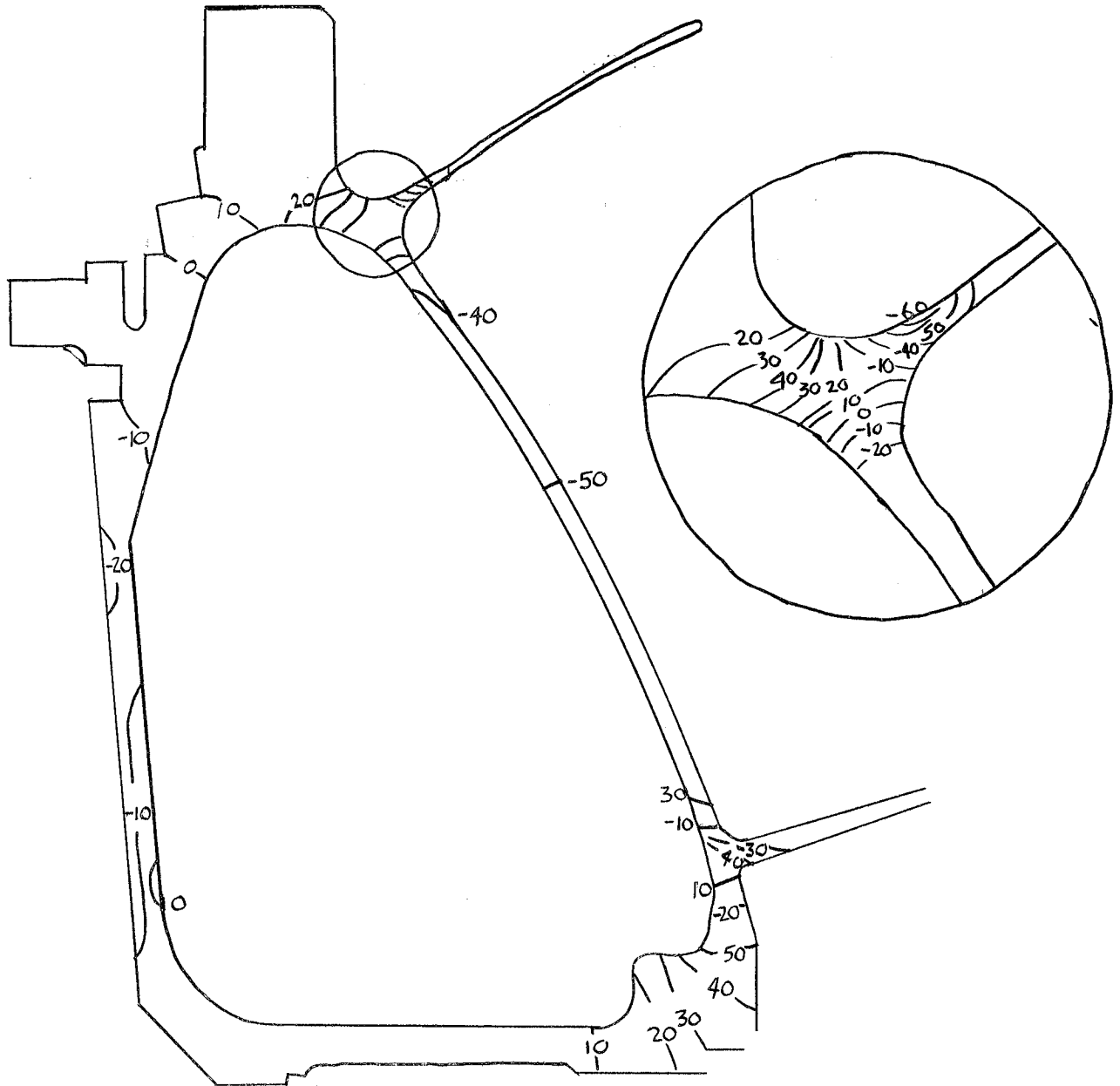


Figure No. C-7

Tangential Stress Distribution - Backplate Assembly

Note: Stress in KSI

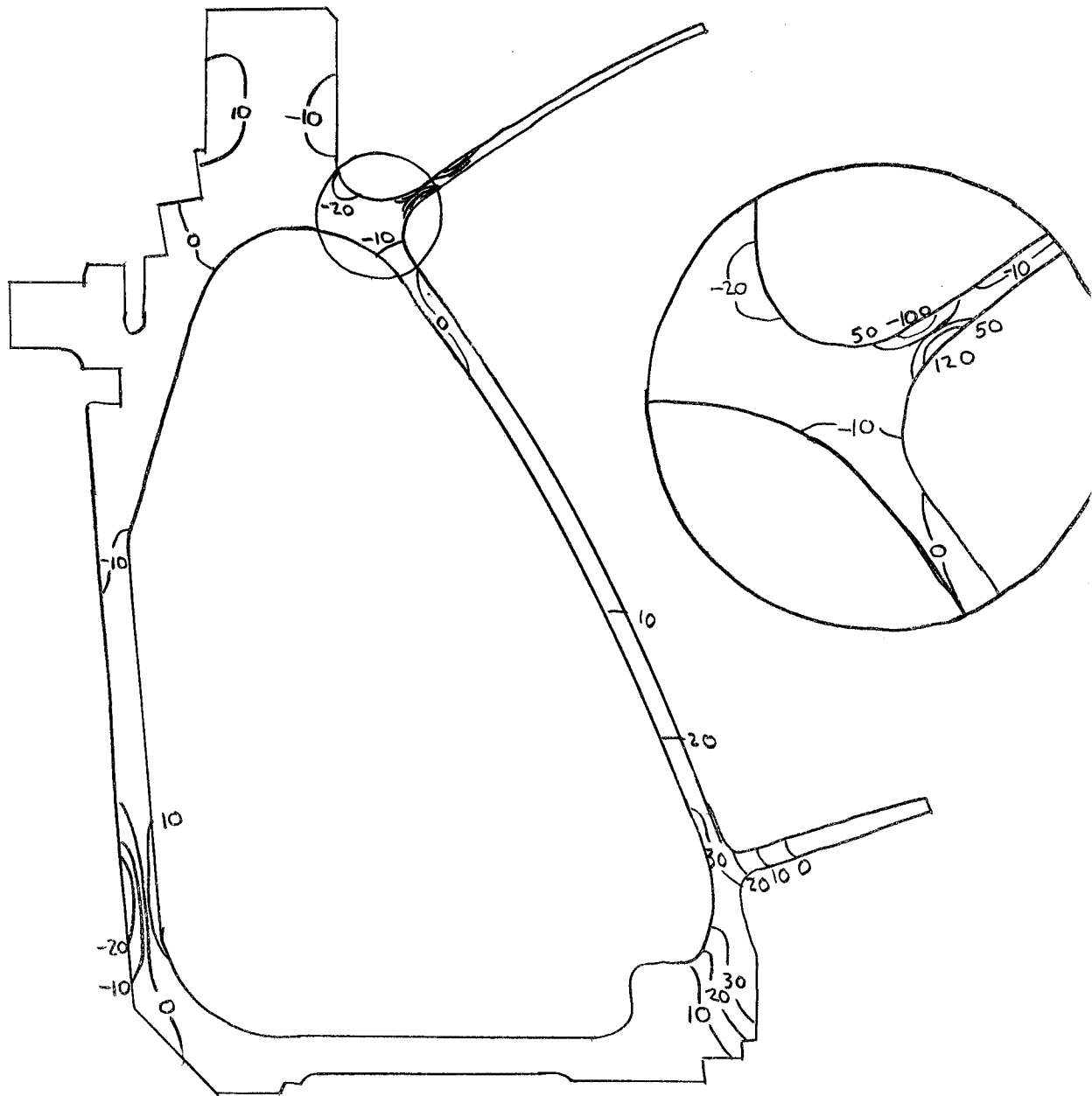
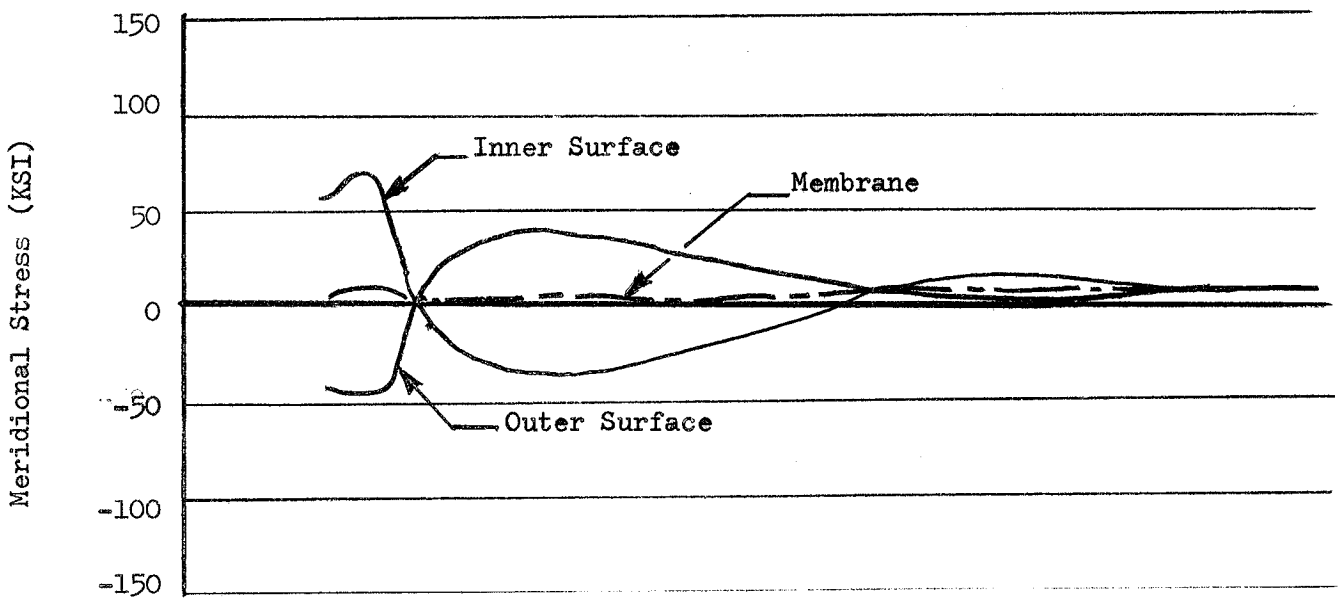
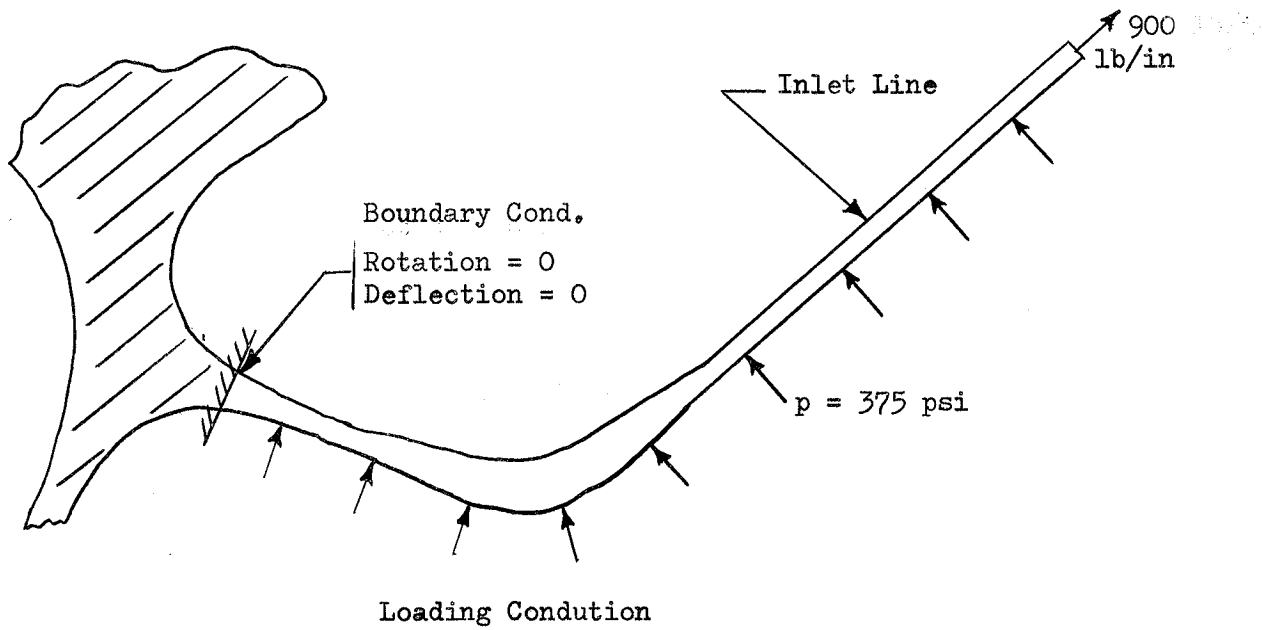


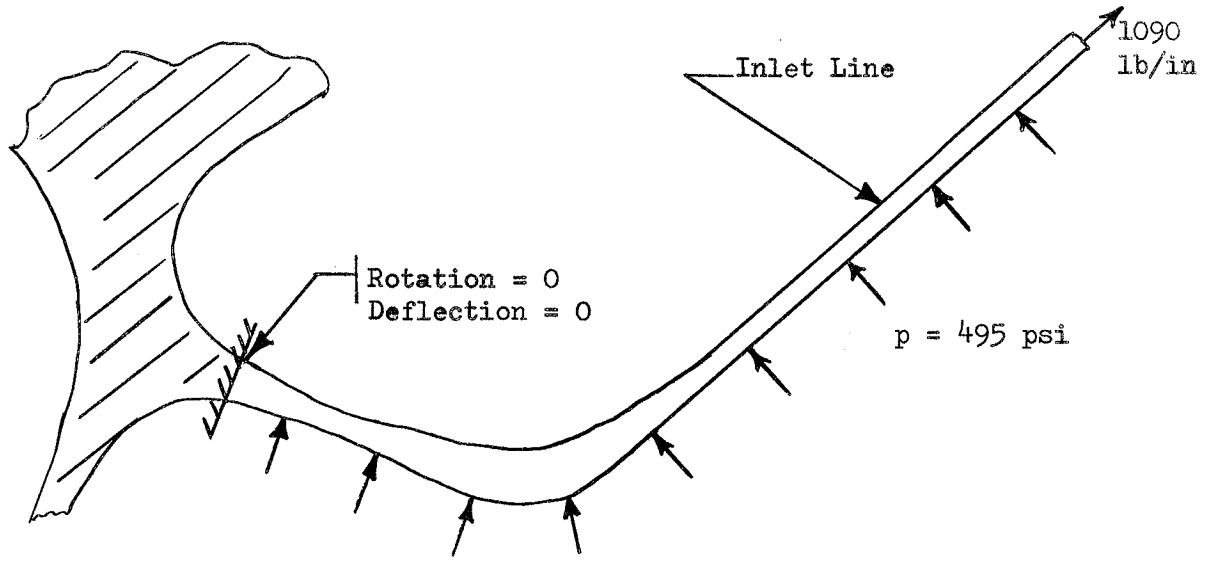
Figure No. C-8

Meridional Stress Distribution - Backplate Assembly

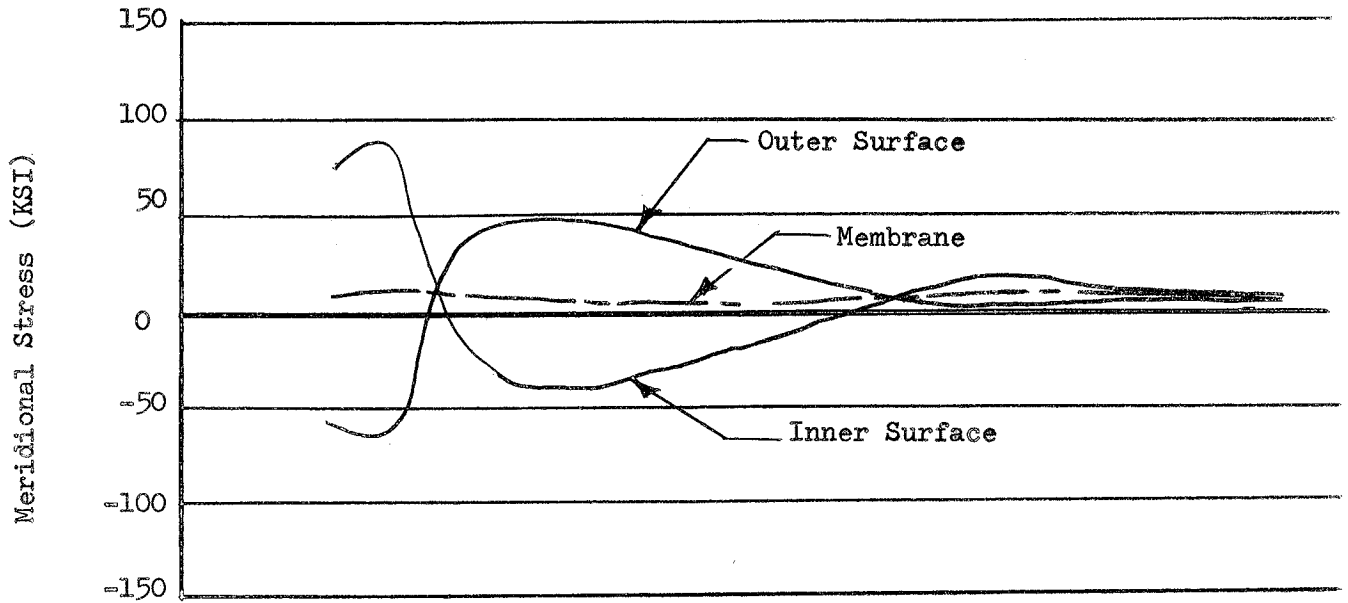


Stress Distribution

Figure No. C-9
Manifold Inlet at Section A
(Limit Condition)



Loading Condition



Stress Distribution

Figure No. C-10

Manifold Inlet at Section A
(Ultimate Condition)

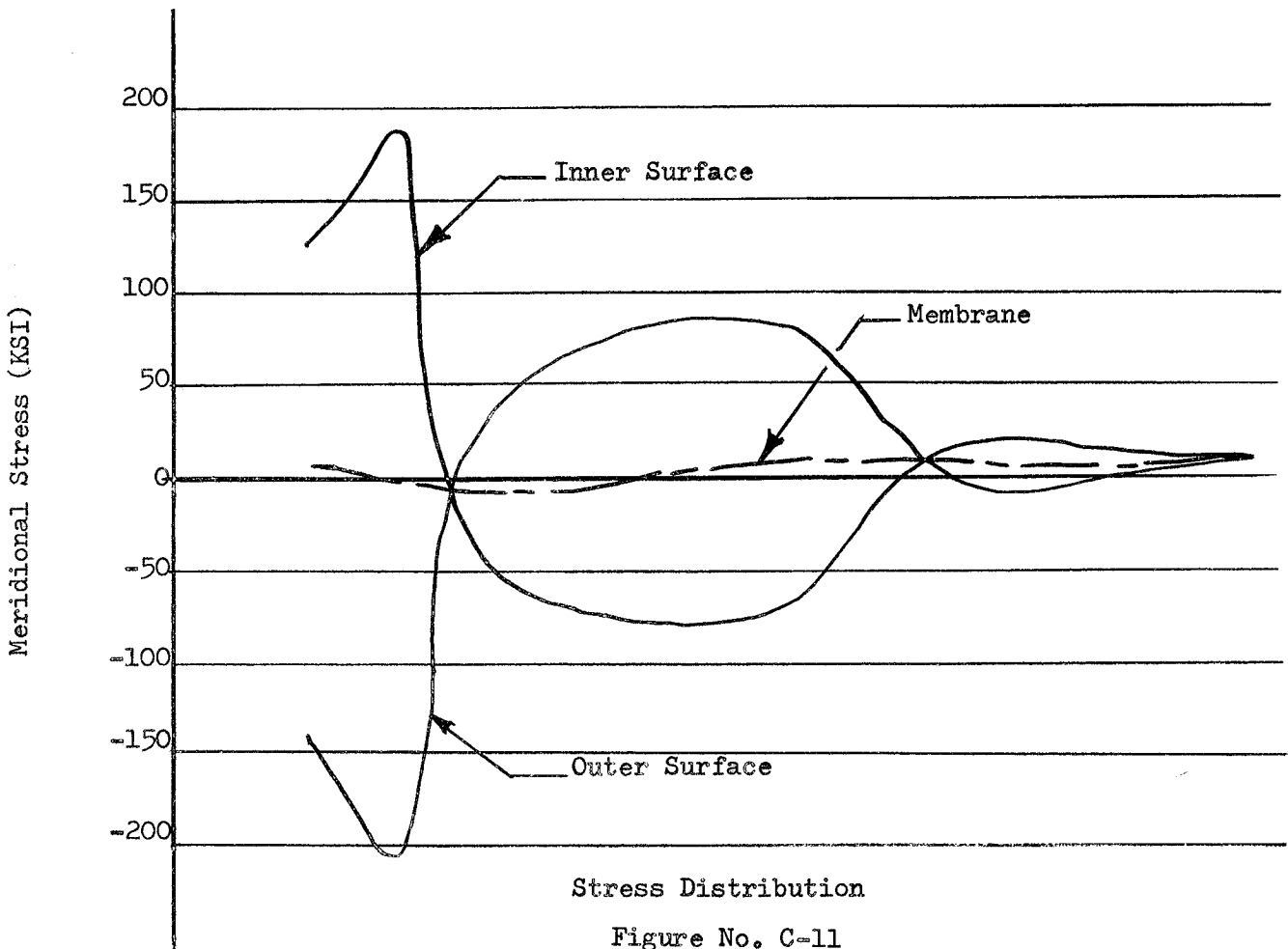
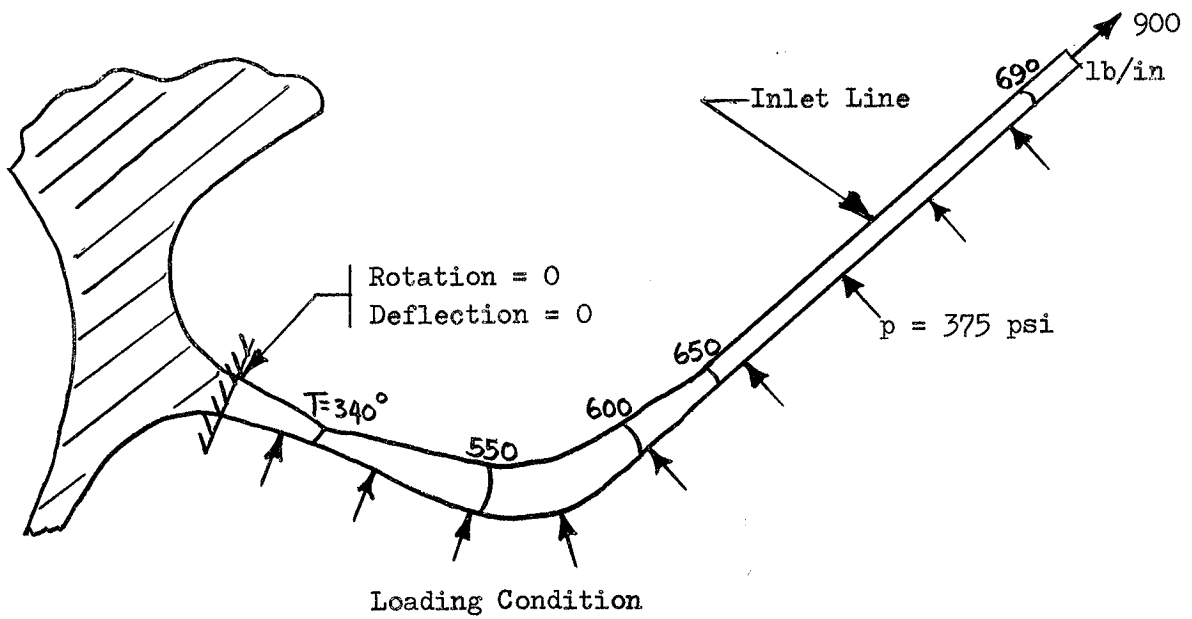


Figure No. C-11
Manifold Inlet at Section A
Limit Load + Thermal Load
(Temperature at 400 sec)

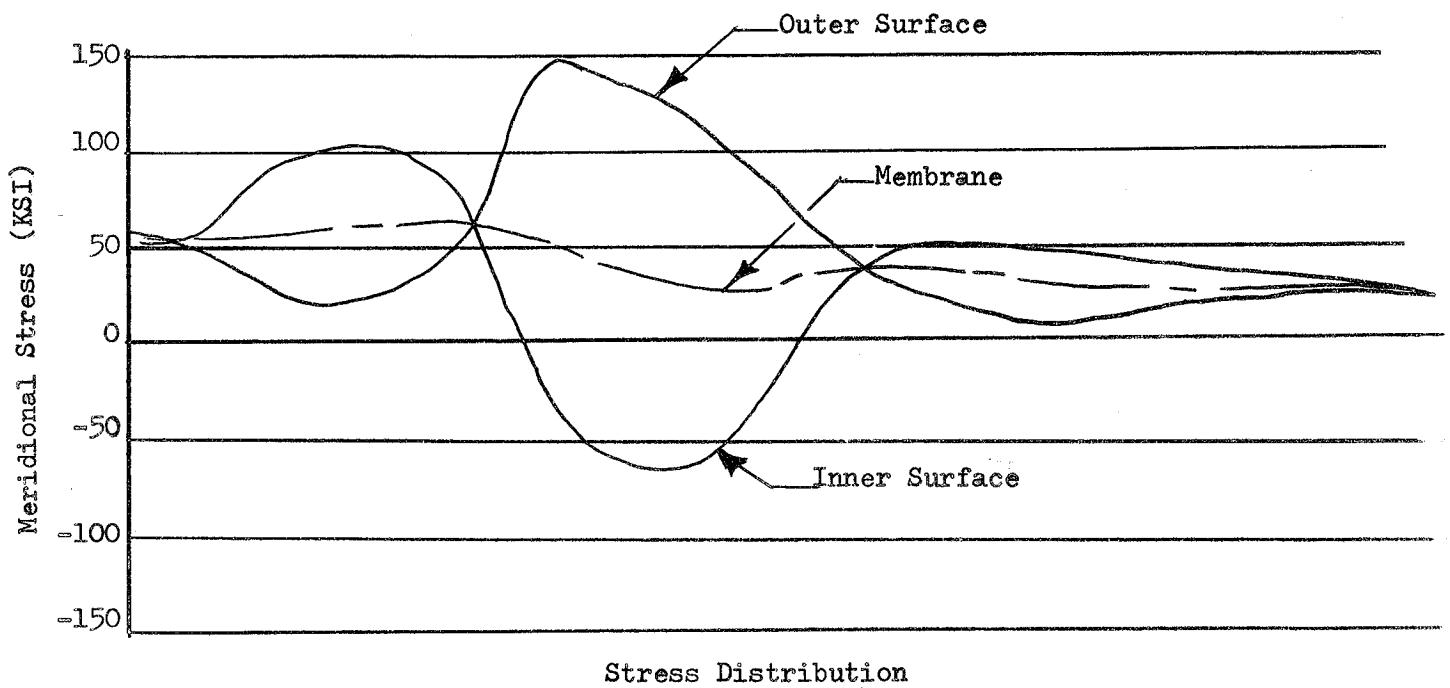
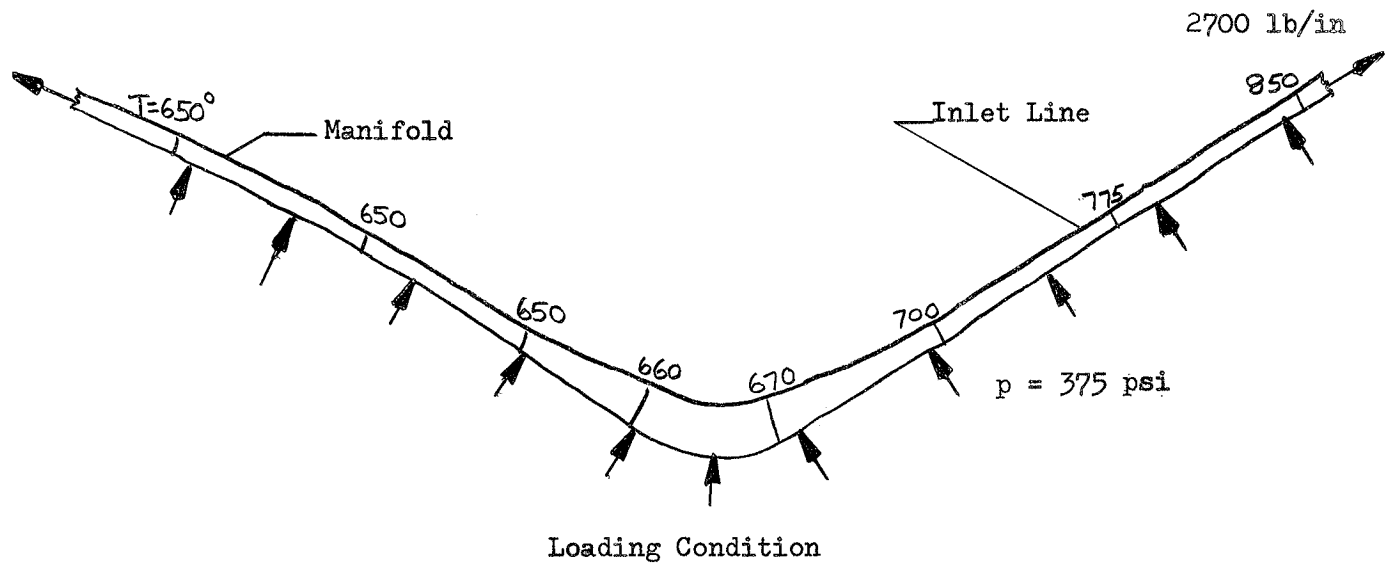
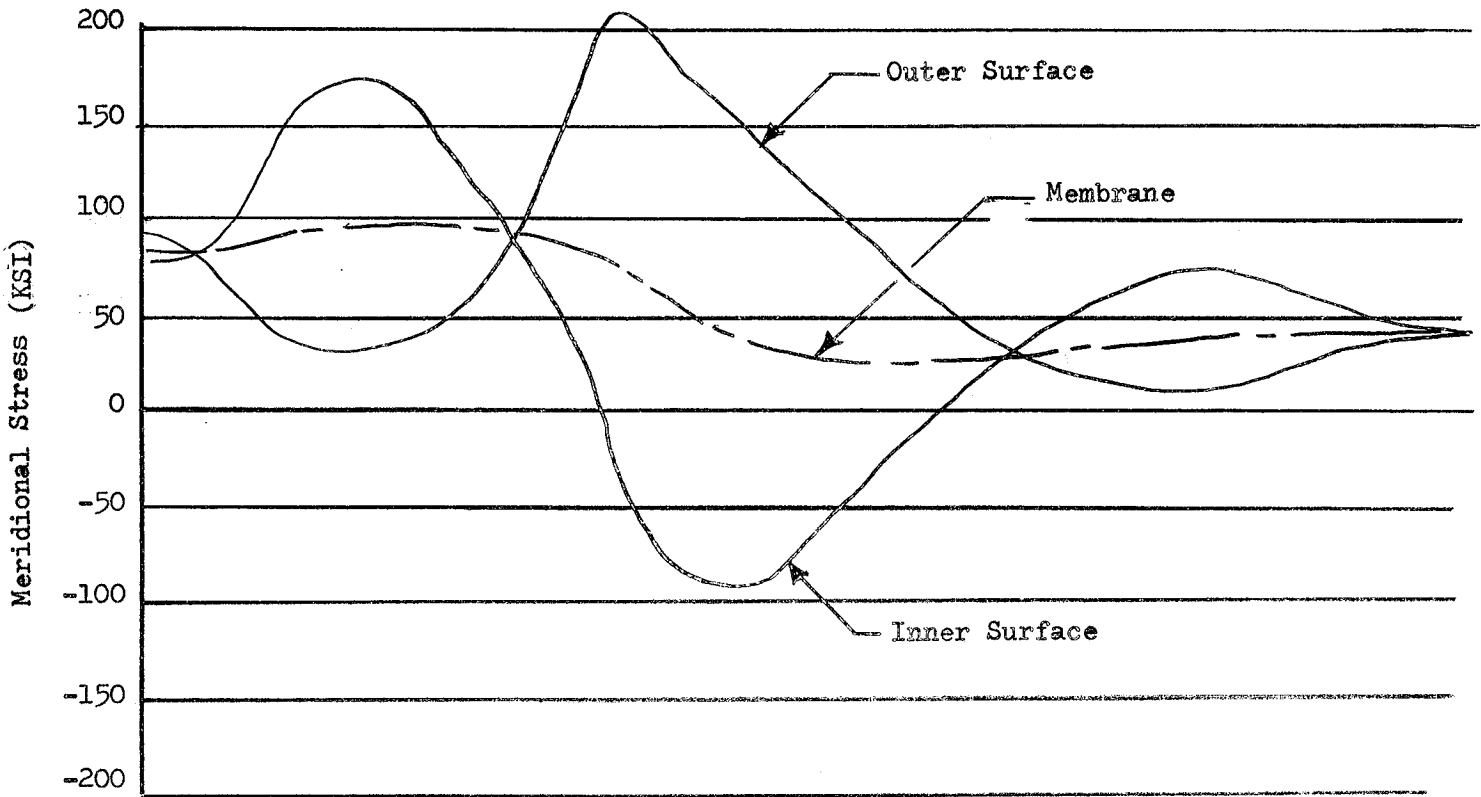
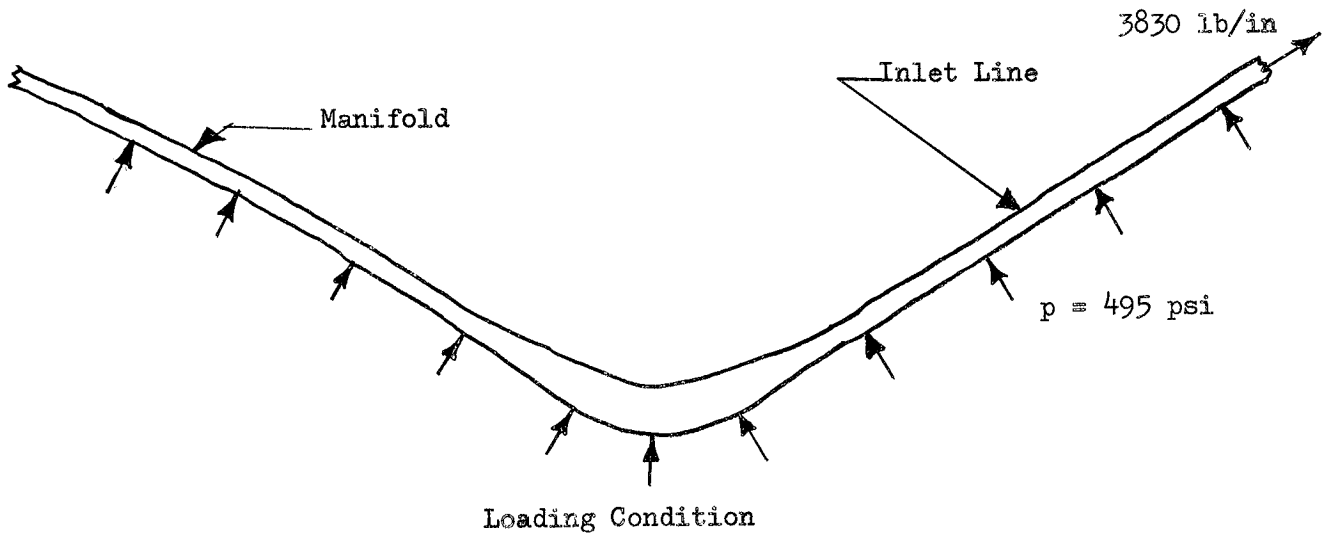


Figure No. C-12

Manifold Inlet at Section B
 Limit Load + Thermal Load
 (Temperature at 400 sec)



Stress Distribution

Figure No. C-13

Manifold Inlet at Section B
(Ultimate Condition)

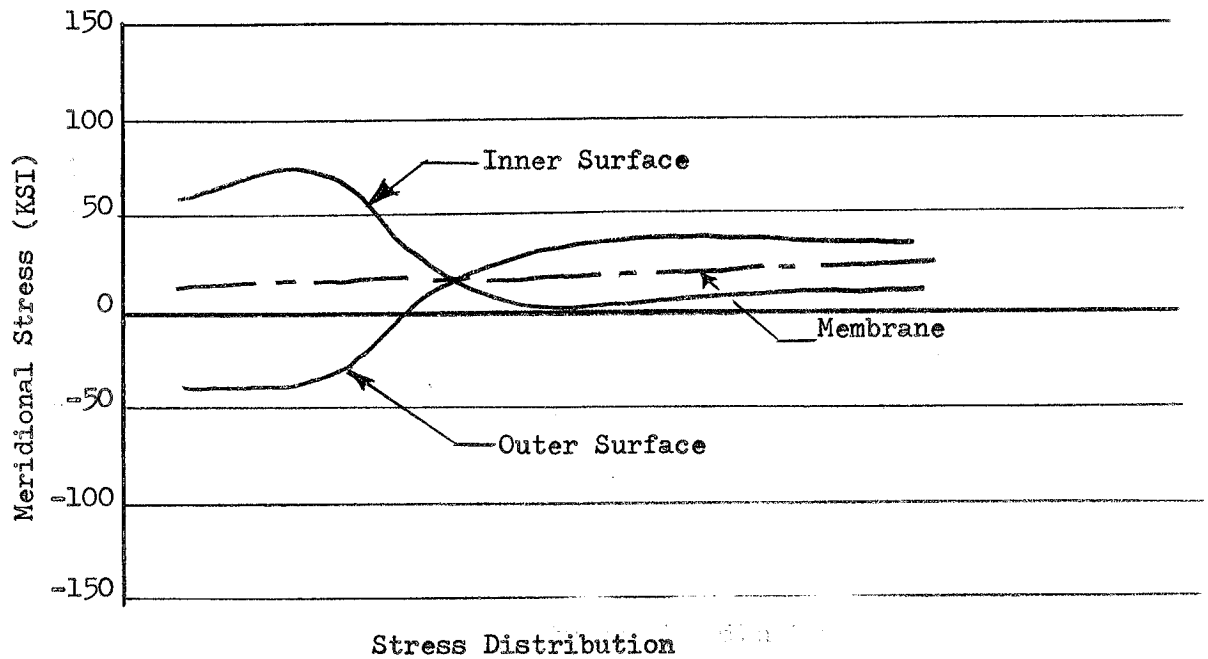
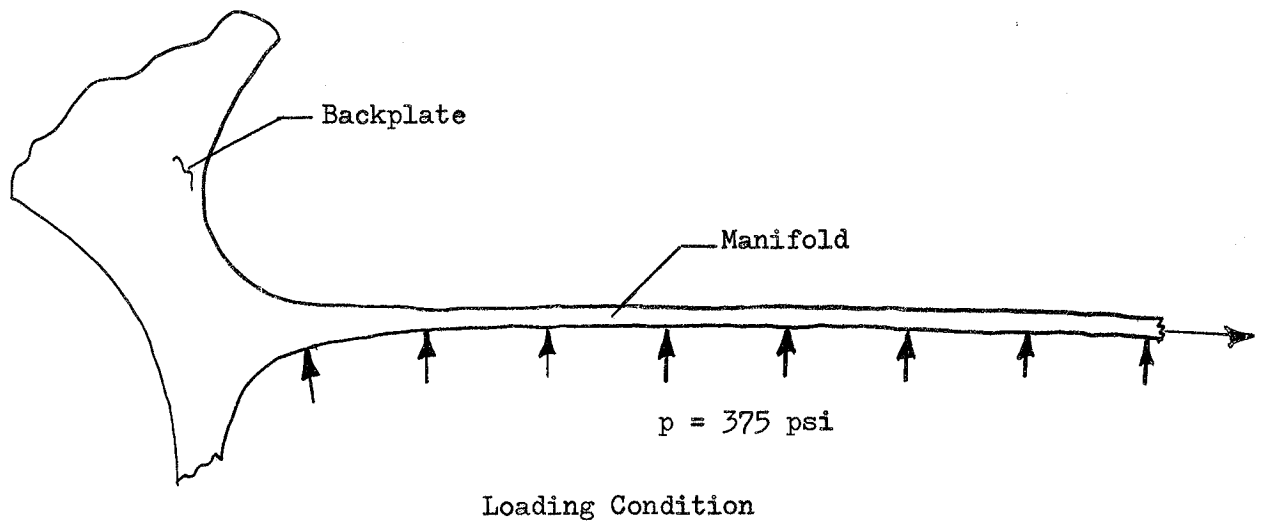


Figure No. C-14
 Manifold at Section C
 (Limit Condition)

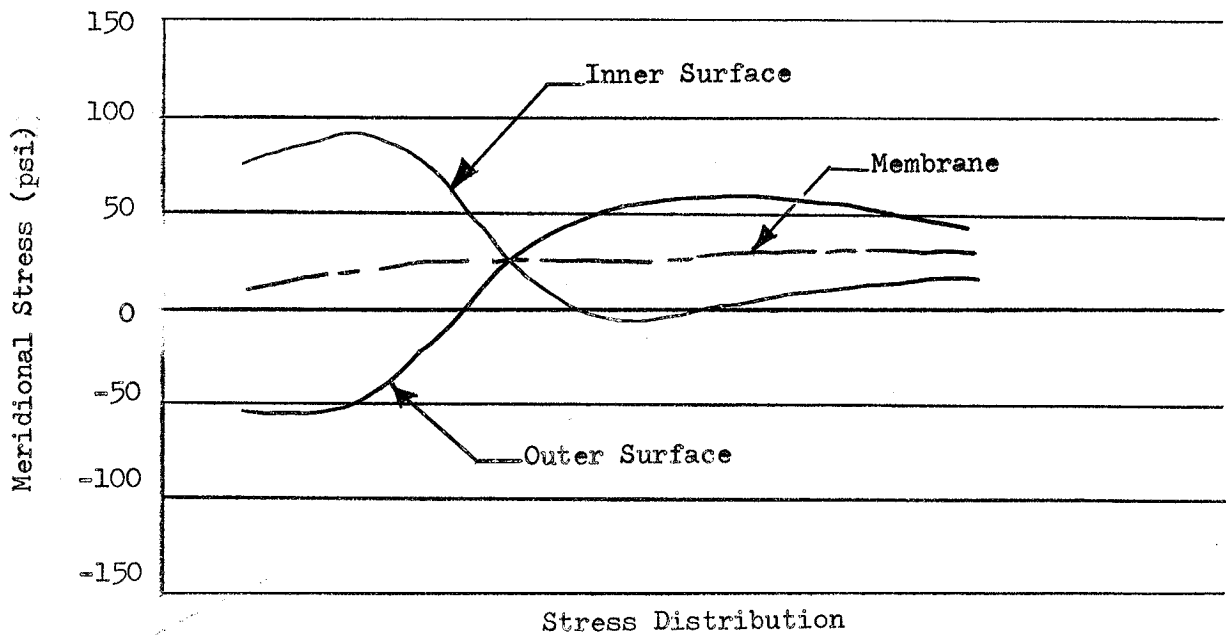
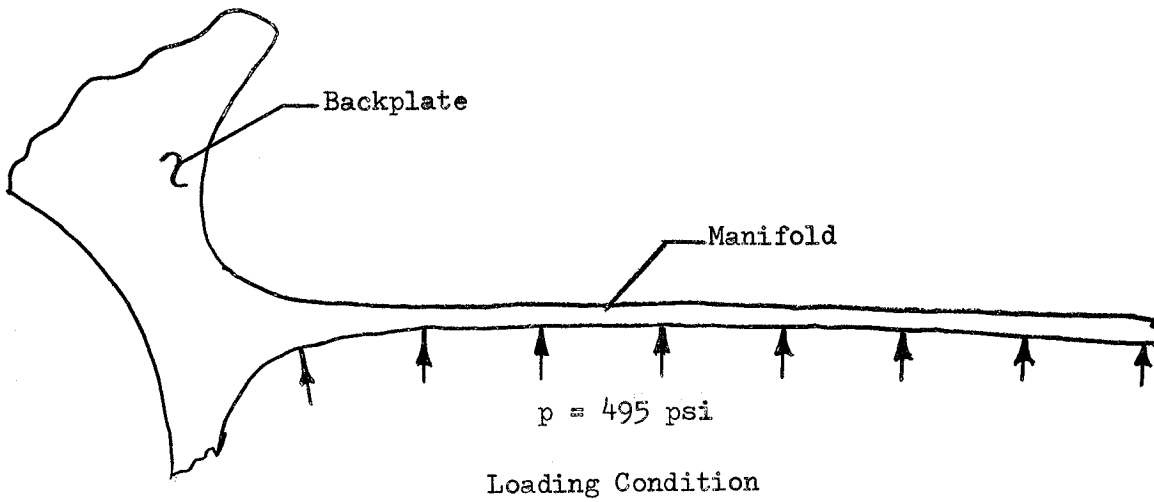
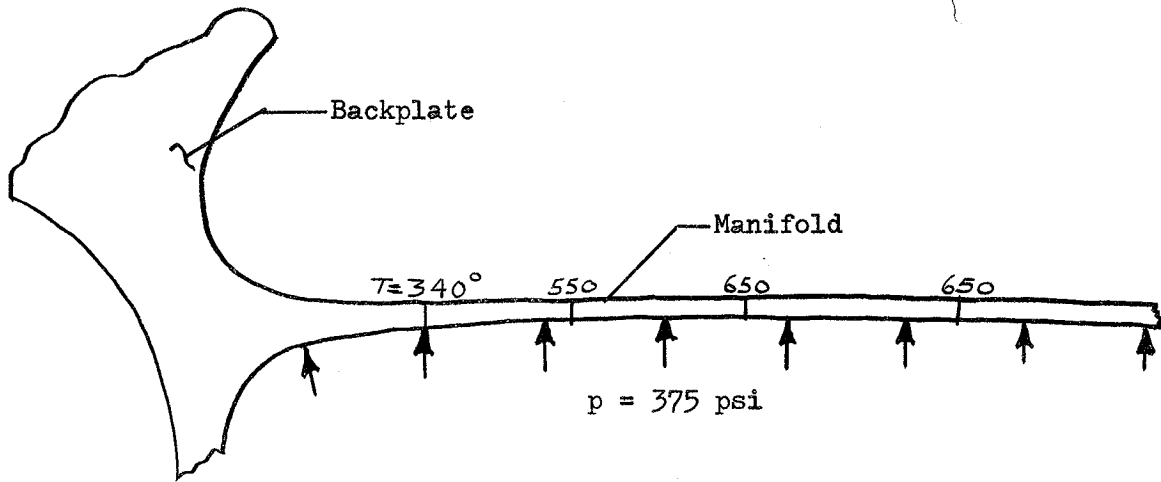
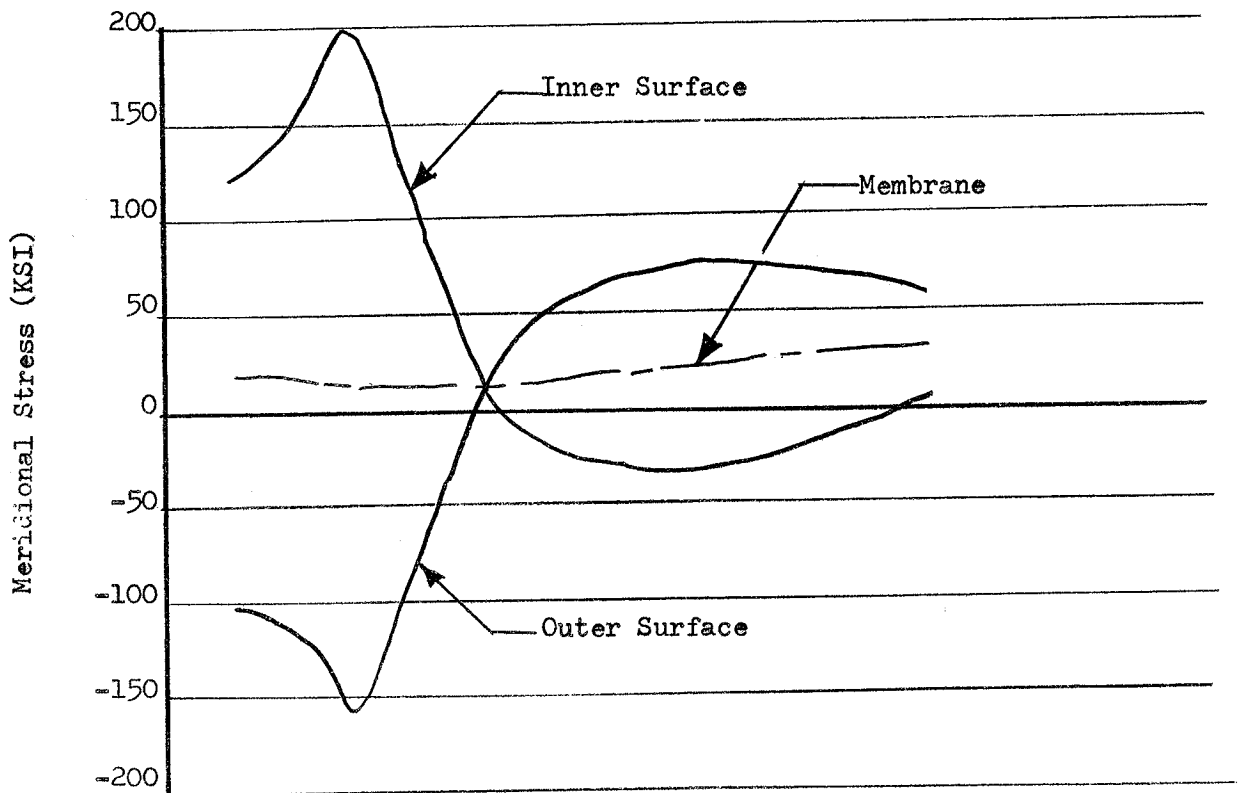


Figure No. C-15
 Manifold at Section C
 (Ultimate Condition)



Loading Condition



Stress Distribution

Figure No. C-16

Manifold at Section C
 Limit Load + Thermal Load
 (Temperature at 400 sec)

APPENDIX D

TECHNOLOGY USED IN FABRICATING THE TURBINE
INLET MANIFOLD, PUMP BACKPLATE, AND TURBINE
SUPPORT STRUCTURE ASSEMBLY FOR THE FLIGHT TYPE
M-1 OXIDIZER TURBOPUMP

TABLE OF CONTENTS

	<u>Page</u>
I. <u>INTRODUCTION</u>	D-2
II. <u>TECHNICAL DISCUSSION</u>	D-2
A. MATERIALS	D-2
B. DETAIL FORMING	D-2
C. WELDING AND SHEET METAL DETAILS	D-2
D. MACHINING OF DETAIL PARTS	D-3
E. DETERMINATION OF WELD PARAMETERS	D-3
F. ASSEMBLY WELDING OF BACKPLATE (286506-9)	D-4
G. ASSEMBLY WELDING OF MANIFOLD (286503-9)	D-5
H. WELDING OF MANIFOLD/BACKPLATE ASSEMBLY (286502-9)	D-5
I. HEAT TREATMENT OF ASSEMBLY	D-6
J. HYDROSTATIC TEST AND HELIUM LEAK CHECK	D-6
K. MACHINING OF ASSEMBLY (286501-9)	D-7

LIST OF FIGURES

<u>Figure No.</u>	<u>Title</u>	
D-1	Manifold Inlet - Rough AGC Drawing No. 286503 (2 sheets)	D-10
D-2	Backplate, Oxidizer Pump - Rough AGC Drawing No. 286506 (9 sheets)	D-12
D-3	Manifold, Inlet-Weldment AGC Drawing No. 286502 (2 sheets)	D-21
D-4	Technical Sheet - Hydrotest AGC Drawing No. 286507	D-23
D-5	Manifold Inlet AGC Drawing No. 286501 (6 sheets)	D-24

I. INTRODUCTION

The turbine inlet manifold, pump backplate, and turbine support structure for the flight-weight turbopump are made as one unitized component. This component is a composite weldment made chiefly from Inconel 718 material and involves fabrication complexity, precision machining, and details requiring high surface finishes. The unit was manufactured by the Rohr Corporation of Chula Vista, California, under subcontract to the Aerojet-General Corporation of Sacramento, California.

II. TECHNICAL DISCUSSION

The techniques and processes used in the fabrication of this part were primarily conventional. However, the experience gained, particularly in the weld preparation, welding, and more difficult machining operations with the relatively new Inconel 718 material, is of interest and not necessarily limited to this specific component.

A. MATERIALS

All raw materials, such as forgings, sheet, plate, bar, and tubing were certified by the supplier for mechanical and chemical specification compliance and reinspected in Rohr Laboratories. All Inconel 718 forgings were procured in the rough-machined condition with a minimum of 3/16-in. excess material for finish machining.

B. DETAIL FORMING

The majority of all detail parts were formed by conventional methods.

The 286503-21 skirt, (Figure D-1), was made from a rolled and welded metal cone and finish formed by explosives. The part was fully annealed prior to finish forming. Three explosive forming steps (shots) were required and the maximum charge used was seven strands of 100 grain primer cord. The forming was accomplished by the open die, open pit process.

The 286506-7 cover, (Figure D-2) was formed on a drop hammer using a conventional punch and die. One full anneal was required prior to finish-forming.

The tubes for the 286506-9 assembly (Figure D-2) were custom-formed using conventional tube forming equipment. A mockup of the assembly was used extensively as a guide.

C. WELDING OF SHEET METAL DETAILS

All rolled and welded rings for the 286503-9 inlet ducts (Figure D-1) were hand gas tungsten arc welded using a suspended bead. The cone for the 286503-21 skirt (Figure D-1) was automatic gas tungsten arc welded in the conventional manner. All welds were x-ray inspected.

D. MACHINING OF DETAIL PARTS

The 286506-5 bearing hub (Figure D-2) was semi-finish machined prior to welding. Holes that become inaccessible after welding were pre-drilled. Key-ways, thread recess, and the 0.035-in. diameter holes were electric discharge machined in the hub prior to welding.

Forgings for the 286503-3 flanges and the 286503-5 transition rings (Figure D-1) were finish machined with excess allowed for weld shrinkage.

Machining of the remaining detail parts consisted mainly of weld joint preparation.

E. DETERMINATION OF WELD PARAMETERS

Welding tests were conducted to evaluate contamination of base and filler metal as well as to determine the contributing causes of weld porosity.

1. Contamination of Base and Filler Metal

One test plate was welded as-received and wire brushed using an air-driven rotary stainless steel brush. The plate was degreased with double-distilled acetone prior to welding. The filler metal was used in the as-received, chemically-cleaned condition. Radiographic inspection revealed excessive porosity throughout the 12-in. weld bead; also, there was a crater void approximately 3/16-in. deep at the termination of the weld. This crater was attributed to insufficient tailing time; by increasing the tailing time the crater was eliminated.

The surface of four test plates was machined to remove all surface oxidation and degreased with double-distilled acetone prior to welding. Filler metal was used in the as-received, chemically-cleaned condition. Radiographic inspection showed that the weld was within the required (MIL-STD-453) specification.

Based upon the above results, the following procedures were used for all welding of Inconel 718 material:

- a. All surface oxidation was removed prior to welding.
- b. The weld area was hand cleaned with double-distilled acetone prior to welding.
- c. Tailing time was extended to eliminate crater cracks at the end of a weld or tackweld.

2. Preflow of Shielding Gas

Three types of tests were conducted to evaluate the effects of pre-flow torch purging. These included no pre-flow gas shielding, 15 sec pre-flow shielding, and 3 minutes purging with 15 sec pre-flow prior to welding.

III. WELDING OF INCONEL 718

Test plates welded with no pre-flow shielding prior to welding exhibited excessive porosity at the beginning of each weld.

Test plates welded with a 15 sec pre-flow shielding exhibited porosity at the beginning of the weld for approximately 1-1/2-in.

Test plates welded with a 3 minute torch purge and 15 sec pre-flow were acceptable for production welding.

Based upon the above results, 3 minute purging of manual and automatic torches with inert gas prior to welding was made standard procedure.

3. Inert Gas Shielding

Helium and Argon inert gas shielding were evaluated for automatic and manual welding of Inconel 718.

Helium provided definite advantages over Argon in welding thick sections (0.090-in. and over) because it eliminated a lack of fusion in multiple pass welding, minimized porosity, and increased the welding speed. Arc stability was more difficult to maintain at lower currents with helium; consequently, all material under 0.090-in. thickness was welded with Argon. The transition from poor arc stability to good arc stability occurred at 65 amperes to 75 amperes.

The Linde Gas Lens was used for automatic and manual welding to eliminate turbulence of the gas, which is a source of weld contamination.

4. Tack Welding

In an attempt to eliminate cold spots on the root side of the weld in areas of tack welding, two methods of tack welding were investigated. Six weld test samples of 0.063-in. Inconel 718 material were prepared for butt welding. Three of the test samples were tack welded on the face side of the weld joint; the remaining were tack welded from the root side of the weld joint. The automatic inert gas shielded tungsten arc welding process was used at optimum machine settings for welding all specimens.

Samples tack welded on the face side of the weld joint exhibited cold spots throughout the root side of the weld.

Specimens tack welded on the root side of the joint exhibited a uniform bead free of cold spots. It was concluded that this method was to be used whenever possible.

F. ASSEMBLY WELDING OF BACKPLATE, 286506-9 (Figure D-2)

The problems encountered with this first main weldment were mainly warpage and distortion rather than metallurgical.

flange (Figure D-1) followed by four equally spaced 3-in. long welds around the same diameter. As welding progressed, the 286503-21 shell (Figure D-1) warped inwardly. Dry ice and shorter welds were used to complete the welding. Although the inward movement of the 286502-21 shell (Figure D-1) did not increase, there was a severe mismatch (.10-in.) of the 286503-21 shell and the 286503-5 flanges. This was corrected by depositing filler metal to the distorted area and then grinding to fair with adjacent parent metal without any sacrifice in structural strength.

Because of the inward movement of the 286503-21 shell (Figure D-1), the weld shrink allowance disappeared and the centerline-to-flange face dimension of the ducts was approximately 0.150-in. short. The ducts were out-of-round and required straightening before the 286503-3 flanges (Figure D-1) could be attached, using weld buildup to compensate for the short dimension.

I. HEAT TREATMENT

After completion of welding, the solution anneal and age operations were performed. The assembly was degreased prior to positioning in the heat treat fixture, which was made from Hastelloy "X" material. Hastelloy "X" has a coefficient of expansion equivalent to Inconel 718.

For temperature control, thermocouples were attached to both light and heavy sections of the assembly as well as to the fixture. The retort was of the sand seal type, also constructed of Hastelloy "X" material. Three tubes were used to purge the inside; one routed inside the 286506-9 cavity (Figure D-2), the second inside the 286502-21 shell (Figure D-3) while the third was near the top center portion. The assembly was cold purged with argon for two hours prior to placing it into the furnace.

The retort was positioned in a preheated furnace which was then elevated to 1950°F, as measured by the attached thermocouples, and held for one hour. It was then removed from the furnace and force-cooled by fans to room temperature. Again, the retort and its contents were inserted into the furnace at 70°F and elevated to 1350°F and held for 10 hours. Then, the temperature was reduced to 1200°F and held for another 10 hours. The retort was removed from the furnace and cooled to room temperature before opening. The assembly was slightly discolored, reflecting the presence of some impurities in the argon gas. Test specimens were included in the retort. These were analyzed and found to be within specification requirements.

J. HYDROSTATIC TEST AND HELIUM LEAK CHECK

Successful hydrostatic test and helium leak check (per 286507, Figure D-4) of the turbine housing was accomplished in a heavy four-piece fixture.

With all elements of the test fixture in place, both cavities were pressurized with water to 245 psi and checked for leaks. The pressure in the upper cavity was then elevated to 375 psi and once again checked for leaks. Pressures held steady in both cavities for the specified time.

Automatic multiple pass welding was used in welding the 286506-3 plate to the 286506-5 inner ring and the 286506-1 outer ring (Figure D-2). The initial welding sequence created cracks in both weld joints. This was corrected as subsequent weld passes were deposited, adding strength to the weld root. When the second unit was welded, the condition of initial cracking was eliminated by depositing the first weld pass on the root side of the weld prior to completing the weld on the face side. Shrinkage from both weld joints moved the inner ring upward and out of position approximately 3/8-in. Four hundred tons were required to cold straighten the assembly on a hydropress.

Welding and straightening was followed by rough machining all over, finish machining inside the cavity, and completion of drilling. Tubes were formed and trimmed to fit. Joints were trimmed short, thus permitting burn-through welds to eliminate contamination pockets. Tubes were individually installed, gas purged, tack welded, and welded. All joints were x-rayed to determine the burn-through quality of welds and the tubes were then hydrostatically tested and leak checked with helium.

The inner cavity was cleaned and inspected prior to fitting and welding the 286506-7 cover plate (Figure D-2). Shrinkage once again moved the inner ring upward. In the process of straightening, the spherical radius of the cover changed to a conical contour. After straightening, the assembly was stress relieved.

G. ASSEMBLY WELDING OF MANIFOLD, 286503-9 (Figure D-1)

The duct assemblies were fabricated by welding five rings together. The 286503-3 flange was omitted at this time as a joint was required to correct for weld shrinkage and tolerance build-up at final assembly.

Weld porosity, which was prevalent throughout the program, was the only source of trouble with this part.

H. WELDING OF MANIFOLD AND BACKPLATE ASSEMBLY, 286502-9 (Figure D-3)

Problems in connection with the final joining of the two major subassemblies were caused mainly by warpage and shrinkage. A subassembly of the 286502-11 flange and the 286502-5 cone (Figure D-3) when welded to the 286506-9 assembly, (Figure D-3), resulted in a short dimension. This was corrected by adding an attached shim after final machining.

The 286506-9 assembly, (Figure D-3) was machined for fit-up of the shell 286502-1 (Figure D-3) allowing additional material for shrinkage.

The inlet ducts were then attached to the other manifold components that were already welded to the backplate. To assure fit-up, it was necessary to skip tack weld at increments of 3/4-in. around the 15.08-in. diameter of the 286503-5

The assembly was then drained and the test fixture removed. After drying, the fixture was repositioned for the helium leak check. Helium was pumped into both cavities and pressurized to 125 psi, showing no indications of leakage by mass spectrometer check. The pressure in the upper cavity was increased to 185 psi and again showed no leaks.

K. FINISH MACHINING 286501-9 (Figure D-5)

After inspecting the 286502-9 assembly (Figure D-3) to determine stock removal allowances and out-of-roundness, the assembly was mounted with the open end down on the lathe fixture. With the assembly in place, the fixture was mounted on a King Vertical Turret Lathe and indicated for concentricities and flatness. By using hydraulic leveling jacks on the fixture, the assembly was positioned concentric and flat to within .001 TIR. For machining of the outside diameter, the assembly was clamped through the bore with a large washer.

During rough machining of the outside diameter, the flange face, and the Conoseals*, the lathe fixture had to be reinforced to maintain concentricity. After rough machining, the assembly was unclamped and allowed to stabilize before re-clamping and finish-machining. The Conoseal contour was machined with a form tool to within a few thousandths of an inch of drawing dimensions, to be finished by subsequent polishing.

When the outside diameter was semi-finish machined, fixture clamps were secured on the outside flange and the center clamping arrangement removed. All surfaces were rough cut with the exception of the five degree angular face which is held to gauge point dimensions. A tracing attachment was installed and coordinated to previously machined surfaces. Single point tracing with a Valenite V-7 carbide tool with a positive rake angle proved satisfactory.

The root areas of the Conoseals were abrasive-polished to the specified 32 micro-in. finish. Other surfaces, requiring 63 micro-in. finish were also polished.

Machining Inconel 718 in the aged condition is slightly more difficult than machining in the annealed condition. Very light cuts work-harden the material and cuts of no less than 0.010-in. were used where possible. The material is very abrasive and requires regular cutter changes.

For the second machining operation, the assembly was mounted on the lathe fixture with the open end up. A plug and a split ring were used to maintain roundness of the 286503-1 ring (Figure D-1) during machining. The inside of the hub was finish-bored with exception of the extremely close tolerance 9.5460/9.5464-in. diameter bore which was ground on a separate set-up. The Conoseal grooves were plunge-cut with a form tool and abrasive polished to the required 32 micro-in. finish.

*Registered Trademark of Aeroquip Corp.

III, W, 10-10-54 (cont.)

Drilling was accomplished on a Burgmaster drilling machine. Previously conducted studies showed that the performance of Cobalt drills far surpassed high speed drills on hole sizes of 1/2-in. diameter and smaller. Broken drills were removed from the holes by electric discharge machining.

Finish boring of the venturies was accomplished on a Lucas Boring Mill, using a rotary index table for positioning. To bore the holes straight and accurate, a bushing was used as a pilot for a four-flute core drill. After core drilling, the lower end of the hole was reamed. Using this diameter as a pilot for the remaining steps, it was possible to ream the holes and maintain concentricity. All tools were of high speed steel.

The remaining operations were of routine mode and were accomplished without incident. Because in-process inspection was practiced throughout, the final inspection was minimized. The completed part was cleaned by flushing with degreasing fluid and protective covers were installed prior to packaging and shipping.

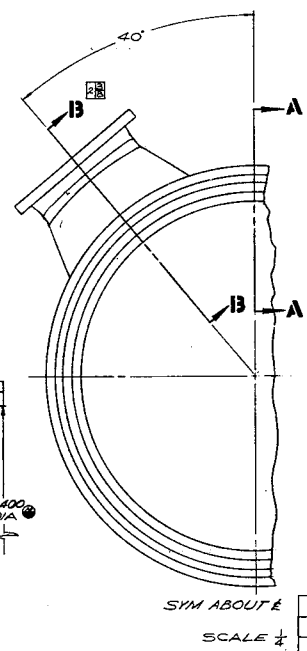
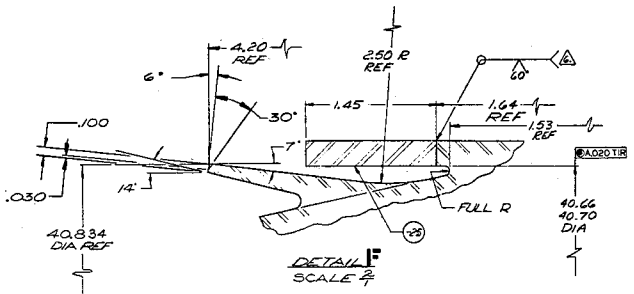
- NOTES: 1 REMOVE ALL BURRS & SHARP EDGES EQUIV. TO .005/DEN UNLESS OTHERWISE NOTED.
 2 INTERPRET DWG PER STANDARDS PREScribed IN MIL-D-70327 & ASA-132.3 1959.
 3 SURFACE ROUGHNESS TO BE $R_{a} 1.6$ UNLESS OTHERWISE NOTED.
 4 ALL FILLETS & CORNER RADII SHALL BE 12R MAX UNLESS OTHERWISE NOTED.
 5 CLASSIFICATION OF CHARACTERISTICS PER MIL-W-2411 DENOTED BY (C) (CRITICAL), (M) (MAJOR) AND (N) SYMBOL (MINOR).
 6 TIG WELD PER MSFC DWG NO. 10509308, CLASS I, AND AGC-46351, MSFC DWG. NO. 10509308 TAKES PRECEDENCE.
 7 PENETRANT INSPECT ALL WELDS PER MIL-I-6866, TYPE I, & AGC-STD-4818 TYPE I CLASS I, MIL-I-6866 TAKES PRECEDENCE.
 8 QUALITY LEVEL PER AGC-STD-4006, CLASS I.
 9 RADIOGRAPHIC INSPECT WELD JOINTS PER MIL-STD-463, LEVEL II AND AGC-STD-4818. MIL-STD-453 TAKES PRECEDENCE.
 10 CLEAN PER MSFC DWG. NO. 10509308.
 11 CLEAN PER AGC-46350 LEVEL II.
 12 PRESERVE & PACKAGE PER DWG. NO. MSFC-10419900, FUSELAGE COMPONENT.
 13 TEMPORARY MARK PER ASD 5215 H WITH PART NO. 286503 AND APPLICABLE DASH NO.
 14 PREPRODUCTION TEST PER AGC-STD-4861.
 15 REMOVED.
 16 REPRODUCTION OF DETAILS & LOCATION OF WELD JOINTS OPTIONAL, ALL CHANGES TO BE SUBMITTED TO AGC ENGINEERING FOR APPROVAL PRIOR TO FABRICATION.
 17 ULTRASONIC INSPECT ROUGH MACH FORGINGS PER AGC-STD-4819 TYPE OPTIONAL, ACCEPT PER AGC-STD-4006, CLASS III BEFORE WELDING.
 18 RADIOGRAPHIC INSPECTION NOT REQD. WELD PER MSFC DWG. NO. 10509308, CLASS III.

19. STRESS RELIEF PER AGC-46604 AS REQUIRED.

20. REMOVED

21. VENDOR FORGING DWG SHALL BE SUBMITTED TO AGC ROYALTY MACHINERY ENGR DEPT FOR APPROVAL PRIOR TO PLACEMENT OF FORGING ORDER. FORGING TEST SPECIMENS SHALL BE TAKEN FROM THE HEAVIEST CROSS-SECTION AND THEIR LOCATIONS SHALL BE SHOWN ON THE FORGING DRAWING.

22. PENETRANT INSPECT -5, -7, -11, -13, 21, 23, 25 PER MIL-I-6866 TYPE I & AGC-STD-4818 TYPE I CLASS I BEFORE WELDING. MIL-I-6866 TAKES PRECEDENCE OVER AGC-STD-4818. ACCEPTANCE CRITERIA PER AGC-STD-4006, CLASS I.

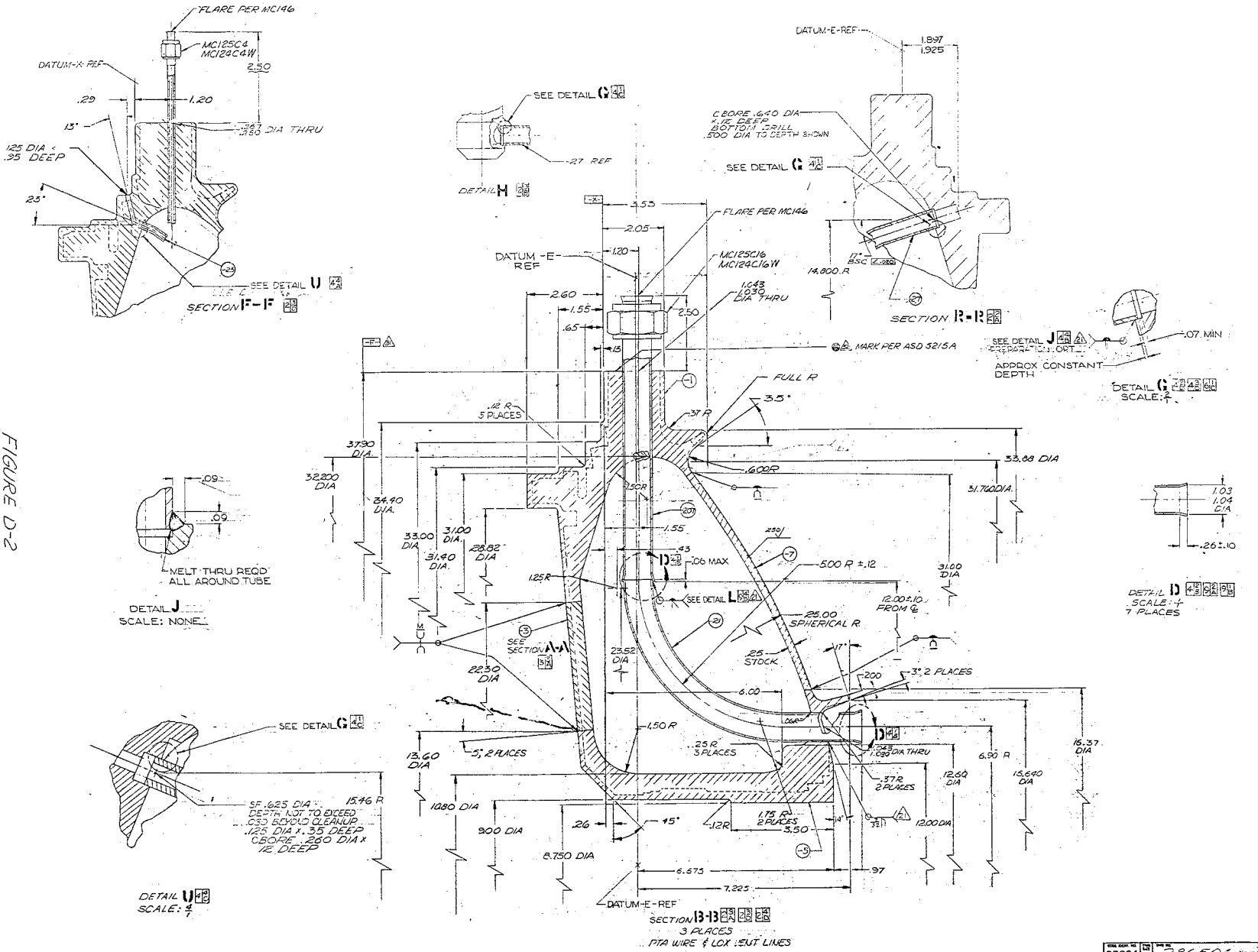


REV	DATE	BY	CHKD	DESCRIPTION
1				WELD ROD
2				INCONEL 718
3				AGC-44151
4				375 THK PLATE
5				INCONEL 718
6				AGC-44152
7				105 THK SHEET
8				INCONEL 718
9				AGC-44152
10				105 THK PLATE
11				INCONEL 718
12				AGC-44152
13				375 THK PLATE
14				INCONEL 718
15				AGC-44152
16				105 THK SHEET
17				INCONEL 718
18				AGC-44152
19				375 THK PLATE
20				INCONEL 718
21				AGC-44152
22				105 THK SHEET
23				INCONEL 718
24				AGC-44152
25				375 THK PLATE
26				INCONEL 718
27				AGC-44152
28				105 THK SHEET
29				INCONEL 718
30				AGC-44152
31				375 THK PLATE
32				INCONEL 718
33				AGC-44152
34				105 THK SHEET
35				INCONEL 718
36				AGC-44152
37				375 THK PLATE
38				INCONEL 718
39				AGC-44152
40				105 THK SHEET
41				INCONEL 718
42				AGC-44152
43				375 THK PLATE
44				INCONEL 718
45				AGC-44152
46				105 THK SHEET
47				INCONEL 718
48				AGC-44152
49				375 THK PLATE
50				INCONEL 718
51				AGC-44152
52				105 THK SHEET
53				INCONEL 718
54				AGC-44152
55				375 THK PLATE
56				INCONEL 718
57				AGC-44152
58				105 THK SHEET
59				INCONEL 718
60				AGC-44152
61				375 THK PLATE
62				INCONEL 718
63				AGC-44152
64				105 THK SHEET
65				INCONEL 718
66				AGC-44152
67				375 THK PLATE
68				INCONEL 718
69				AGC-44152
70				105 THK SHEET
71				INCONEL 718
72				AGC-44152
73				375 THK PLATE
74				INCONEL 718
75				AGC-44152
76				105 THK SHEET
77				INCONEL 718
78				AGC-44152
79				375 THK PLATE
80				INCONEL 718
81				AGC-44152
82				105 THK SHEET
83				INCONEL 718
84				AGC-44152
85				375 THK PLATE
86				INCONEL 718
87				AGC-44152
88				105 THK SHEET
89				INCONEL 718
90				AGC-44152
91				375 THK PLATE
92				INCONEL 718
93				AGC-44152
94				105 THK SHEET
95				INCONEL 718
96				AGC-44152
97				375 THK PLATE
98				INCONEL 718
99				AGC-44152
100				105 THK SHEET

PAGE D-10
 FIGURE D-1

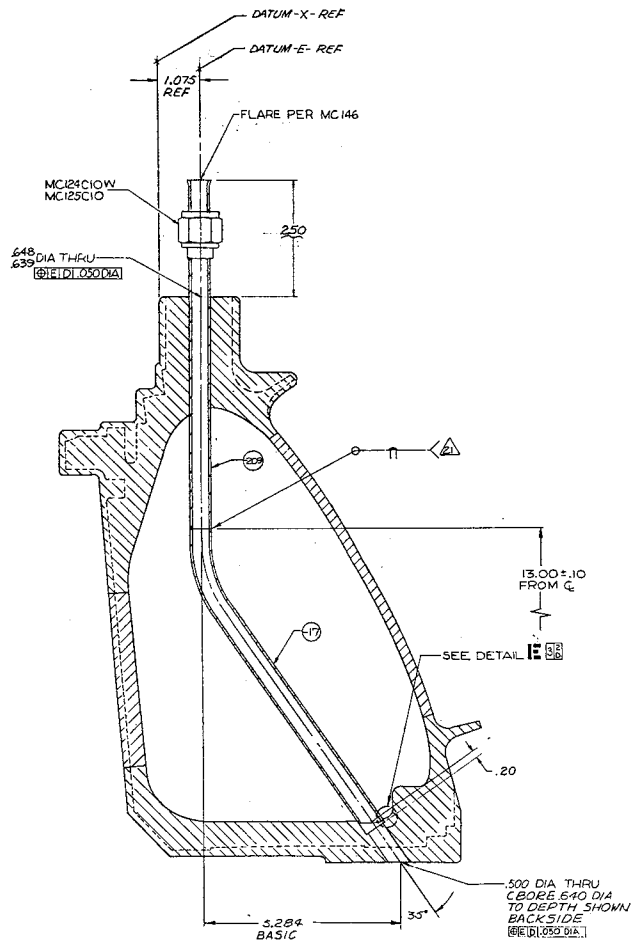
UNLESS OTHERWISE SPECIFIED		MATERIALS TO BE USED	
FINISH	AS SHOWN	TEMPERATURE	AS SHOWN
TOLERANCES	UNLESS OTHERWISE SPECIFIED	STRENGTH	AS SHOWN
WELDING	AS SHOWN	WELDING	AS SHOWN
INSPECTION	AS SHOWN	INSPECTION	AS SHOWN
SCALE	AS SHOWN	SCALE	AS SHOWN
DATE	1/1/52	DATE	1/1/52
DESIGNER	J. J. WELLS	DESIGNER	J. J. WELLS
CHECKED		CHECKED	
APPROVED		APPROVED	
AERONAUTICAL CORPORATION		AERONAUTICAL CORPORATION	
MANIFOLD INLET		MANIFOLD INLET	
ROUGH, HOT GAS		ROUGH, HOT GAS	
FIG. NO.	05824	FIG. NO.	286503
REV.		REV.	
DATE		DATE	

FIGURE D-2
PAGE 0-15

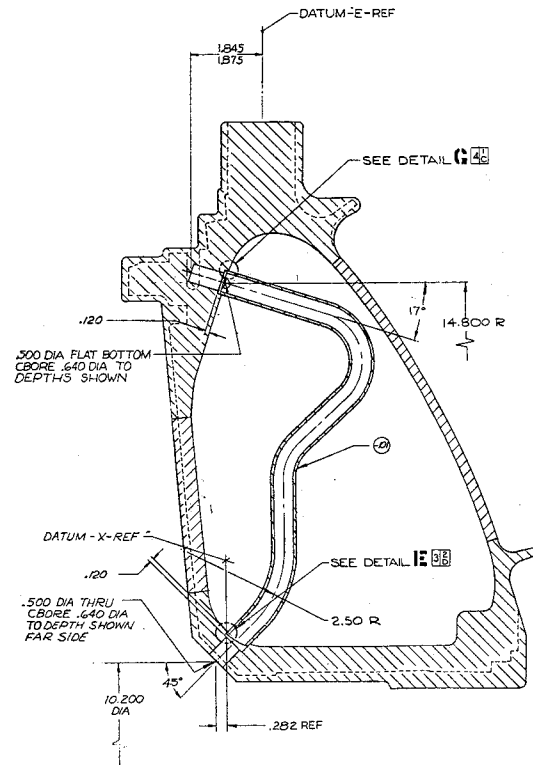


05824 286506

FIGURE D-2
PAGE D-17



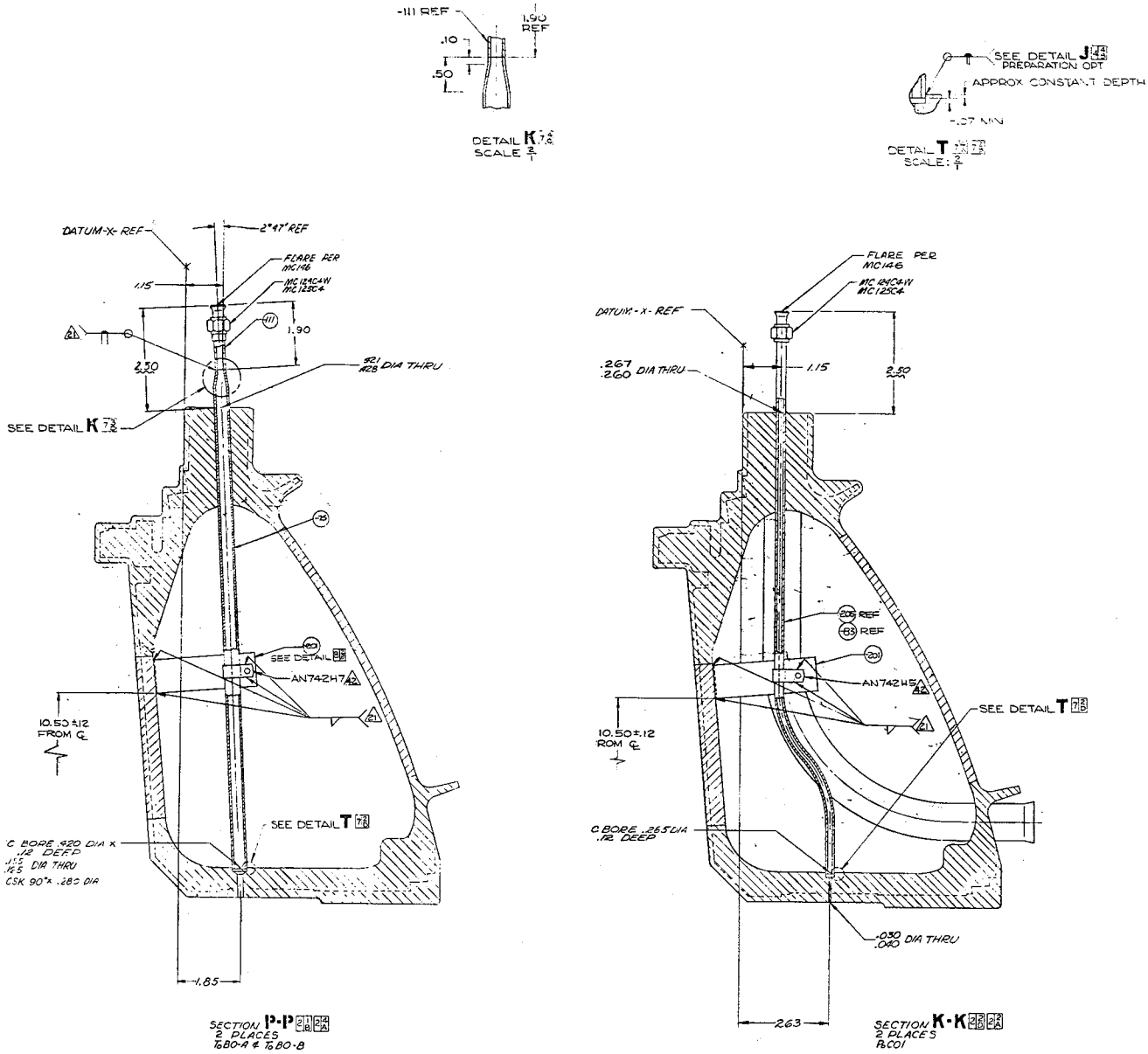
SECTION L-L
PURGE FLOW
3 PLACES

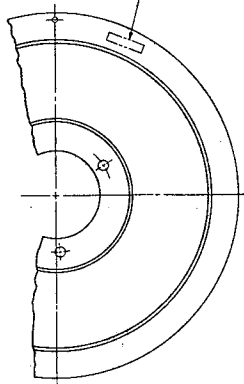
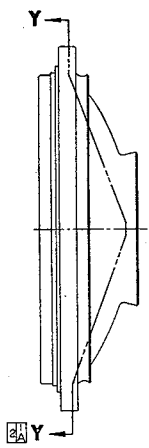
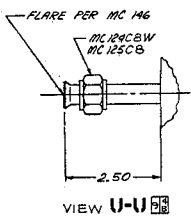
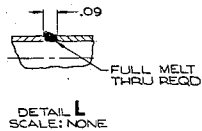


SECTION N-N
BYPASS FLOW
3 PLACES

DATE	05824	REV	E	FIG NO	286506
WORK		REVISION		DATE	10-22-61
					SHEET 6

FIGURE D-2
PAGE D-18





MARK PER ASD5215H WITH VENDOR'S
PART NO., SERIAL NO., AGC SOURCE
CONTROL DWG NO. 286506-9 AND
AGC ASSIGNED SERIAL NO.

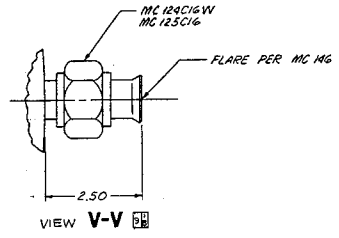
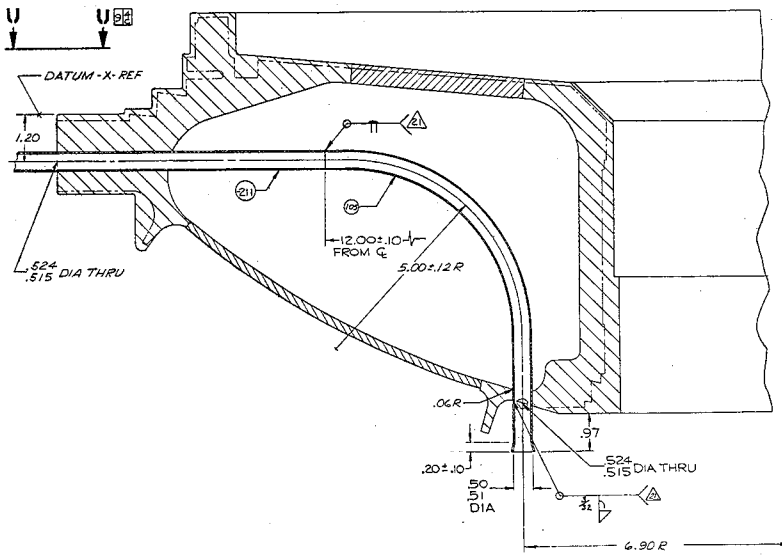
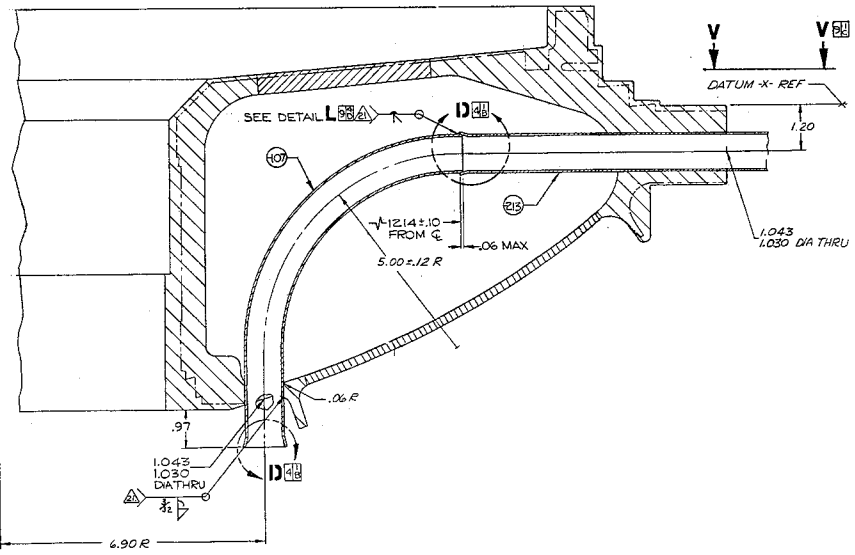


FIGURE D-2
PAGE D-20



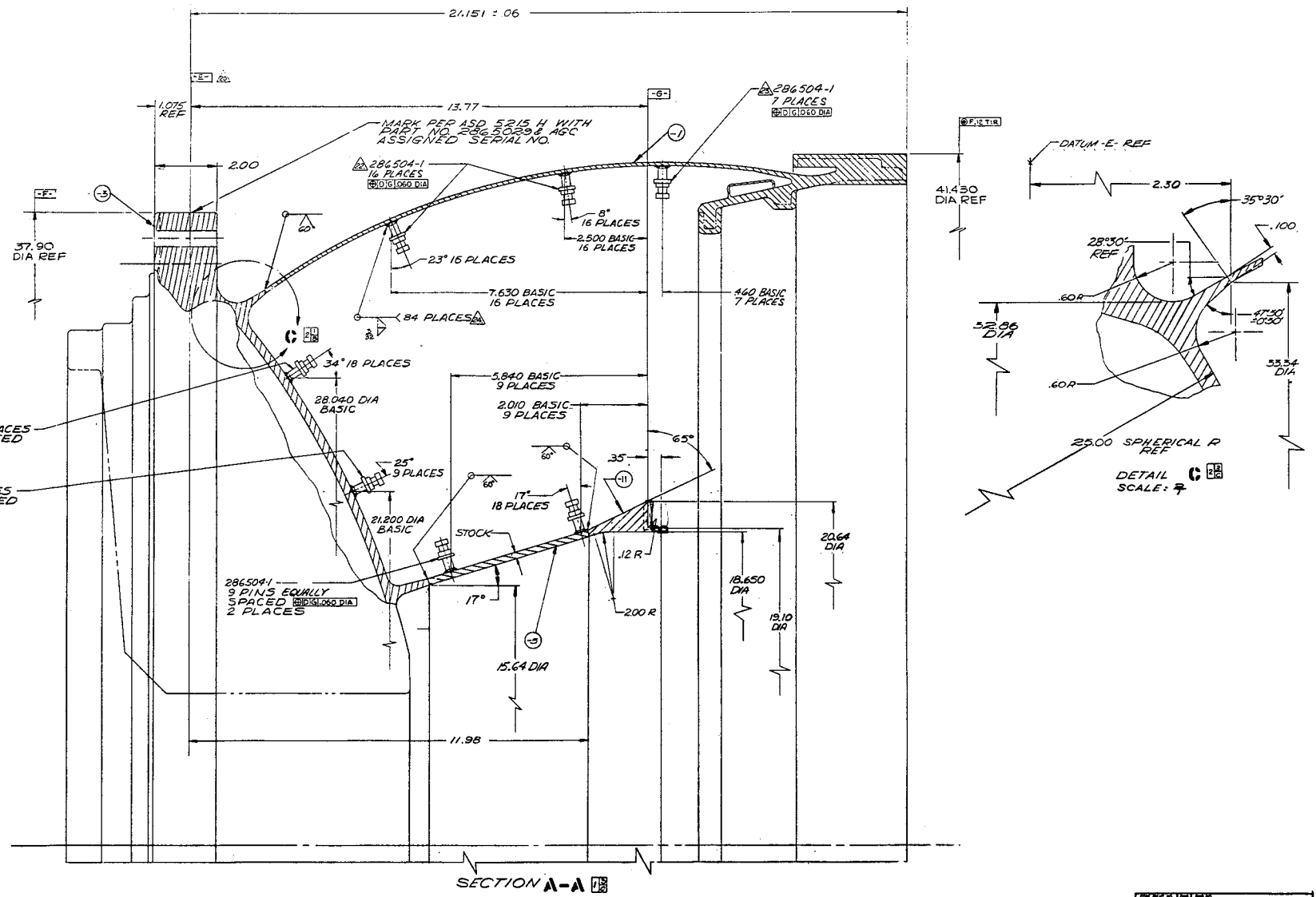
SECTION H-H
2 PLACES
NEUTRAL & HOT GAS PURGE LINES



SECTION S-S
2 PLACES
ROTATED 41°15' CW & 138°45' CCW
NEUTRAL & HOT GAS VENT LINES

REV	DATE	BY	CHK	APP	DESCRIPTION
05824	E				286506
MAX	+	REVISIONS	7/21/67	REV	9

FIGURE D-3
PAGE D-22



NOTES:

1. THIS DRAWING TO BE USED IN CONJUNCTION WITH DRAWING 286502.
 2. HYDROSTATIC PROOF TEST CAVITIES **A** AND **B** SIMULTANEOUSLY. HOLD FOR TWO MINUTES MIN.
 3. LEAK TEST CAVITIES **A** AND **B** SIMULTANEOUSLY. HOLD FOR TWO MINUTES MIN. LEAKAGE NOT TO EXCEED 1×10^{-3} STD CC/SEC.
 4. VENDOR IS TO PROVIDE HYDROTEST TOOLING AS ILLUSTRATED ON THIS DRAWING AND IS TO SUBMIT TOOLING DRAWINGS TO AGC COGNIZANT ENGINEERING DEPT. PRIOR TO CONDUCTING HYDROTEST.
 5. PHANTOM LINE ILLUSTRATIONS OF HYDROTEST TOOLING ARE SHOWN ONLY FOR PURPOSE OF DEFINING THE WORKING CONDITIONS AND LOCATIONS OF SEALS AND CLAMPS.
- INDICATED SURFACES OF 286502-9 MAY BE MACHINED .010 MAX BEYOND CLEANUP TO ASSURE SEALING SURFACE, PROVIDED SUFFICIENT STOCK IS LEFT TO MEET REQUIREMENTS OF END PRODUCT.

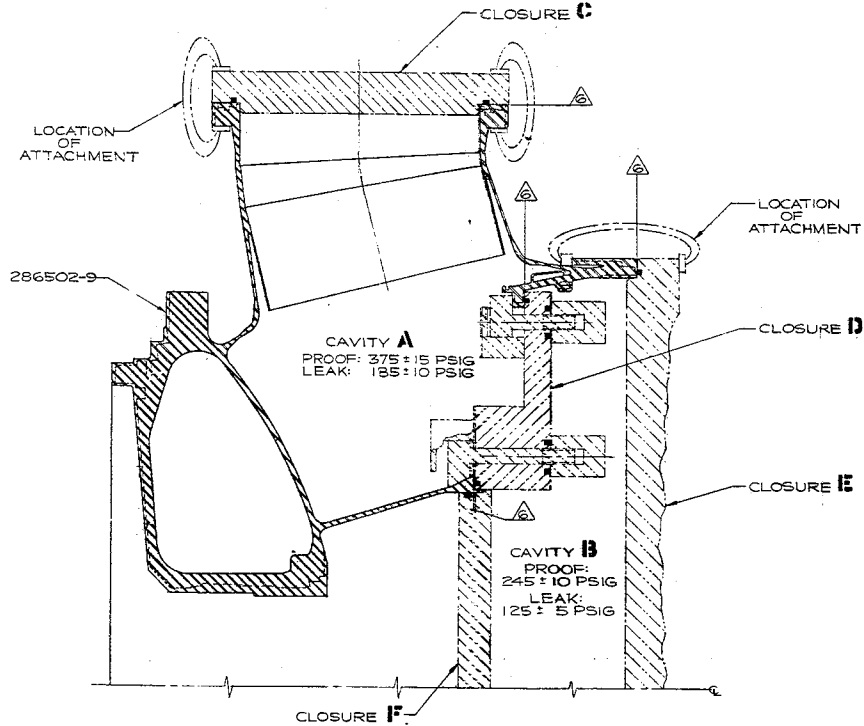


FIGURE D-4
PAGE D-23

REV	DATE	BY	CHKD	DESCRIPTION
1				

UNLESS OTHERWISE SPECIFIED	STAINLESS STEEL 304
ALL DIMENSIONS ARE IN INCHES	
FINISH	RA 32
TOLERANCES	FRACTIONAL DECIMALS
0.001 - 0.005	± .0005
0.005 - 0.010	± .0008
0.010 - 0.030	± .0012
0.030 - 0.060	± .0015
0.060 - 0.125	± .0020
0.125 - 0.250	± .0025
0.250 - 0.500	± .0030
0.500 - 1.000	± .0040
1.000 - 2.000	± .0050
2.000 - 5.000	± .0060
5.000 - 10.000	± .0070
10.000 - 25.000	± .0080
25.000 - 50.000	± .0090
50.000 - 100.000	± .0100
100.000 - 250.000	± .0120
250.000 - 500.000	± .0150
500.000 - 1000.000	± .0200
1000.000 - 2500.000	± .0250
2500.000 - 5000.000	± .0300
5000.000 - 10000.000	± .0400
10000.000 - 25000.000	± .0500
25000.000 - 50000.000	± .0600
50000.000 - 100000.000	± .0700
100000.000 - 250000.000	± .0800
250000.000 - 500000.000	± .0900
500000.000 - 1000000.000	± .1000
1000000.000 - 2500000.000	± .1200
2500000.000 - 5000000.000	± .1500
5000000.000 - 10000000.000	± .1800
10000000.000 - 25000000.000	± .2000
25000000.000 - 50000000.000	± .2500
50000000.000 - 100000000.000	± .3000
100000000.000 - 250000000.000	± .3500
250000000.000 - 500000000.000	± .4000
500000000.000 - 1000000000.000	± .4500
1000000000.000 - 2500000000.000	± .5000
2500000000.000 - 5000000000.000	± .5500
5000000000.000 - 10000000000.000	± .6000
10000000000.000 - 25000000000.000	± .6500
25000000000.000 - 50000000000.000	± .7000
50000000000.000 - 100000000000.000	± .7500
100000000000.000 - 250000000000.000	± .8000
250000000000.000 - 500000000000.000	± .8500
500000000000.000 - 1000000000000.000	± .9000
1000000000000.000 - 2500000000000.000	± .9500
2500000000000.000 - 5000000000000.000	± 1.0000
5000000000000.000 - 10000000000000.000	± 1.1000
10000000000000.000 - 25000000000000.000	± 1.2000
25000000000000.000 - 50000000000000.000	± 1.3000
50000000000000.000 - 100000000000000.000	± 1.4000
100000000000000.000 - 250000000000000.000	± 1.5000
250000000000000.000 - 500000000000000.000	± 1.6000
500000000000000.000 - 1000000000000000.000	± 1.7000
1000000000000000.000 - 2500000000000000.000	± 1.8000
2500000000000000.000 - 5000000000000000.000	± 1.9000
5000000000000000.000 - 10000000000000000.000	± 2.0000
10000000000000000.000 - 25000000000000000.000	± 2.1000
25000000000000000.000 - 50000000000000000.000	± 2.2000
50000000000000000.000 - 100000000000000000.000	± 2.3000
100000000000000000.000 - 250000000000000000.000	± 2.4000
250000000000000000.000 - 500000000000000000.000	± 2.5000
500000000000000000.000 - 1000000000000000000.000	± 2.6000
1000000000000000000.000 - 2500000000000000000.000	± 2.7000
2500000000000000000.000 - 5000000000000000000.000	± 2.8000
5000000000000000000.000 - 10000000000000000000.000	± 2.9000
10000000000000000000.000 - 25000000000000000000.000	± 3.0000
25000000000000000000.000 - 50000000000000000000.000	± 3.1000
50000000000000000000.000 - 100000000000000000000.000	± 3.2000
100000000000000000000.000 - 250000000000000000000.000	± 3.3000
250000000000000000000.000 - 500000000000000000000.000	± 3.4000
500000000000000000000.000 - 1000000000000000000000.000	± 3.5000
1000000000000000000000.000 - 2500000000000000000000.000	± 3.6000
2500000000000000000000.000 - 5000000000000000000000.000	± 3.7000
5000000000000000000000.000 - 10000000000000000000000.000	± 3.8000
10000000000000000000000.000 - 25000000000000000000000.000	± 3.9000
25000000000000000000000.000 - 50000000000000000000000.000	± 4.0000
50000000000000000000000.000 - 100000000000000000000000.000	± 4.1000
100000000000000000000000.000 - 250000000000000000000000.000	± 4.2000
250000000000000000000000.000 - 500000000000000000000000.000	± 4.3000
500000000000000000000000.000 - 1000000000000000000000000.000	± 4.4000
1000000000000000000000000.000 - 2500000000000000000000000.000	± 4.5000
2500000000000000000000000.000 - 5000000000000000000000000.000	± 4.6000
5000000000000000000000000.000 - 10000000000000000000000000.000	± 4.7000
10000000000000000000000000.000 - 25000000000000000000000000.000	± 4.8000
25000000000000000000000000.000 - 50000000000000000000000000.000	± 4.9000
50000000000000000000000000.000 - 100000000000000000000000000.000	± 5.0000
100000000000000000000000000.000 - 250000000000000000000000000.000	± 5.1000
250000000000000000000000000.000 - 500000000000000000000000000.000	± 5.2000
500000000000000000000000000.000 - 1000000000000000000000000000.000	± 5.3000
1000000000000000000000000000.000 - 2500000000000000000000000000.000	± 5.4000
2500000000000000000000000000.000 - 5000000000000000000000000000.000	± 5.5000
5000000000000000000000000000.000 - 10000000000000000000000000000.000	± 5.6000
10000000000000000000000000000.000 - 25000000000000000000000000000.000	± 5.7000
25000000000000000000000000000.000 - 50000000000000000000000000000.000	± 5.8000
50000000000000000000000000000.000 - 100000000000000000000000000000.000	± 5.9000
100000000000000000000000000000.000 - 250000000000000000000000000000.000	± 6.0000
250000000000000000000000000000.000 - 500000000000000000000000000000.000	± 6.1000
500000000000000000000000000000.000 - 1000000000000000000000000000000.000	± 6.2000
1000000000000000000000000000000.000 - 2500000000000000000000000000000.000	± 6.3000
2500000000000000000000000000000.000 - 5000000000000000000000000000000.000	± 6.4000
5000000000000000000000000000000.000 - 10000000000000000000000000000000.000	± 6.5000
10000000000000000000000000000000.000 - 25000000000000000000000000000000.000	± 6.6000
25000000000000000000000000000000.000 - 50000000000000000000000000000000.000	± 6.7000
50000000000000000000000000000000.000 - 100000000000000000000000000000000.000	± 6.8000
100000000000000000000000000000000.000 - 250000000000000000000000000000000.000	± 6.9000
250000000000000000000000000000000.000 - 500000000000000000000000000000000.000	± 7.0000
500000000000000000000000000000000.000 - 1000000000000000000000000000000000.000	± 7.1000
1000000000000000000000000000000000.000 - 2500000000000000000000000000000000.000	± 7.2000
2500000000000000000000000000000000.000 - 5000000000000000000000000000000000.000	± 7.3000
5000000000000000000000000000000000.000 - 10000000000000000000000000000000000.000	± 7.4000
10000000000000000000000000000000000.000 - 25000000000000000000000000000000000.000	± 7.5000
25000000000000000000000000000000000.000 - 50000000000000000000000000000000000.000	± 7.6000
50000000000000000000000000000000000.000 - 100000000000000000000000000000000000.000	± 7.7000
100000000000000000000000000000000000.000 - 250000000000000000000000000000000000.000	± 7.8000
250000000000000000000000000000000000.000 - 500000000000000000000000000000000000.000	± 7.9000
500000000000000000000000000000000000.000 - 1000000000000000000000000000000000000.000	± 8.0000
1000000000000000000000000000000000000.000 - 2500000000000000000000000000000000000.000	± 8.1000
2500000000000000000000000000000000000.000 - 5000000000000000000000000000000000000.000	± 8.2000
5000000000000000000000000000000000000.000 - 10000000000000000000000000000000000000.000	± 8.3000
10000000000000000000000000000000000000.000 - 25000000000000000000000000000000000000.000	± 8.4000
25000000000000000000000000000000000000.000 - 50000000000000000000000000000000000000.000	± 8.5000
50000000000000000000000000000000000000.000 - 100000000000000000000000000000000000000.000	± 8.6000
100000000000000000000000000000000000000.000 - 250000000000000000000000000000000000000.000	± 8.7000
250000000000000000000000000000000000000.000 - 500000000000000000000000000000000000000.000	± 8.8000
500000000000000000000000000000000000000.000 - 1000000000000000000000000000000000000000.000	± 8.9000
1000000000000000000000000000000000000000.000 - 2500000000000000000000000000000000000000.000	± 9.0000
2500000000000000000000000000000000000000.000 - 5000000000000000000000000000000000000000.000	± 9.1000
5000000000000000000000000000000000000000.000 - 100.000	± 9.2000
100.000 - 25000000000000000000000000000000000000000.000	± 9.3000
25000000000000000000000000000000000000000.000 - 500.000	± 9.4000
500.000 - 1000.000	± 9.5000
1000.000 - 2500.000	± 9.6000
2500.000 - 5000.000	± 9.7000
5000.000 - 100.000	± 9.8000
100.000 - 25000.000	± 9.9000
25000.000 - 500.000	± 10.0000

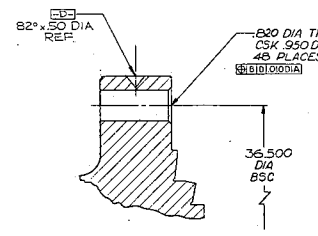
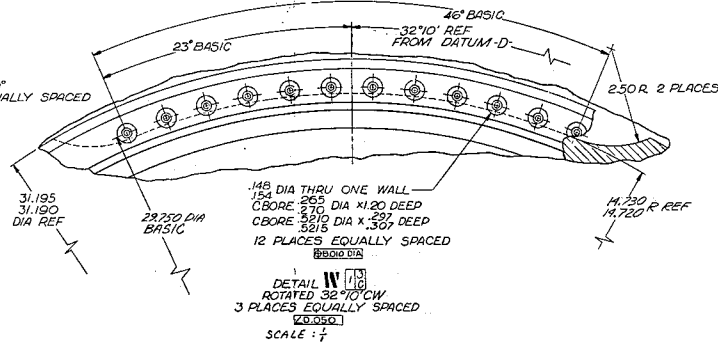
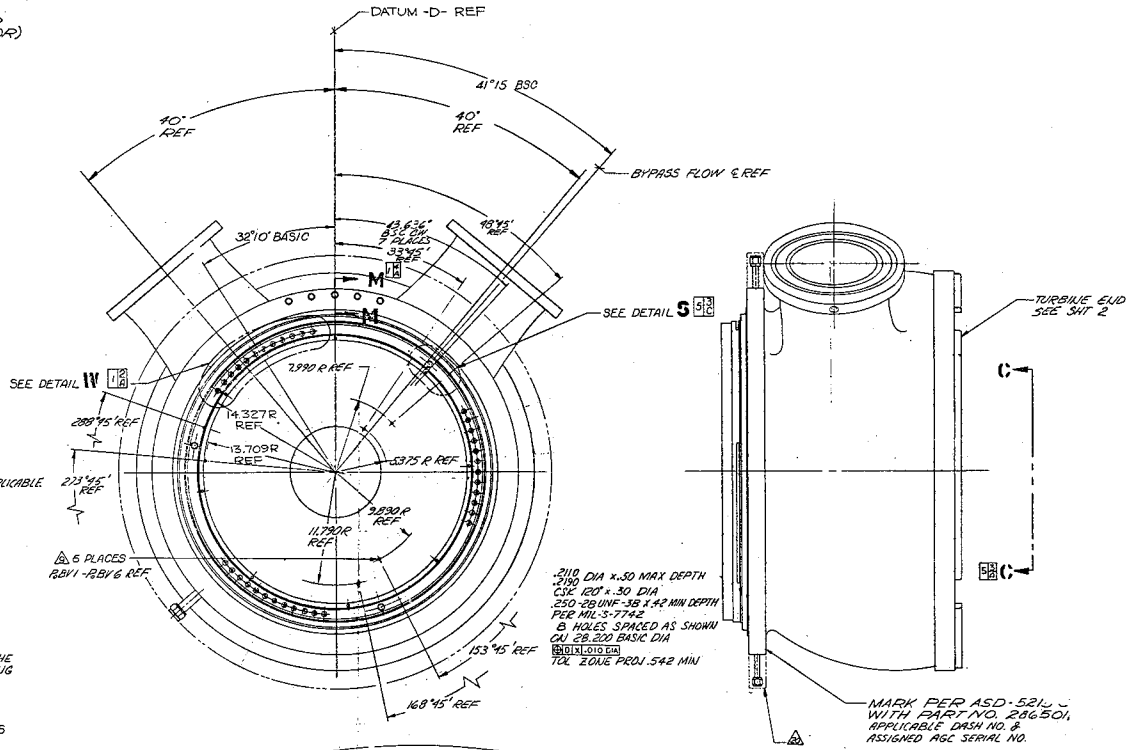
- NOTES: 1. INTERPRET DWG PER STD. PRESCRIBED IN MIL-D-70327 & ASAY32.3. CORRELATED DATUMS INDICATED BY D, E & F.
 2. REMOVE ALL BURRS & SHARP EDGES EQUIV. TO 004/015 R UNLESS OTHERWISE NOTED.
 3. CLEAN PER AGC-466.50, LEVEL H.
 4. PRESERVE & PACKAGE PER MSFC DWG NO. 10419900 FUSELAGE COMPONENT.
 5. REMOVED.
 6. CLASSIFICATION OF CHARACTERISTICS PER MIL-W-9411 DENOTED BY (CRITICAL) & NO SYMBOL (MINOR).

7. PROOF TEST IN ACCORDANCE WITH PROOF TEST ASSY AND REQUIREMENTS AS DEPICTED ON DRAWING 710912.
 8. REMOVED

9. DEBURR .030/.040 HOLE, CORNER RADII'S TO BE .005 MAX.
 10. SURFACE ROUGHNESS TO BE 125 MICRON INCH UNLESS OTHERWISE NOTED.
 11. ALUMINUM PROTECTIVE CLOSURE REQ'D, ONE INCH DIA. MIN.
 12. ALL FILLET RADII TO BE .005/.015 R UNLESS OTHERWISE NOTED.
 13. DATUM -E- IS A PLANE PASSING THRU THE CENTERS OF THREE .375/.376 DIA HOLES.

14. TIG WELD PER MSFC DWG NO. 10509308, CLASS I, AND AGC-46351. MSFC DWG TAKES PRECEDENCE IN CASE OF CONFLICT. WELD MISMATCH MUST BE HELD BELOW .5% OF MATL THK.
 15. PENETRANT INSPECT ALL WELDS PER MIL-F-6866, TYPE I, AND AGC-STD-4816, TYPE I, CLASS I. MIL-F-6866 TAKES PRECEDENCE IN CASE OF CONFLICT.
 16. QUALITY LEVEL PER AGC-STD-4005, CLASS I.
 17. RADIOGRAPHIC INSPECT WELD JOINTS PER MIL-STD-453 LEVEL II AND AGC-STD-4818, MIL-STD TAKES PRECEDENCE IN CASE OF CONFLICT. QUALITY PER MSFC DWG NO. 10509308.

18. REMOVED.
 19. WELD .5 TO .3 THEN SOLUTION ANNEAL AND AGE PER AGC-46604 PRIOR TO WELDING .3 TO .1 OR .3 TO .7 AS APPLICABLE.
 20. PROTECTIVE CLOSURES REQ'D ON ALL PORTS.
 21. PROTECTIVE CLOSURES REQ'D DURING AND AFTER MACHINING EXCEPT AS NOTED.
 22. PROTECTIVE CLOSURES MAY BE REMOVED WHEN MACHINING THIS AREA.
 23. TEMPORARY MARK PER ASD5215 WITH PART NO. 286501 AND APPLICABLE DASH NO.
 24. USE CRES 19-9 W/M WELD ROD PER AMS 5782.
 25. ANGLE TAKEN FROM DATUM -D-.
 26. REMOVED.
 27. PROOF TEST WELDED TUBE AT 500 ± 10 PSIG.
 28. LEAK TEST AT 250 ± 10 PSIG WITH HELIUM, HOLD FOR TWO HOURS, MIN. LEAKAGE NOT TO EXCEED 1.10" STD 1/4 IN.
 29. TIE THRU END OF BB645 AND BB646 TUBE AS REQ'D.
 30. TIE DOWN LOOPS ARE PROVIDED FOR HOLDING IN PLACE THE FOUR FLEXIBLE TUBE ENDS TO PREVENT BREAKAGE DURING SHIPMENT. SEE SUGGESTED METHOD IN DETAIL I.
 31. LOCATE TUBE BEFORE WELDING BY MEANS OF FIXTURING SUCH THAT INDICATED DIM. CAN BE MET AFTER WELDING.
 32. DATUMS S-1 & R ARE THE VIRTUAL (EFFECTIVE) CENTERLINES OF AND10056 FITTING ENDS.



SECTION M-M
SCALE: 1/2

DETAIL W
ROTATED 32.10° CW
3 PLACES EQUALLY SPACED
SCALE: 1/2

QTY	PART NO.	DESCRIPTION	MATERIAL	FINISH	QTY	DATE
1	WELD ROD	CRES 19-9 W/M	AMS 5782			
1	WELD ROD	ALCONEL 718	AGC-44131			
2	2	BB646	VENT TUBE		2	5/8
2	2	BB645	PURGE TUBE		2	5/8
1	-7				3	2
7	-5				2	3
1	-3				3	2
1	-1				3	2

REVISION	DATE	BY	DESCRIPTION
1	11/14/74	J. J. J.	ISSUED FOR MANUFACTURE

MANUFACTURED BY	INSPECTED BY	DATE
ASSEMBLED BY	TESTED BY	DATE
WELDED BY	WELDED DATE	

ENGINEER	DESIGNER	DRAWN
APPROVED	CHECKED	SCALE

ORDER NO.	05824	REV.	E
QUANTITY	1	PRICE	286501

FIGURE D-5
PAGE D-24

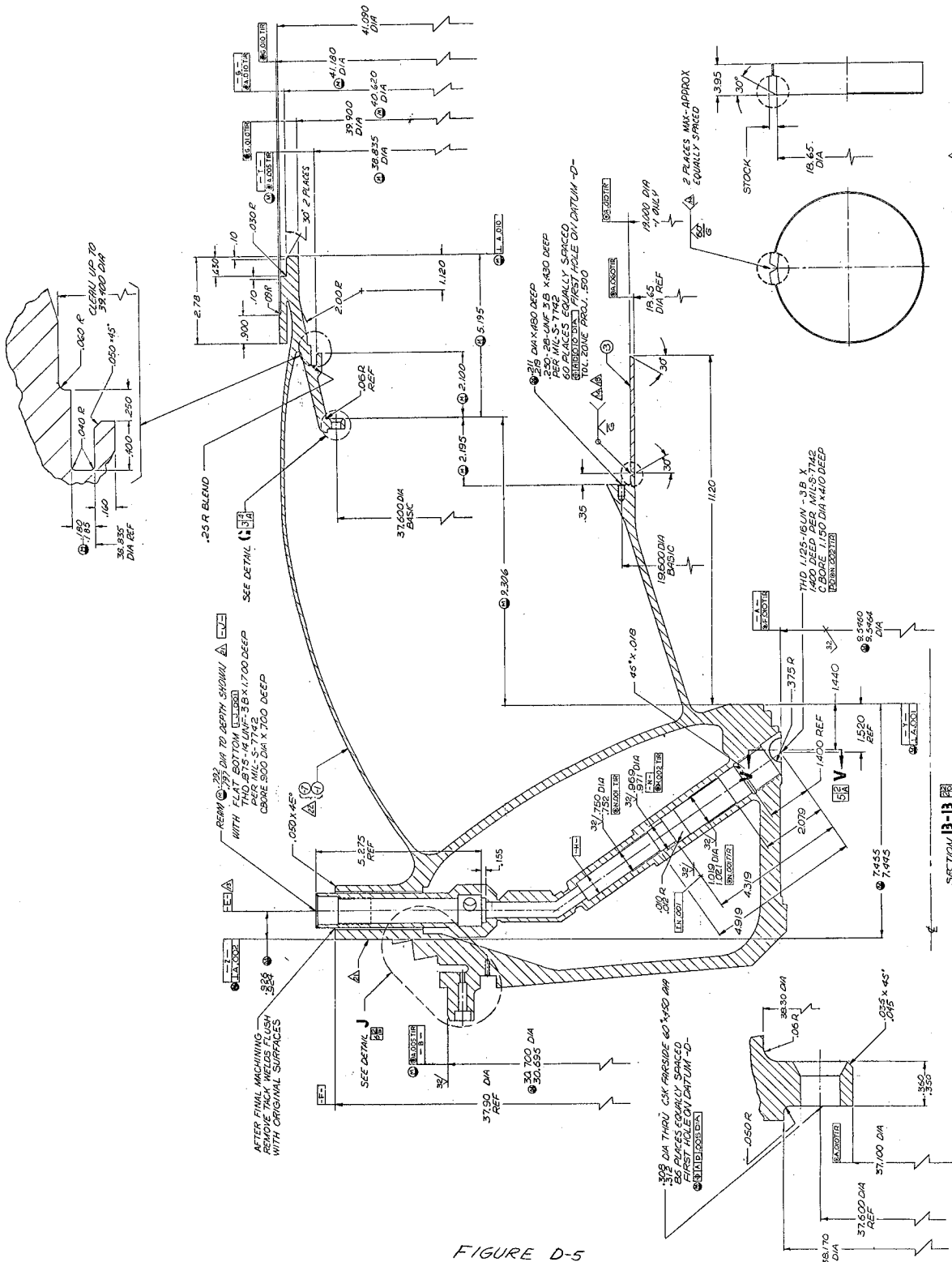


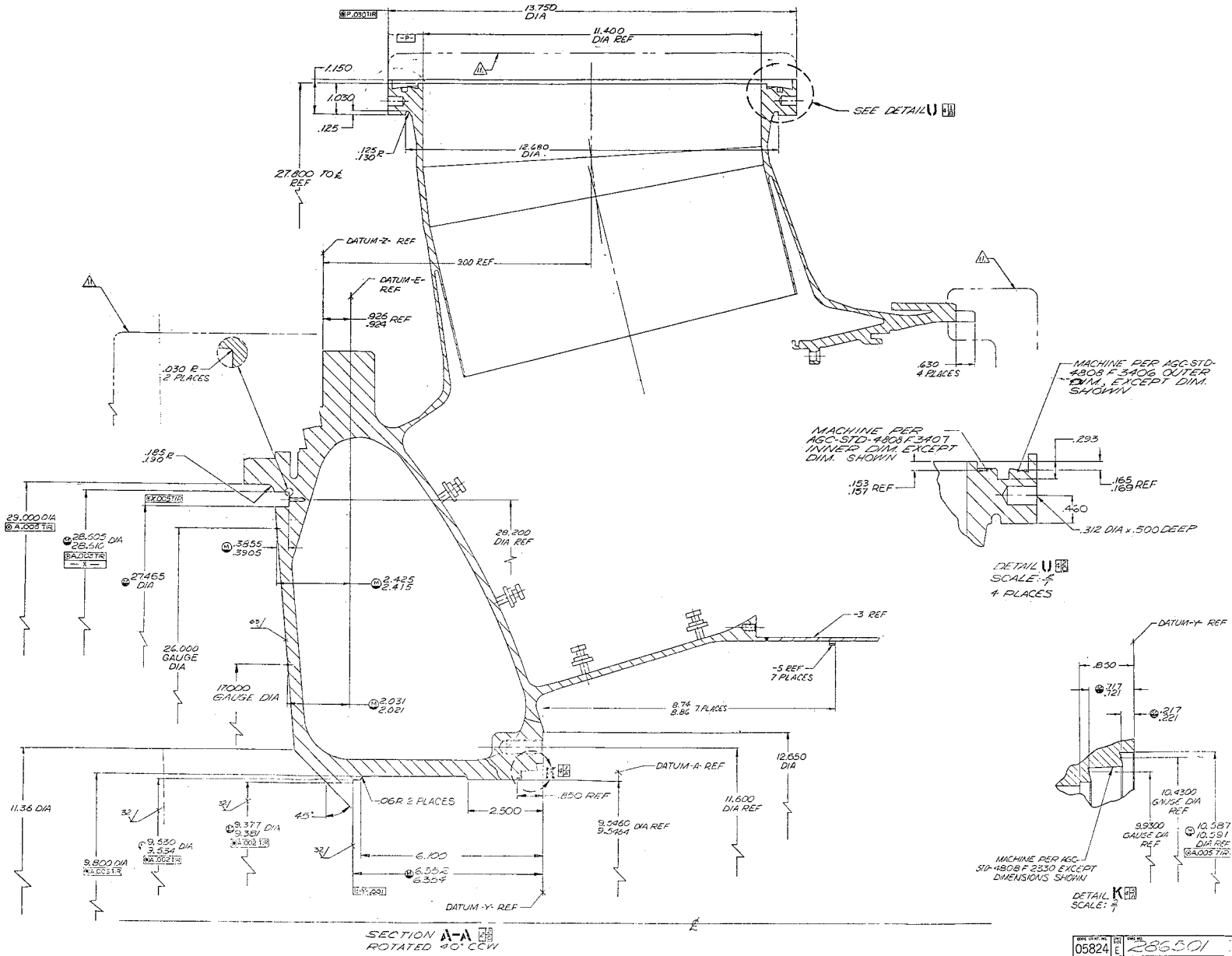
FIGURE D-5
PAGE D-26

3 DETAIL A
SCALE: 1/4

SECTION B-B
3 PLACES EQUALLY SPACED

DETAIL C
SCALE: 3/8

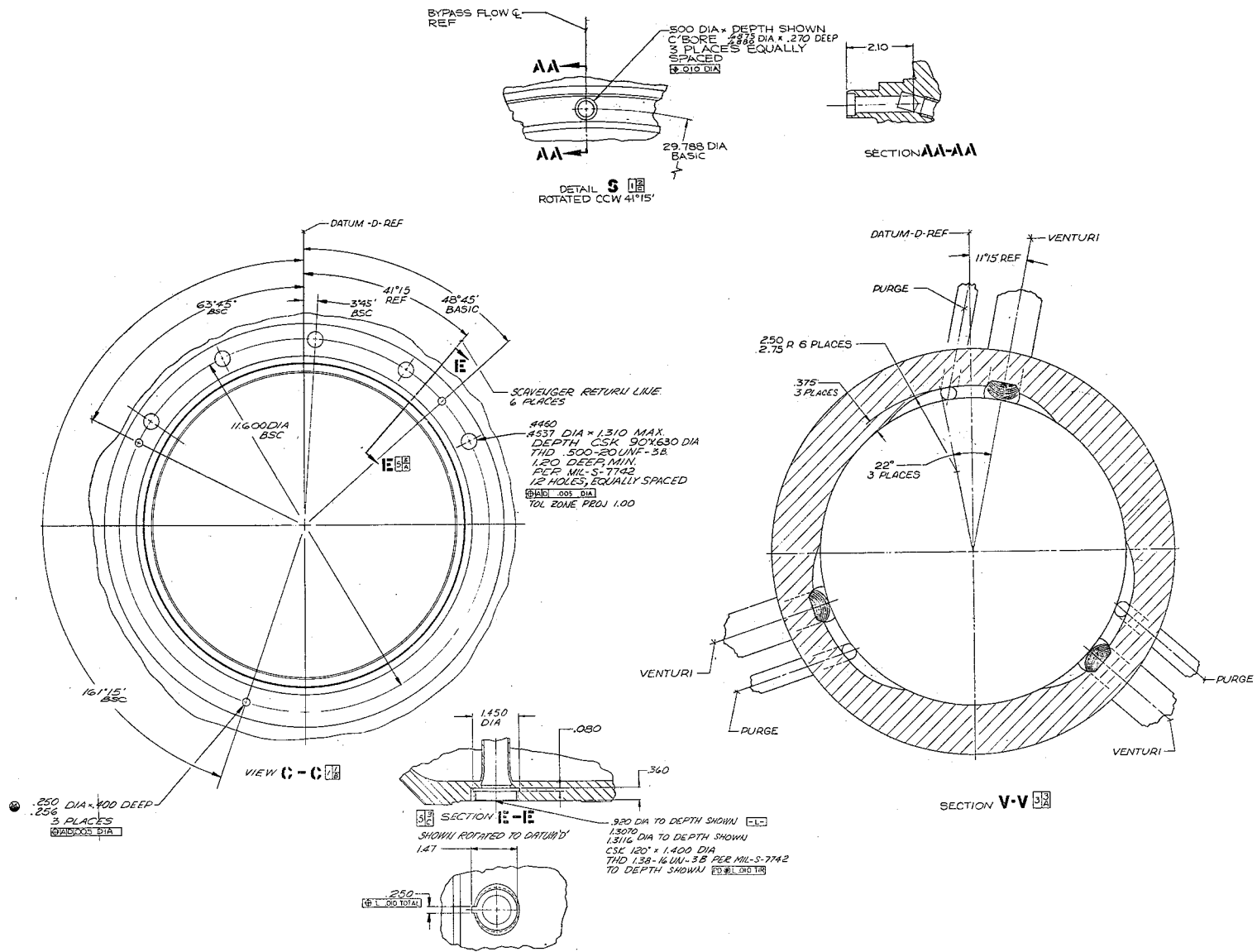
FIGURE D-5
PAGE D-27



SECTION A-A
ROTATED 90° CCW

REV	DATE	BY	CHKD	APP'D
05824	E	286501		

FIGURE D-5
PAGE D-28



05824	286501
REV	DATE
1	11/11/51

REPORT NASA CR 54815 DISTRIBUTION LIST

W. F. Dankhoff (3 Copies)
NASA
Lewis Research Center
21000 Brookpark Road
Cleveland, Ohio 44135
Mail Stop 500-305

H. Hinckley (1 Copy)
Mail Stop 500-210

Patent Counsel (1 Copy)
Mail Stop 77-1

Lewis Library (2 Copies)
Mail Stop 60-3

M. J. Hartmann (1 Copy)
Mail Stop 5-9

W. L. Stewart (1 Copy)
Mail Stop 5-9

J. C. Montgomery (1 Copy)
Mail Stop 501-1 SNPO-C

Major E. H. Karalis (1 Copy)
AFSC Liaison Office
Mail Stop 4-1

Office of Reliability and
Quality Assurance (1 Copy)
Mail Stop 500-203

F. J. Dutee (1 Copy)
Mail Stop 23-1

D. F. Lange (1 Copy)
Mail Stop 501-1

J. B. Esgar (1 Copy)
Mail Stop 49-1

D. D. Scheer (1 Copy)
Mail Stop 500-305

C. F. Zalabak (1 Copy)
Mail Stop 500-305

NASA Representative (6 Copies)
NASA Scientific and Technical
Information Facility
Box 5700
Bethesda, Maryland

Library (1 Copy)
NASA
Ames Research Center
Moffett Field, California 94035

Library (1 Copy)
NASA
Flight Research Center
P. O. Box 273
Edwards AFB, California 93523

Library (1 Copy)
NASA
Goddard Space Flight Center
Greenbelt, Maryland 20771

Library (1 Copy)
NASA
Langley Research Center
Langley Station
Hampton, Virginia 23365

Library (1 Copy)
NASA
Manned Spacecraft Center
Houston, Texas 77058

Library (1 Copy)
NASA
George C. Marshall Space
Flight Center
Huntsville, Alabama 35812

Library (1 Copy)
NASA
Western Operations Office
150 Pico Boulevard
Santa Monica, California 90406

Library (1 Copy)
Jet Propulsion Laboratory
4800 Oak Grove Drive
Pasadena, California 91103

A. O. Tischler (2 Copies)
Code RP
NASA
Washington, D. C. 20546

J. W. Thomas, Jr. (5 Copies)
I-E-E
NASA
George C. Marshall Space Flight Center
Huntsville, Alabama

E. W. Gomersall (1 Copy)
NASA
Mission Analysis Division
Office of Advanced Research and
Technology
Moffett Field, California 94035

Dr. Keith Boyer (1 Copy)
Los Alamos Scientific Laboratory
CMF-9
P. O. Box 1663
Los Alamos, New Mexico

A. Schmidt (1 Copy)
National Bureau of Standards
Cryogenic Division
Boulder, Colorado

Dr. G. Wislicenus (1 Copy)
Penn State University
Naval Ordnance Laboratory
University Park, Pennsylvania

Dr. A. Acosta (1 Copy)
California Institute of Technology
1201 East California Street
Pasadena, California

Dr. E. B. Konecci (1 Copy)
NASA
Executive Office of the President
Executive Office Building
Washington, D. C.

Dr. M. Vavra (1 Copy)
Naval Post-Graduate School
Monterey, California

H. V. Main (1 Copy)
Air Force Rocket Propulsion Laboratory
Edwards Air Force Base
Edwards, California

Dr. George Serovy (1 Copy)
Iowa State University
Ames, Iowa

T. Iura (1 Copy)
Aerospace Corporation
2400 East El Segundo Blvd.
P. O. Box 95085
Los Angeles, California 90045

REPORT NASA CR 54815 DISTRIBUTION LIST (Cont'd)

Chemical Propulsion Information
Agency (1 Copy)
John Hopkins University
Applied Physics Laboratory
8621 Georgia Avenue
Silver Spring, Maryland

Robert O. Bullock (1 Copy)
Garrett Corporation
Airesearch Manufacturing Division
402 S. 36th Street
Phoenix, Arizona 85034

Pratt and Whitney Aircraft
Corporation (1 Copy)
Florida Research and Development
Center
P. O. Box 2691
West Palm Beach, Florida 33402

Library Dept. 586-306 (1 Copy)
Rocketdyne
Division of North American Aviation
6633 Canoga Avenue
Canoga Park, California 91304

John Stanitz (1 Copy)
Thompson-Ramo-Wooldridge, Inc.
23555 Euclid Avenue
Cleveland, Ohio 44117

Dr. M. J. Zucrow (1 Copy)
Purdue University
Lafayette, Indiana 47907